

For Reference

NOT TO BE TAKEN FROM THIS ROOM

Ex LIBRIS
UNIVERSITATIS
ALBERTAEASIS



T H E U N I V E R S I T Y O F A L B E R T A

RELEASE FORM

NAME OF AUTHOR .CHRISTIAAN.WILLEM.LUURSEMA.....
TITLE OF THESIS .PERTURBED.ANGULAR.DISTRIBUTION.ON.THE
.879.keV.LEVEL.IN...⁷⁰Ga.....
.....
DEGREE FOR WHICH THESIS WAS PRESENTED MASTER.OF.SCIENCE
YEAR THIS DEGREE GRANTED 1975.....

Permission is hereby granted to THE UNIVERSITY OF
ALBERTA LIBRARY to reproduce single copies of this
thesis and to lend or sell such copies for private,
scholarly or scientific research purposes only.

The author reserves other publication rights, and
neither the thesis nor extensive extracts from it may
be printed or otherwise reproduced without the author's
written permission.

THE UNIVERSITY OF ALBERTA

PERTURBED ANGULAR DISTRIBUTION ON THE
879 keV LEVEL IN ^{70}Ga

by



CHRISTIAAN WILLEM LUURSEMA

A THESIS

SUBMITTED TO THE FACULTY OF GRADUATE STUDIES AND RESEARCH
IN PARTIAL FULFILMENT OF THE REQUIREMENTS FOR THE DEGREE
OF MASTER OF SCIENCE

DEPARTMENT OF PHYSICS

EDMONTON, ALBERTA

FALL, 1975

THE UNIVERSITY OF ALBERTA
FACULTY OF GRADUATE STUDIES AND RESEARCH

The undersigned certify that they have read, and recommend to the Faculty of Graduate Studies and Research, for acceptance, a thesis entitled "A Perturbed Angular Distribution on the 879 keV Level in ^{70}Ga " submitted by Christiaan Willem Luursema in partial fulfilment of the requirements for the degree of Master of Science.

ABSTRACT

This work deals with the time-dependent quadrupole interaction of ^{70}Ga in a Zn lattice for the 879 keV level with spin 4.

The quadrupole frequency has a value $\omega_q = e^2qQ/\hbar = 315 \text{ MHz}$ and it changes $(+3 \pm 6)\%$ from 300 K to 600 K. The derived quadrupole moment is 0.5 b when the field gradient is estimated according to the proposed universal correlation between the local and lattice part of the field gradient. The temperature dependence might indicate a larger quadrupole moment.

The measured anisotropy coefficients are consistent with a CN-model for spin 4 and the published anisotropies of the decay of the 1102 keV level with spin 4⁻.

The time-integrated values of the attenuation coefficients give in combination with the unperturbed values the indication that the assumption of a static electric field gradient is probably not correct for all nuclei at higher temperatures.

The measurements do not yield a definite value of the spin of the 879 keV level or of the asymmetry parameter η .

ACKNOWLEDGEMENTS

I would like to thank Dr. Dave Hutcheon for his enormous help in all aspects of this work.

I greatly appreciate discussions with my supervisor, Dr. Sheppard, in all phases of my work.

I wish to thank Dr. J. T. Sample and Dr. R. Lawson for their work on my committee.

The help of Jock Elliot in operating the machine was always much appreciated and necessary.

I would like to thank the rest of the staff, academic and non-academic, for the various ways in which they helped me.

My sincere thanks to Mrs. Wahl and graphics for the marvelous job they did on the technical perfection of this thesis.

TABLE OF CONTENTS

CHAPTER		PAGE
I	INTRODUCTION	1
II	THEORY OF QUADRUPOLE INTERACTION	5
	II.1 Angular Distribution	5
	II.2 Perturbed Angular Distribution	10
	II.3 The Hamiltonian for Quadrupole Inter- action	15
III	EQUIPMENT	19
IV	DATA ANALYSIS	30
V	THE EXPERIMENTS	39
	V.1 ^{70}Zn (p,n) ^{70}Ga	39
	V.2 The ^{18}F Trial	47
	V.3 ^{69}Ga (d,p) ^{70}Ga	58
VI	DISCUSSION OF THE RESULTS	59
	VI.1 The Frequencies	59
	VI.2 The Anisotropy Coefficients	64
	VI.3 General Conclusions	68
	REFERENCES	70
	APPENDIX I: TARGET HEATING	72
	APPENDIX II: LEVEL SCHEME OF ^{70}Ga in the INTERMEDIATE COUPLING MODEL	75
	APPENDIX III: PROGRAM TDPAD. INTERNAL REPORT	78

LIST OF TABLES

TABLE		PAGE
1	UNPERTURBED VALUES OF THE LEGENDRE POLY- NOMINALS. THE FIT IS DONE WITHOUT TIME- RESOLUTION	45
2	SCALING FACTORS FOR ω FOR DIFFERENT SPINS . .	46
3	DATA FROM VARIOUS RUNS FOR ^{70}Ga	48
4	SUBLIMATION RATE OF ZINC AS FUNCTION OF THE TEMPERATURE	74

LIST OF FIGURES

FIGURE		PAGE
1	Euler angles. α is rotation around the z-axis, β rotation around y_1 - axis, γ rotation around z' - axis	6
2	The electronic arrangement with two timing counters	20
3	The electronic arrangement with single timing counter and the monitor counter	21
4	The normal beam stop target holder with surrounding devices	23
5	Hot target chamber. The 5 feedthroughs are for the heating-wire (2), the thermocouple (2) and the current collector	25
6	The control box circuit diagram. This circuit switches the power on or off if the reading of the thermocouple is lower or higher than the required setting	26
7	The calibration of the control box as function of the reading of the thermocouple	27
8	Background suppressing target holder	29
9-18	The values of $G_2(t)$ term as function of time for different values of spin, η , $\delta\omega$ and the resolution time τ . Note that Fig. 9 is the $G_4(t)$ term for spin 2. For all curves the first case is represented by the solid curve, the second by the dashed and the third by the the dash dot line	33
9	Spin = 2 $\eta = 0.0, 0.5, 1.0$ $\delta\omega = 0.0$ $\tau = 0.0$. The $G_4(t)$ term	34
10	Spin = 2 $\eta = 0.0, 0.5, 1.0$ $\delta\omega = 0.0$ $\tau = 0.0$. The $G_2(t)$ term	34
11	Spin = 3 $\eta = 0.0, 0.5, 1.0$ $\delta\omega = 0.0$ $\tau = 0.0$	35

FIGURE		PAGE
12	Spin = 5/2 $\eta = 0.0, 0.5, 1.0$ $\delta\omega = 0.0$ $\tau = 0.0$	35
13	Spin = 4 $\eta = 0.0, 0.5, 1.0$ $\delta\omega = 0.0$ $\tau = 0.0$	36
14	Spin = 5 $\eta = 0.0, 0.5, 1.0$ $\delta\omega = 0.0$ $\tau = 0.0$	36
15	Spin = 4 $\eta = 0.4$ $\delta\omega = 0.0$ $\tau = 0.0, 1.0, 2.5$ channels for $\omega = 5$ rad/channel	37
16	Spin = 4 $\eta = 0.0$ $\delta\omega = 0.0$ $\tau = 0.0, 1.0, 2.5$ channels for $\omega = 5$ rad/channel	37
17	Spin = 4 $\eta = 0.4$ $\delta\omega = 0.0, 2.0, 5.0\%$ $\tau = 0.0$	38
18	Spin = 4 $\eta = 0.0$ $\delta\omega = 0.0, 2.0, 5.0\%$ $\tau = 0.0$	38
19	Level scheme of ^{70}Ga with the transitions of interest	40
20	A typical spectrum of $^{70}\text{Zn} (p,n) ^{70}\text{Ga}$. The labels are the energies in keV	41
21-34	These figures show the experimental values for the various runs, with the least square fit as given by Table 3. For the 340 k run we also show the difference between the various η values in the fitting	49
21	$a_4 G_4(t)$ of 188 keV at 340 K	50
22	$a_2 G_2(t)$ of 188 keV at 340 K	50
23	$a_4 G_4(t)$ of 691 keV at 340 K	51
24	$a_2 G_2(t)$ of 691 keV at 340 K	51
25	$a_2 G_2(t)$ of 691 keV at 410 K	52
26	$a_2 G_2(t)$ of 188 keV at 410 K	52
27	$a_2 G_2(t)$ of 691 keV at 420 K	53
28	$a_2 G_2(t)$ of 188 keV at 420 K	53
29	$a_2 G_2(t)$ of 691 keV at 510 K	54
30	$a_2 G_2(t)$ of 188 keV at 510 K	54
31	$a_4 G_4(t)$ of 188 keV at 560 K	55
32	$a_2 G_2(t)$ of 188 keV at 560 K	55

FIGURE		PAGE
33	$a_4 G_4(t)$ of 691 keV at 560 K	56
34	$a_2 G_2(t)$ of 691 keV at 560 K	56
35	The dependence of ω_q on the temperature of ^{70}Ga in Zinc	60
36	Correlation of ionic and extraionic field gradients in metals	62
37	Variation of the quadrupole frequency of different ions in Zn with the temperature and the variation of the lattice part of the field gradient with the temperature	63
38	The time-integrated attenuation coefficient as function of ω_q	66
39	Comparison between the experimental and calculated level scheme for ^{70}Ga . The calculation is done with one phonon in the Intermediate Coupling Model	77

CHAPTER I

INTRODUCTION

When a nucleus in an excited state is formed in a reaction, the population of the magnetic substates is not necessarily equal, but the nucleus may be aligned. This causes the decay of the nucleus to be anisotropic. The degree of anisotropy yields information about the spins and of the levels involved in the decay. When the excited state formed has an electric or magnetic multipole moment and experiences an appropriate field for this moment, it will precess. This is the well-known Larmor precession for the case of the magnetic dipoles. This precession will also rotate the angular distribution of the decay of the level. To see the effect of the precession the level has to have a lifetime. The technique which looks at the time-dependence of this precession in times longer than five nanoseconds is called time-dependent perturbed angular distribution method.

This thesis describes studies of perturbation of γ ray angular distributions due to the interaction of the nuclear quadrupole moment and the electric field gradient (E.F.G.) at the nuclear site.

The interaction is characterized by the spin of the level and the quadrupole frequency e^2qQ/\hbar , where eq is the largest component of the field gradient and Q is the quadrupole

moment of the nucleus. All three parameters are obtainable from a time-dependent angular correlation or distribution measurement (TDPAC or TDPAD). In the correlation experiment the nucleus is aligned by the detected first decay, which feeds the level, and the angular distribution of the second decay, depopulating the level, is measured. The distribution experiments involves the nucleus aligned in a reaction. TDPAC is the most applied technique of these two, for TDPAD experiments require a pulsed beam to define the time of creation of the level, while TDPAC uses the populating decay as time reference point. University of Alberta has a pulsed beam with a width of 1 ns and the level of interest is not populated by a long-lived parent, TDPAD was the way to perform these experiments.

Since the frequency is a product of two unknown quantities, i.e. q and Q , the results of one measurement don't yield definite values for both quantities. By looking at the behaviour at various temperatures or in different hosts or compare the value of the frequency with those of other ions in the same host, one is able to obtain more information about the various contributions to the field gradient, i.e. the lattice part, the local part and radiation damage. The other possibility to calculate one value and deduce the other is up to the present, in most cases, impossible.

Three sets of measurements were carried out. The first concerned the interaction of ^{70}Ga in a metallic Zn

target. In the study of the spin and parities of levels in the isotope ^{70}Ga there appeared a discrepancy between the data obtained from particle work and the γ ray anisotropy of the 879 keV level (Do72). Since this level has a half-life of 23 ns, and the Zn target used in the γ ray study is non-cubic there is the possibility of a perturbation of the anisotropy due to a quadrupole interaction. The other collaborators of the published paper (Hu75) had measured the time dependence of the anisotropy at room temperature. In order to estimate the effects of radiation damage the measurements were extended to investigate the temperature dependence of the interaction.

Two experiments in addition to the interaction of Ga in Zn, were begun. One was an attempt to measure the quadrupole interaction of ^{70}Ga in Ga metal, the other an experiment to compare the quadrupole interactions of ^{18}F (1121 keV level) and ^{19}F (197 keV, $Q = 0.11$ b). Both these experiments need only the final data-taking, but this was prevented by a major shutdown of the beam-line.

For the experiments various requirements were present, especially for the target chamber. The Ga in Zn experiment had no particular requirement for the room temperature run, but for the study of temperature dependence a hot target chamber was developed, which was capable of keeping the target at a well defined temperature as high as 600 K, did not produce background radiation and showed isotropic absorption.

The annihilation radiation of the decay of ^{18}F ($T_{1/2} = 110$ min.) produced so much background, that it was necessary to shield a part of this radiation from the detectors. This was done with the background suppressing target holder, which uses up to 5 targets in the same measurement. The Ga in Ga metal experiment required a cooling device, because the melting point of Ga is only 29.8°C and the purpose was to look at a solid target. It also required the use of a less efficient detector, for the yield of the reaction of interest was very high. The Low Energy Photon Spectrometer (LEPS) detector was used for this purpose.

All experiments were analyzed with the assumption that the interaction originated from a static electric field gradient. This assumption implies that the radiation damage either is negligible or is "frozen in" for a time long compared to the lifetime of the level of interest. This was justified by the measurements of Bleck et al. (Bl72) and McDonald et al. (Mc72). But the results of this work indicate that the field gradient experienced by the nuclei is probably not static for all nuclei.

CHAPTER 11

THEORY OF QUADRUPOLE INTERACTION

11.1 Angular Distributions

In the derivations we follow the sign conventions and definitions of Rose and Brink [Ro67] and Brink and Satchler [Br62].

A nuclear state with spin I , can be completely described with a density matrix ρ , whose matrix elements are defined by

$$\rho_{mm'} = \langle I m | \rho | I m' \rangle$$

One can expand the density-matrix in so-called statistical tensors ρ_Q^{λ}

$$\langle I m | \rho | I m' \rangle = \sum_{\lambda} \rho_Q^{\lambda} (I -m I m' | \lambda q) (-1)^{I-m} \quad (11.1)$$

or

$$\rho_Q^{\lambda} = \sum_m (-1)^{I-m} (I -m I m' | \lambda q) \langle I m | \rho | I m' \rangle \quad (11.2)$$

These statistical tensors behave under rotation over the Euler angles α, β, γ (Fig. 1) as

$$(\rho')_{Q'}^{\lambda} = \sum_Q \rho_Q^{\lambda} D_{QQ'}^{\lambda}(\alpha\beta\gamma) \quad (11.3)$$

where $D_{qq'}^\lambda(\alpha\beta\gamma)$ is the rotation matrix.

When we look at systems with cylindrical symmetry around the Z-axis a rotation around the z-axis will not change the density matrix. Such a rotation is $\alpha \neq 0$, $\beta = 0$, $\gamma = 0$ and $D_{qq'}^\lambda(\alpha, 0, 0) = e^{-iq\alpha} \delta_{qq'}$,

and

$$\begin{aligned} (\rho')_{q'}^\lambda &= \sum_q e^{-iq\alpha} \delta_{qq'} \rho_q^\lambda \\ &= e^{-iq'\alpha} \rho_{q'}^\lambda \delta_{qq'} \end{aligned}$$

But $(\rho')_q^\lambda = \rho_q^\lambda$

which means that only the terms with $q = 0$ do not disappear.

The remaining terms are simply related to the alignment parameters $B_\lambda(I)$ as defined by Ro67 by

$$\rho_0^\lambda(I) = \frac{1}{(2I+1)^{\frac{1}{2}}} B_\lambda(I) \quad (\text{II.4})$$

When a state as described above decays with a γ - ray to a state with spin I_2 we have an angular distribution as derived in Ro67

$$W(\theta) = \sum_{k \text{ even}} B_k(I_1) R_k(I_1 I_2) P_k(\cos \theta), \quad (\text{II.5})$$

where $P_k(\cos \theta)$ is the Legendre polynomial in the cosine of the angle with the z-axis.

$R_k(I_1 I_2)$ transition dependent parameter.

$$R_k(I_1 I_2) = \sum_{(L\pi)(L'\pi')} \frac{\{R_k(LL'I_1 I_2) \delta_L^{<\pi>} \delta_{L'}^{<\pi'>}\}}{\sum_L |\delta_L^{<\pi>}|^2} \quad (II.6)$$

$R_k(LL'I_1 I_2)$ is a product of Clebsch-Gordan and Racah coefficients (see formula 3.31 of Ro67).

L and L' are the allowed multipolarities of the decay and $<\pi>$ indicate an Electric or Magnetic transition.

$\delta^{<\pi>}$ is the so-called mixing-ratio defined by

$$\delta_L^{<\pi>} = \frac{\langle I_1 || T_L^{<\pi>} || I_2 \rangle / (2L + 1)}{\langle I_1 || T_{\bar{L}}^{<\pi>} || I_2 \rangle / (2\bar{L} + 1)} \quad (II.7)$$

where $T_L^{<\pi>}$ is the transition-operator for the $L^{<\pi>}$ transition and \bar{L} the lowest-order multipolarity in the transition. The angular distribution of the second γ -ray from the state with spin I_2 to the state with spin I_3 is given by

$$W(\theta) = \sum_k B_k(I) R_k(I_2 I_3) U_k(I_1 I_2) P_k(\cos \theta) \quad (II.8)$$

with $U_k(I_1 I_2) = \sum_{L_{12}} (\delta_{L_{12}})^2 U_k(L_{12} I_1 I_2) / \sum (\delta_{L_{12}})^2$

$$U_k(L_{12} I_1 I_2) = (-1)^k \frac{W(I_1 I_1 I_2 I_2; k L_{12})}{W(I_1 I_1 I_2 I_2; 0 L_{12})}, \quad (II.9)$$

where W is the Racah coefficient and

L_{12} is the multipolarity of the γ -decay from I_1 to I_2 . Usually and also here we take only mixing between two multipolarities, for the transition probability becomes negligibly smaller with higher multipolarity.

Formula II.8 is only valid if the state with spin I_2 is unperturbed, i.e. the lifetime is short compared to the time in which an interaction can disturb the density matrix.

For practical purposes the angular distributions are described by

$$W(\theta) = A_0 \sum_{k \text{ even}} a_k P_k(\cos \theta) \quad (\text{II.10})$$

where

$$a_k = \frac{B_k U_k R_k}{B_0 U_0 R_0} \quad (\text{II.11})$$

($U_k = 1$ when we observe the first decay and R_k is the value for the observed decay).

When level 1 is perturbed, i.e. has a time-dependent density matrix, we end up with a time-dependent angular distribution for both decays.

$$\begin{aligned} W(\theta) &= A_0 \sum_k a_k(t) P_k(\cos \theta) \\ &= \sum_k B_k(I, t) U_k R_k P_k(\cos \theta) \\ &= \sum_k B_k(I, 0) U_k R_k P_k(\cos \theta) G_k(t) \\ &= A_0 \sum_k a_k G_k(t) U_k R_k P_k(\cos \theta) \end{aligned} \quad (\text{II.12})$$

Where $G_k(t) \equiv \frac{a_k(t)}{a_0(0)}$

From this we see that the second decay, for which in general $U_k \neq 1$, has the same time-dependence as the first decay, only

the unperturbed value $a_k(0)$ will be different.

II.2 Perturbed Angular Distribution

The expression for $G_k(t)$ can be evaluated for any case with a known interaction-Hamiltonian, which is time-dependent in one system. From (II.2) and (II.4) follows

$$G_k(t) = \frac{a_k(t)}{a_k(0)} = \frac{B_k(I,t)}{B_k(I,0)} = \frac{\rho^k(t)}{\rho^k(0)} \quad (\text{II.13})$$

In solving the expression for G we have to work in three coordinate systems:

(a) The laboratory system, which is defined by the plane of detection. In this system, $a_k(0)$ and $G_k(t)$ are defined.

(b) The "creation" system. In this system we know the density matrix as formed by the beam and subsequent reaction, or any other method.

(c) The crystal system, which gives us the interaction-Hamiltonian, defined by an externally applied field or hyperfine fields.

To calculate $G_k(t)$ we follow the following procedure:

- (1) Transform $\rho_q^\lambda(t)$ from the laboratory system to the crystal system.
- (2) Form the density matrix in the crystal system.
- (3) Calculate the time-dependence in this system of the density matrix as function of the density matrix at time zero.

(4) Expand the time zero density matrix in statistical tensors.

(5) Transform back to the laboratory system and we end up with

$$\rho_q^\lambda(t) = \sum_{q'\lambda'} G_{qq'}^{\lambda\lambda'}(t) \rho_{q'}^{\lambda'}(0).$$

The time-dependence of the density matrix is given by the equation of motion.

$$i\hbar\rho(t) = [H, \rho]$$

We consider only time-independent Hamiltonians so

$$\rho(t) = e^{-iHt/\hbar} \rho(0) e^{iHt/\hbar} \quad (\text{II.14})$$

We also use the formulas II.1,2,3.

$$\begin{aligned} \rho_{q'}^{\lambda'}(t) &= \sum_{q''} (\rho')_{q''}^{\lambda'}(t) D_{q''q'}^{\lambda'}(\Omega) \\ &= \sum_{q''m} (I=m \ I \ m' | \lambda' q'') (-1)^{\lambda' - I - m} \\ &\quad \langle I \ m | \rho'(t) | I \ m' \rangle D_{q''q'}^{\lambda'}(\Omega) \\ &= \sum_{q''m''m'} (I-m \ I \ m' | \lambda' q'') \\ &\quad (-1)^{\lambda' - I - m} D_{q''q'}^{\lambda'}(\Omega) \times \\ &\quad \times \langle I \ m | e^{-iHt/\hbar} | I \ m'' \rangle \langle I \ m'' | \rho'(0) | I \ m' \rangle \times \\ &\quad \times \langle I \ m' | e^{iHt/\hbar} | I \ m' \rangle \end{aligned}$$

$$\begin{aligned}
&= \sum_{q'' m m'' m'''} \lambda (I-m \ I \ m' \ | \ \lambda' \ q'') \times \\
&\quad \times (-1)^{\lambda-I-m} D_{q'' q'}^{\lambda'}(\Omega) \times \\
&\quad \times \langle I \ m | e^{-iHt/\hbar} | I \ m'' \rangle \langle I m''' | e^{iHt/\hbar} | I \ m' \rangle \times \\
&\quad \times (\rho')_{q''}^{\lambda'}(0) (I \ -m'' \ I \ m'' \ | \ \lambda \ q'') (-1)^{\lambda-I-m''} \\
&= \sum_{q'' m m'' m'''} \lambda (I-m \ I \ m' \ | \ \lambda' \ q'') (-1)^{\lambda+\lambda'-2I-m-m''} \times \\
&\quad \times \langle I \ m | e^{-iHt/\hbar} | I \ m'' \rangle \langle I \ m'' \ | \ e^{iHt/\hbar} | I \ m' \rangle \times \\
&\quad \times (I \ -m'' \ I \ m'' \ | \ \lambda \ q'') \rho_q^{\lambda}(0) D_{qq''}^{\lambda}(-\Omega) D_{q'' q'}^{\lambda'}(\Omega) \\
&\equiv \sum_{\lambda q} G_{qq'}^{\lambda\lambda'}(t, \Omega) \rho_q^{\lambda}(0) \tag{II.15}
\end{aligned}$$

This is the general expression for the perturbation coefficient due to a static Hamiltonian. It is applicable in all cases of geometry.

There are a couple of experimental conditions, which can reduce this expression to more workable formulae.

(a) The 'creation' system, in which ρ is cylindrically symmetric, coincides with the laboratory system. That means $\rho_q^{\lambda}(0) = 0$ for $q \neq 0$.

So

$$\rho_{q'}^{\lambda'}(t) = \sum_{\lambda} G_{0q'}^{\lambda\lambda'}(t) \rho_0^{\lambda}(0) \tag{II.16}$$

(b) A random orientation of the crystal systems with respect to the laboratory system, as encountered in microcrystalline samples. Then we can perform an integration over Ω .

$$\frac{1}{4\pi} \int D_{0q''}^{\lambda}(-\Omega) D_{q''q'}(\Omega) d\Omega =$$

$$\frac{1}{4\pi} \int D_{q''0}^{*\lambda}(\Omega) D_{q''q'}(\Omega) d\Omega = \frac{1}{2\lambda+1} \delta_{q''0} \delta_{q'0} \delta_{\lambda\lambda'}$$
(II.17)

Here we can integrate over two angles α and β , for γ may be taken zero and still we will describe the rotation. When we are averaging over the total solid angle the factor 4π drops out. Substitute (II.17) and (II.16) in (II.15)

$$\rho_0^{\lambda}(t) = \sum_{q'', mm''} (I -m I m' | \lambda q'') (-1)^{2\lambda - 2I - m - m''} \times$$

$$\times \langle I m | e^{-iHt/\hbar} | I m'' \rangle \langle I m'' | e^{iHt/\hbar} | I m' \rangle \times$$

$$(I -m'' I m'' | \lambda q'') \rho_0^{\lambda}(0) \frac{1}{2\lambda+1}$$
(II.18)

(c) The interaction Hamiltonian is diagonal in $|I m\rangle$

$$\langle I m | e^{-iHt/\hbar} | I m'' \rangle = e^{iHt/\hbar} \delta_{mm''}$$

This substituting in (II.18)

$$\begin{aligned}
 \rho_0^\lambda(t) &= \sum_{q', m} (I -m \ I \ m' | \lambda \ q'') (-1)^{2\lambda-2I-2m} e^{-iE_m t/\hbar} \times \\
 &\quad \times e^{iE_{m'} t/\hbar} (I -m \ I \ m' | \lambda \ q'') \rho_0^\lambda(0) \frac{1}{2\lambda+1} \\
 &= \sum_{q', m} (I -m \ I \ m' | \lambda \ q'')^2 \cos\{(E_m - E_{m'})t/\hbar\} \rho_0^\lambda(0)
 \end{aligned}
 \tag{II.19}$$

$(-1)^{2\lambda-2I-2m} = 1$ for the exponent is always even.

$(E_m - E_{m'}) = -(E_{m'} - E_m)$ so the sine functions will cancel each other and we are left with the cosines.

Formula (II.19) is the often derived formula useful for an axially symmetric quadrupole interaction, measured in a microcrystalline sample. For a magnetic field $(E_m - E_{m'})$ is a constant for the allowed transitions of $\Delta m = \pm 1$, and this will further reduce the expression.

For a Hamiltonian, which is not diagonal in the $|I m\rangle$ representation, we have to diagonalize it to a set of eigenvectors $|n\rangle$. The transformation from $|I m\rangle$ to $|n\rangle$ is described by the transformation matrix U . U is unitary and $U^{-1}U = 1$.

$$\sum_{mm'} \langle m | H | m' \rangle =$$

$$\sum_{mm'} \langle m | U^{-1} U H U^{-1} U | m' \rangle =$$

$$\sum_{m'' m'''} \langle m'' | n \rangle \langle m''' | m'' \rangle \langle n | H | n' \rangle \langle m'' | m''' \rangle \langle n' | m' \rangle =$$

$$\sum_{mm'n} U_{mn} E_n \delta_{nn'} U_{n'm'}^{-1} =$$

$$\sum_{mm'n} U_{mn} E_n \delta_{nn'} U_{m'n}^*$$

Use in (II.18)

$$\begin{aligned} \rho_0^\lambda(t) = & \sum_{q''mm''nn'} (I -m I m' | \lambda q'') (-1)^{2\lambda - 2I - m - m''} \times \\ & \times U_{mn} U_{m''n}^* e^{-iE_n t/h} U_{m''n'} U_{m'n'}^* e^{iE_{n'} t/h} \times \\ & \times (I -m'' I m'' | \lambda q'') \rho_0^\lambda(0) \frac{1}{2\lambda + 1} \end{aligned} \quad (\text{II.20})$$

This is the formula for the perturbed angular distribution for a non-axially symmetric Hamiltonian, from a cylindrically symmetric state at time zero in a microcrystalline sample. As is evident the perturbation factor $G(t) = \rho(t)/\rho(0)$ is only dependent on the multipolarity of the γ -decay and the Hamiltonian.

II.3 The Hamiltonian for Quadrupole Interaction

The electrostatic Hamiltonian of a charge distribution in an external field is (De53)

$$H_{el} = \int \rho(\vec{x}) V(\vec{x}) d^3x$$

Where $\rho(\vec{x})$ the local charge density is.

A Taylor expansion of the potential about the origin is

$$V(x) = V(0) + \vec{x} \cdot \vec{\nabla} V(0) + \frac{1}{2} \sum_i \sum_j \frac{\partial^2 V}{\partial x_i \partial x_j} (0) x_i x_j + \dots$$

$$\begin{aligned}
\text{So } H_{el} &= \int \rho(\vec{x}) V(0) d^3x + \\
&+ \int \rho(\vec{x}) \vec{x} \cdot \vec{\nabla} V(0) d^3x + \\
&+ \int \rho(\vec{x}) \sum_{ij} x_i x_j \frac{\partial^2 V}{\partial x_i \partial x_j} (0) d^3x + \dots
\end{aligned}
\tag{II.21}$$

The first term is the energy of the nucleus in its surroundings and not important for this problem. The second term vanishes because the nucleus is in a minimum of the potential so $\vec{\nabla} V = 0$. The third term is the quadrupole interaction, the higher order terms are neglected. We can write the quadrupole interaction as

$$H = \frac{1}{2} \sum_{ij} T_{ij}^{(2)} V_{ij}^{(2)} \tag{II.22}$$

where $T^{(2)}$ is the second-rank tensor, the quadrupole moment tensor, and $T_{ij} = \int \rho(\vec{x}) x_i x_j d^3x$ and $V_{ji}^{(2)} = \frac{\partial^2 V}{\partial x_i \partial x_j} (0)$ is the component of the field gradient tensor.

It is always possible to make the field gradient tensor diagonal by a suitable choice of the coordinate system. Furthermore the Laplace equation is valid for V describes only the external field.

$$V_{xx} + V_{yy} + V_{zz} = 0 \tag{II.23}$$

By defining the axis properly the usual condition is

$$|V_{zz}| \geq |V_{yy}| \geq |V_{xx}| \tag{II.24}$$

$$\text{Define } \eta = (V_{xx} - V_{yy})/V_{zz} \quad (\text{II.25})$$

From (II.23) and (II.24) it follows that $0 \leq \eta \leq 1$. In this way the field gradient is described by V_{zz} and η and the orientation of the coordinate system.

$T^{(2)}$ and $V^{(2)}$ can be expanded in spherical tensors

$$T^{(2)} = \sum_{q=-2}^{+2} T_q^2 \quad \text{and}$$

$$V^{(2)} = \sum_q V_q^2.$$

$$\text{So} \quad H = \frac{1}{2} \sum_q T_q^2 V_{-q}^2.$$

For a diagonal field tensor

$$V_{\pm 1}^2 = 0$$

$$V_0^2 = V_{zz} \quad (\text{II.26})$$

$$V_{\pm 2}^2 = \frac{1}{\sqrt{6}} (V_{xx} - V_{yy}) = \frac{1}{\sqrt{6}} \eta V_{zz}$$

$$\langle I \ m | H | I \ m' \rangle =$$

$$\langle I \ m | \frac{1}{2} \sum_q T_q^2 V_{-q}^2 | I \ m' \rangle =$$

$$\frac{1}{2} \sum_q V_{-q}^2 \langle I \ m | T_q^2 | I \ m' \rangle =$$

$$\frac{1}{2} \sum_q (-1)^4 \langle I || T^{(2)} || I \rangle V_{-q}^2 (I \ m' \ 2 \ q | I \ m)$$

The quadrupole moment of the nucleus is defined as

$$eQ \equiv \int \rho_n (r^2 - z^2) d^3x$$

$$= 2 \int \rho_n x^2 d^3x$$

$$= 2 \langle II | T_0^2 | II \rangle$$

$$= 2 (-1)^4 (I \ I \ 2 \ 0 | I \ I) \langle I || T^{(2)} || I \rangle$$

So $\langle I \ m | H | I \ m' \rangle =$

$$\frac{1}{4} \sum_q eQ (I \ m' \ 2 \ q | I \ m) (I \ I \ 2 \ 0 | I \ I)^{-1} V_{-q}^2$$

Calculate the Clebsch-Gordan coefficients and substitute the values for the components of V

$$q = 0 \quad \langle I \ m | H | I \ m' \rangle = (3m^2 - I(I+1)) \frac{eQ}{4I(2I-1)} V_{zz} \delta_{mm'}$$

$$q = \pm 1 \quad \langle I \ m | H | I \ m' \rangle = 0 \quad (II.27)$$

$$q = \pm 2 \quad \langle I \ m | H | I \ m \mp 2 \rangle =$$

$$\{(I \mp m - 1)(I \mp m)(I \pm m + 1)(I \pm m + 2)\}^{\frac{1}{2}} \frac{eQ}{4I(2I-1)} \frac{\eta}{\sqrt{6}} V_{zz}$$

These values are also derived by Matthias, Schneider and Steffen (Ma62 and Ma63) using the expansion of the Coulomb potential in spherical harmonics. It should be noted that the definitions in this reference for both T and V differ a constant factor from the definition used above.

CHAPTER III

EQUIPMENT

Beam

We used the 7 MeV Van de Graaff accelerator of the University of Alberta, with a pulsed beam of 1 ns width with a repetition rate of 1 MHz.

Detectors

As detectors we used 4 Ge(Li) detectors, 2 in each experiment, with volumes of 20.7, 23.0 and 27.4 cc and the LEPS detector. The three large detectors combine good energy resolution with good time resolution and a wide efficiency range. The LEPS detector (3 cc) is very good for low energies (less than 400 KeV) and less sensitive to higher energy γ -rays reducing the counting-rate by a large factor.

Electronics

We had two electronic setups, one for two time dependent measurements at one time and one for one timing and one monitor. The double timing had the drawback that the tuning was more complicated and that the sum boxes were not able to handle high counting rates. The single timing cost more time, but was easy to set up, and could handle high counting rates. The time-resolution of the system was typically 2.7 ns FWHM for 843 keV and 8.0 ns for 188 keV.

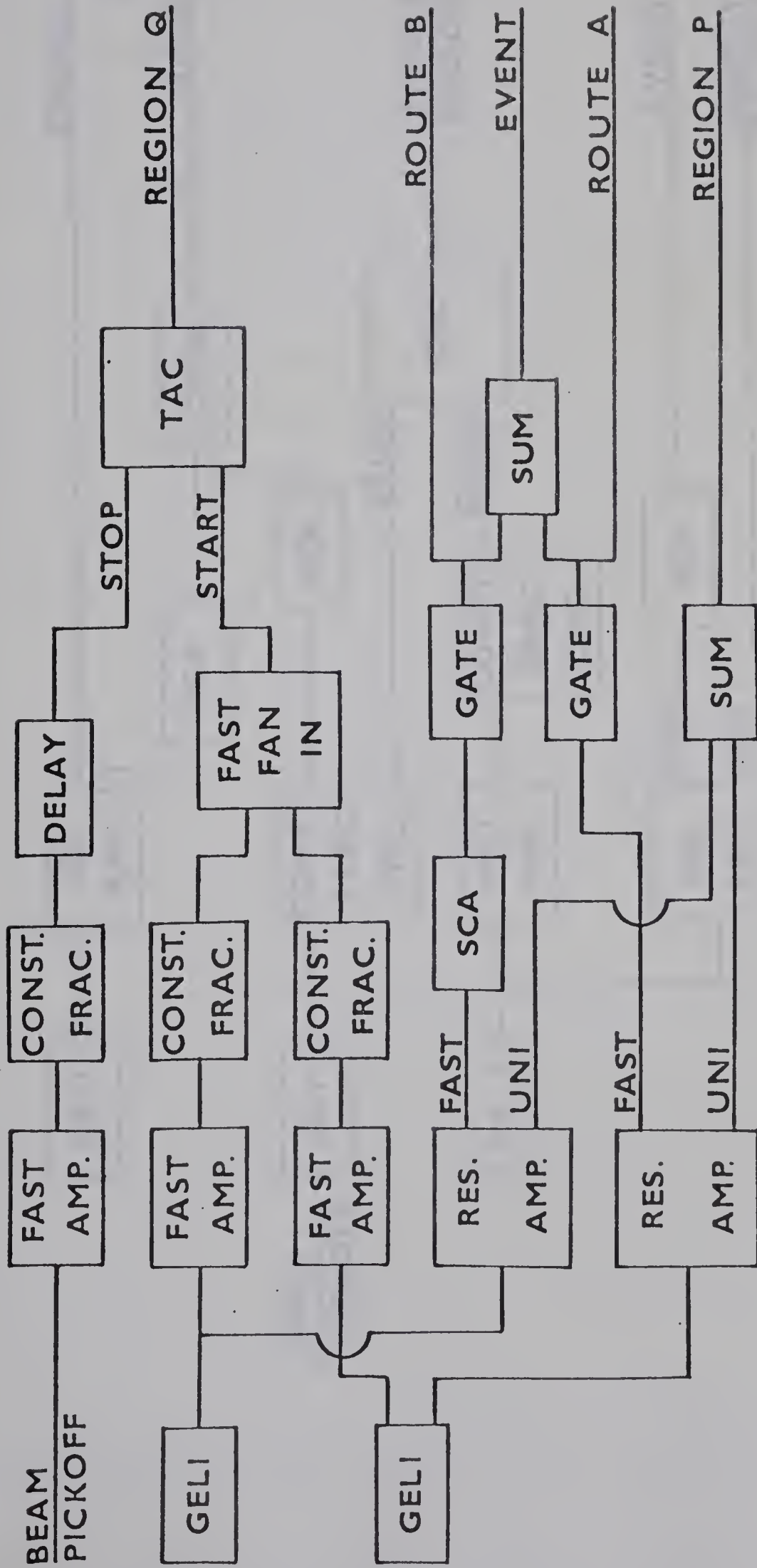


Fig 2: The electronic arrangement with two timing counters

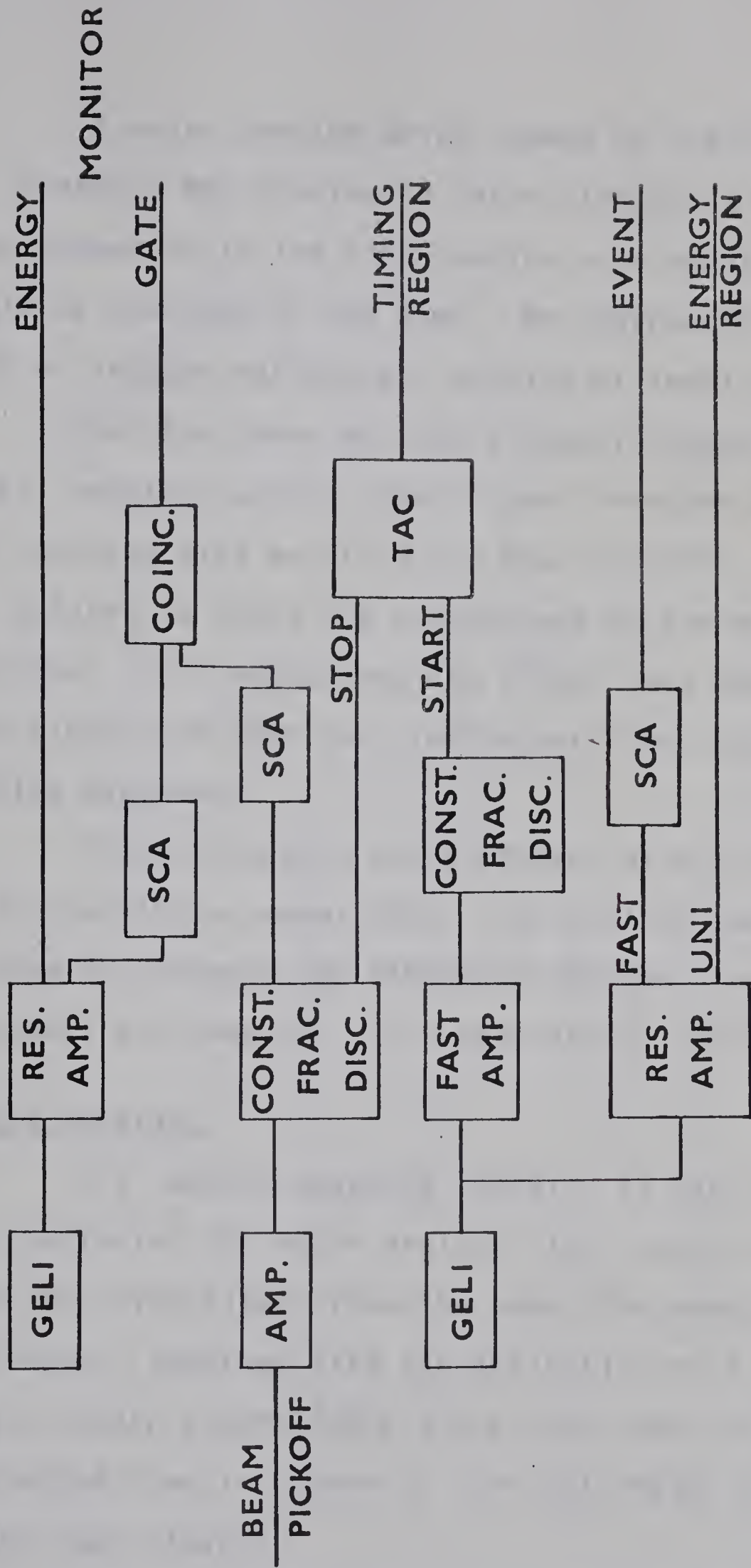


Fig 3: The electronic arrangement with the single timing counter and the monitor counter

A major problem which showed up was the appearance of 10 and 30 MHz ripples in phase with the 1 MHz beam pick-off. This showed up in the time spectra as a modulation of the yield as function of the time. We suppressed it partly with a 50 ns delayed reflection, gaining at least a factor 4.

For the timer we used a time-to-amplitude converter (TAC), supplied with a start-signal from the Ge(Li) detector. The stopping side was from the beam pick-off. This signal was delayed to place the prompt peak on the end of the spectrum. This set-up had the effect that there was always a stop-signal and that the time in our time spectrum was running backwards.

The calibration was performed with a commercial calibrator (Ortec model 462). For on-line sorting of data we used the program TWO PARAMETER SORTING, available on the Honeywell 516 computer. For description see Chapter IV.

Target Mounting

(1) Normal beamstop target. In the figure 4 are also indicated the other devices, i.e. pulse pick-off which gives the time-signal from the beam, the energy slits and the collimator, together with the definition of θ_Y . The other target holder assemblies replace that shown to the right of the dotted line in Figure 4. The collimator is not shown in the next figures

(2) Hot target chamber. For heating up experiments we designed a target chamber with a heating system and control

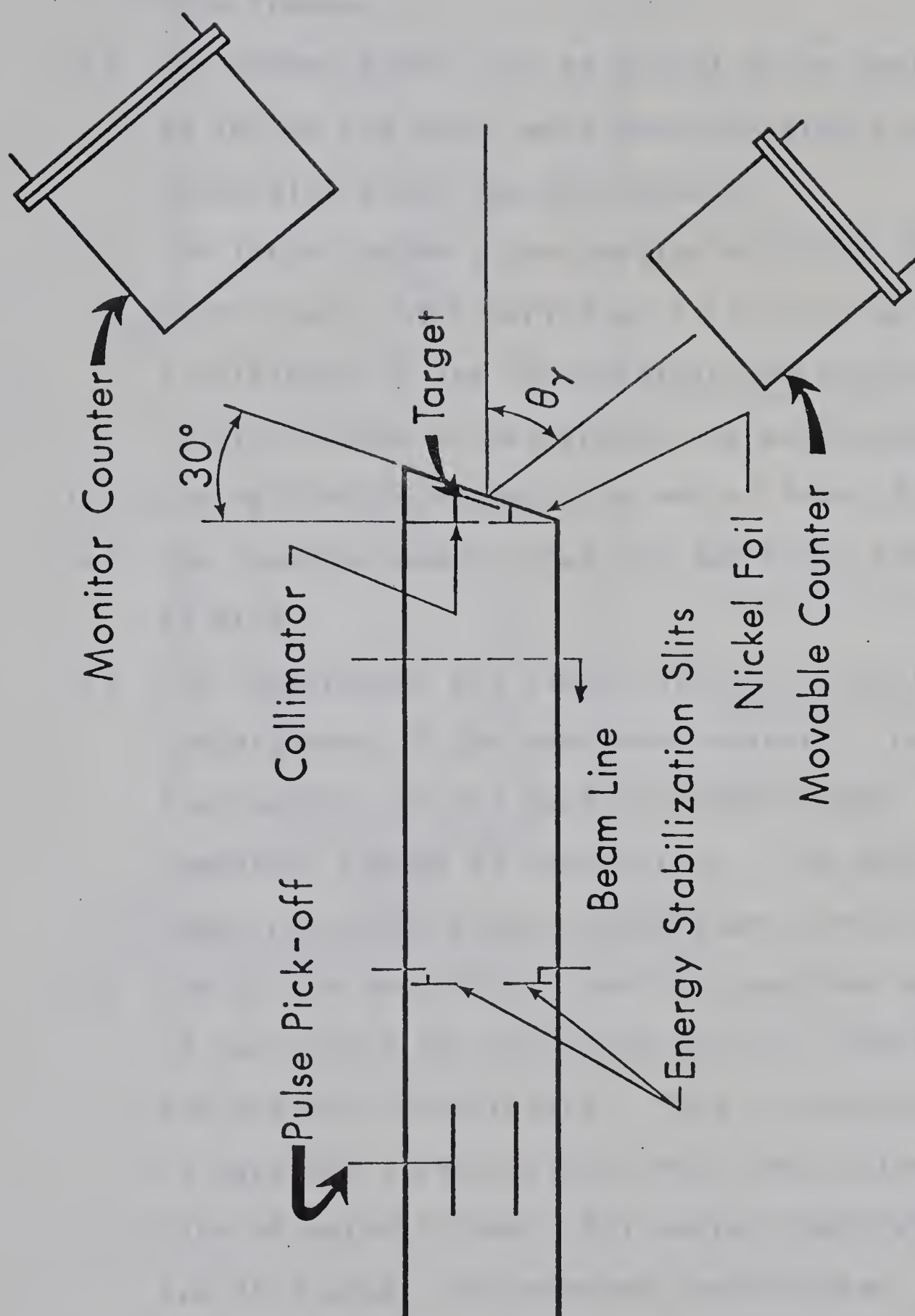


Fig 4: The normal beam stop target holder with surrounding devices

unit. After some trials this final set-up had these properties:

- (a) Ceramics were high temperature castable ceramics from Aramco.
- (b) The target holder can be placed at an angle up to 30° to the beam, made possible with a rotatable connection above the heating-wire.
- (c) The target holder, the heating wire and the nickel hat, which served as a Faraday cup and as a shielding of the surroundings, were electrically isolated to the ground and each other.
- (d) The obtainable temperature was at least 600 K.
- (e) The required power input for 560 K was approximately 35 Watt.
- (f) The temperature was stable within 0.1 K, for each temperature, if the beam was constant. Large fluctuations of the beam resulted in the temporary change in temperature. Too much power input resulted in large temperature variations.
- (g) Due to the heat input from the beam the temperature of the centre of the target was 70 - 100 K above the measured temperature. This is calculated in Appendix I and verified with the sublimation rate of natural zinc. All quoted temperatures are 85 K above the measured temperatures.
- (h) The thermocouple was a standard Fe/Constantan thermocouple. The results were interpreted with

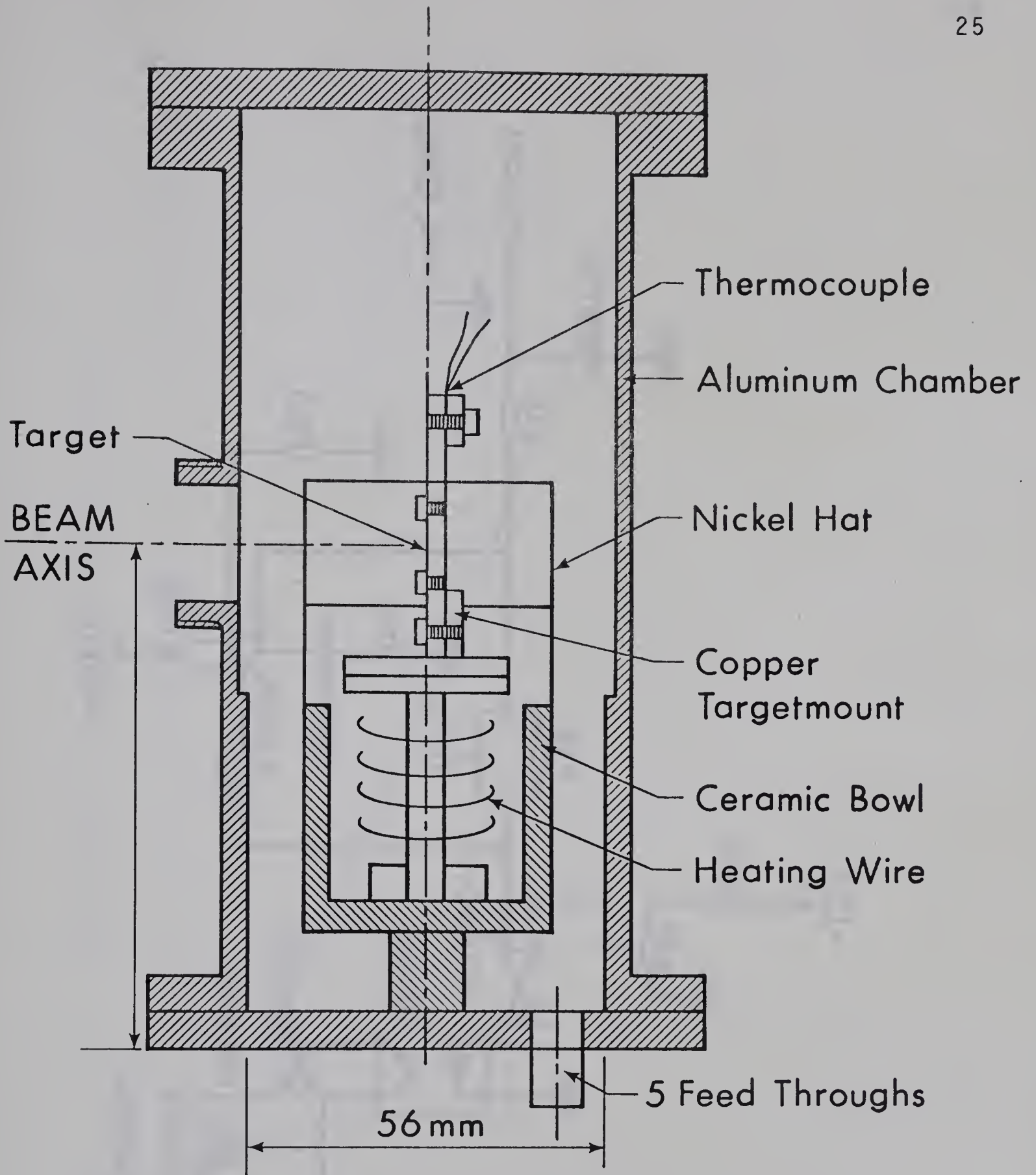


Fig 5: Hot target chamber. The 5 feedthroughs are for the heating-wire (2) the thermocouple (2) and the current collector

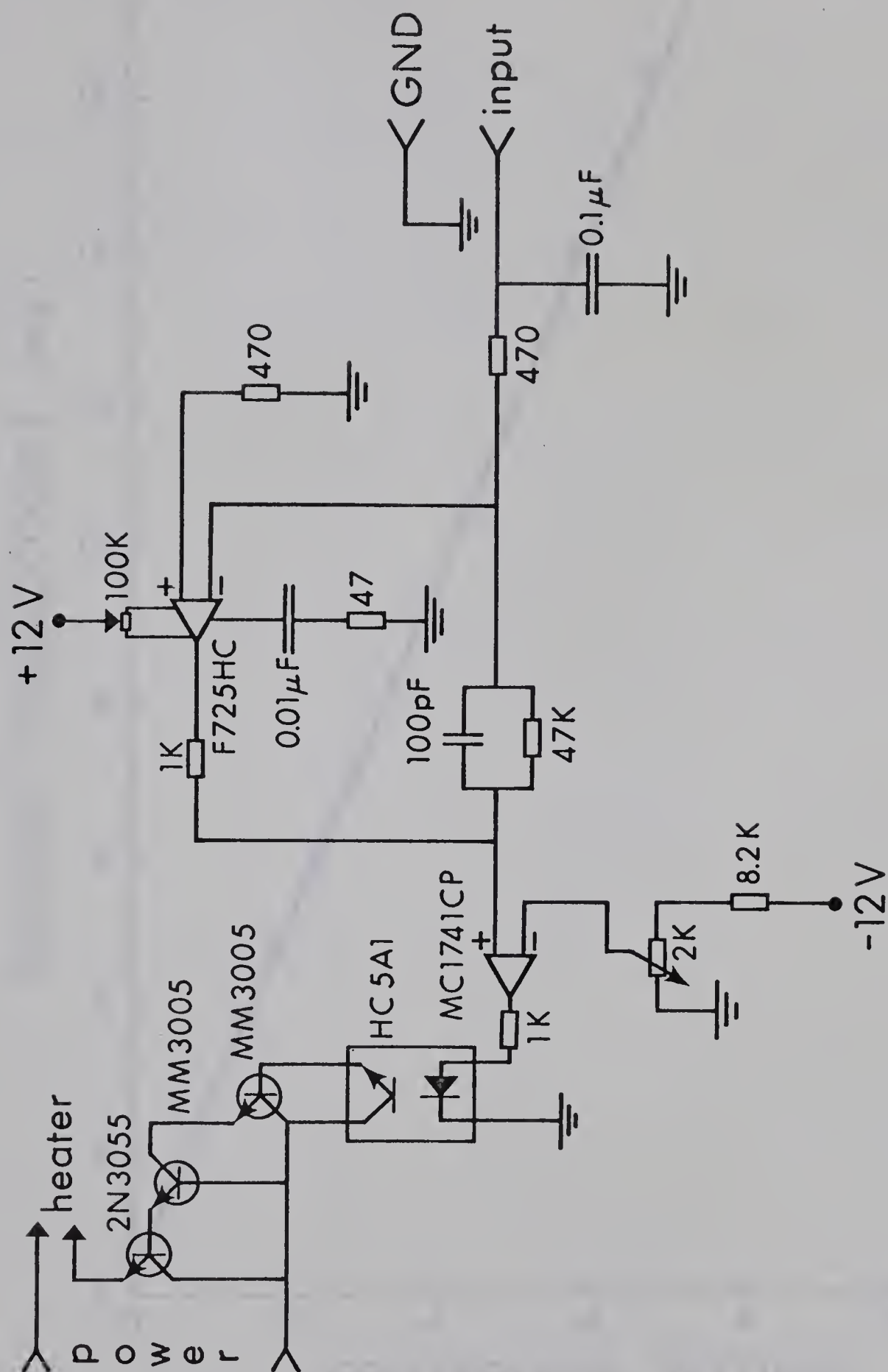


Fig 6: The control box circuit diagram. This circuit switches the power on or off if the reading of the thermocouple is lower or higher than required

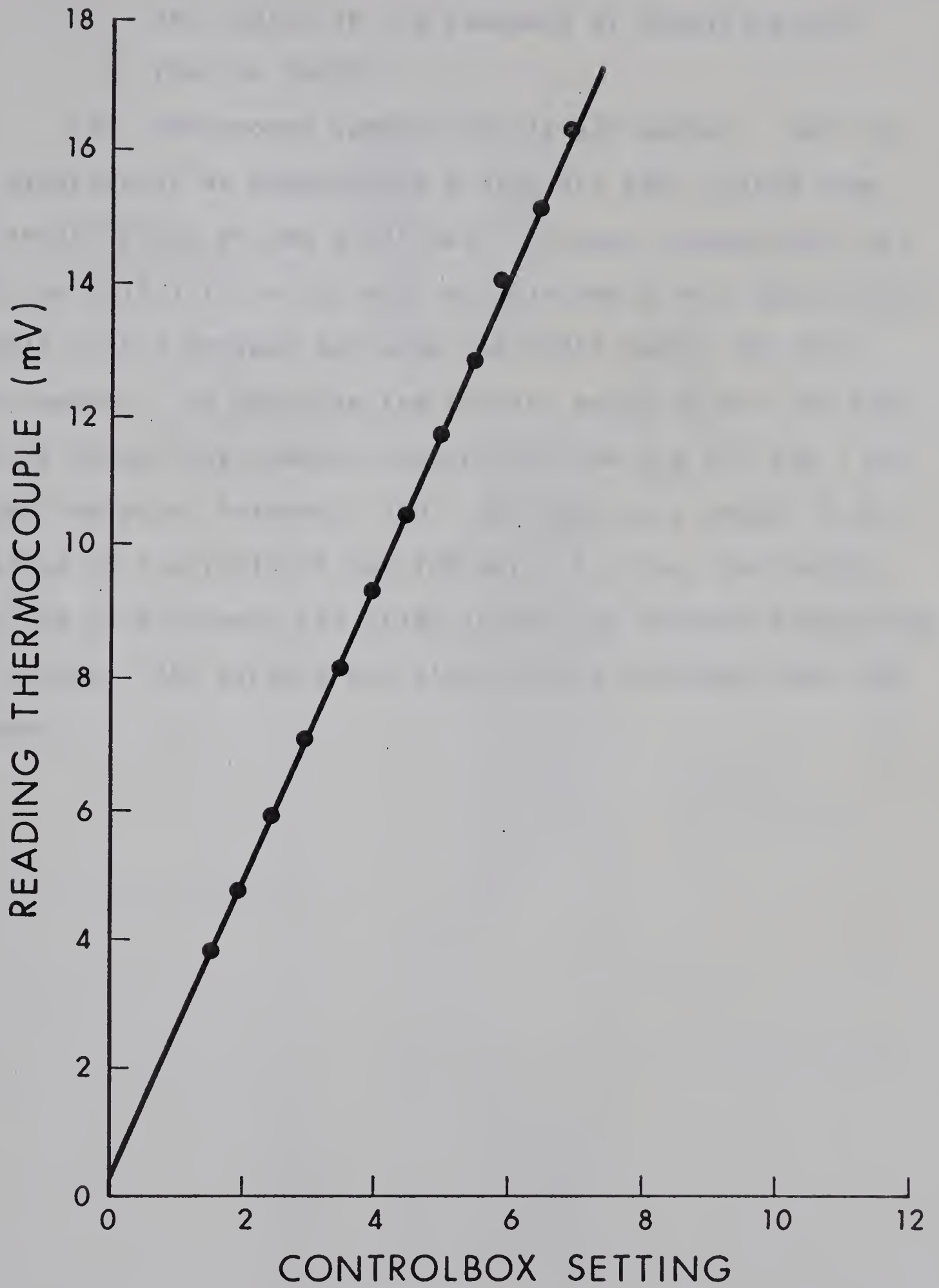


Fig 7: The calibration of the controlbox as function of the reading of the thermocouple

the tables in the Handbook of Chemistry and Physics (Ha72).

(3) Background suppressing target holder. For the ^{18}F experiments we encountered a high 511 keV γ -yield from the annihilation of the β^+ of the ^{18}F decay. Using the fact that the half-life is 110 min, we shielded in this set-up four targets with 2 cm lead and used the fifth target for the measurements. By changing the targets every 30 min. we were able to reduce the compton background from the 511 keV γ ray in the region of interest, 180 - 200 keV, by a factor 3 to 4 relative to the yield of the 188 keV ^{18}F γ ray. The ladder with the five targets can slide in and out without disrupting the vacuum. The targets are electrically isolated from the chamber.

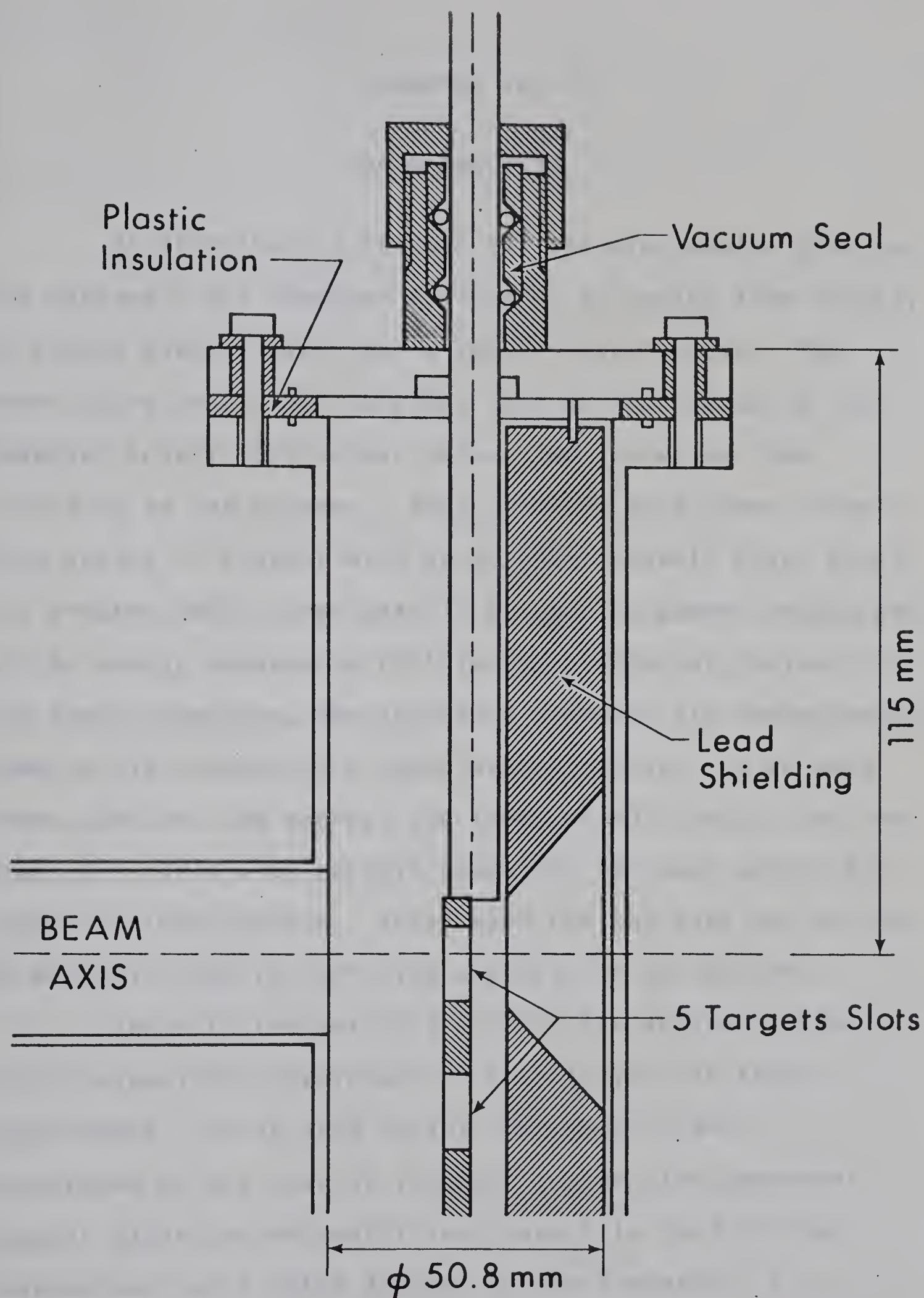


Fig. 8: The background suppressing target holder.

CHAPTER IV

DATA ANALYSIS

As described in Chapter III the electronics give to the Honeywell 516 computer 3 signals, an analog time-signal, an analog energy-signal and a logic 'event'-pulse. The event-pulse serves the purpose, that during the pulse the computer accepts both other pulses and processes them according to the program. ADC's convert both other signals from analog to digital with up to 4096 channels after which the program TWOP stores both in a separate memory region and if the energy happens to fall in one of the set regions in the energy spectrum, the so-called windows, its corresponding time is also stored in a third memory region. So we have three spectra, the energy, the times of all γ ray's and the times of γ ray's with certain energies, for each window one complete time-spectrum. After each run the data was written on magnetic tape for off-line analysis on the XDS 940.

The off-line analysis is with the program TDPAD (Lu75) especially developed for the analysis of these experiments. It is able to fit time spectra and background of the peak of interest to the time-dependent angular distribution coefficients and fits that to the theoretical curve which depends on the frequency, its relative spread, the spin, the asymmetry parameter η , the unperturbed value of a_2 and a_4 , the $A_0(t)$ and the interaction

frequency $\omega_q = (e^2 Qq)/\hbar$.

The TDPAD-program is essentially fitting to the formulae (II.11) and (II.20), using the Hamiltonian given by (II.27).

The perturbation-coefficient as described is

$$G_k(t) = \sum_N s_{kN} \cos(N\omega_q t) \quad (\text{IV.1})$$

For the axially-symmetric case N is integer, but deviates in general from integral values for $\eta \neq 0$. The s_{kN} are easily obtainable from (II.20),

$$N \equiv (E_n - E_{n'})/(\hbar\omega_q) \text{ and } \omega_q = (e^2 Qq)/\hbar.$$

Because all nuclei do not feel the same field gradient, due to slight displacements in the microcrystals, we have a relative frequency spread $\delta\omega$. We assume the Lorentzian frequency distribution given in (Ha73).

$$G'_k(t) = \sum_N s_{kN} e^{-N\omega_q \delta\omega t} \cos N\omega_q t \quad (\text{IV.2})$$

Both (IV.1) and (IV.2) are the theoretical curves for infinite time resolution. This is experimentally unobtainable, so we have to take into account the time resolution of the system. This is a Gaussian distribution and can be described by

$$G''_k(t) = \sum_N s_{kN} e^{-N\omega_q \delta\omega t} e^{(N\omega_q \tau)^2/2} (\cos N\omega_q t) \quad (\text{IV.3})$$

where τ is the time resolution.

The fit is to

$a_k(t) = a_k(0) G_k'(t) + c$, where c is a time-independent constant. $G_k(t)$ is calculated by numerically diagonalizing of the Hamiltonian.

The theoretical curves, as they are calculated with the formulas (IV.1), (IV.2) and (IV.3) are shown in the figures, for a couple of typical spins and spins of interest, with various asymmetry parameters, resolution times and frequency spreads.

In the literature ω_0 is often given instead of ω_q is noted. ω_0 is defined as the smallest energy-difference for an axially symmetric field

$$\omega_0 = \frac{3}{4I(2I-1)} \omega_q \quad \text{for integer spin}$$

$$\omega_0 = \frac{6}{4I(2I-1)} \omega_q \quad \text{for half-integer spin.}$$

We prefer to use ω_q for it is dependent only on the interaction parameters Q and q and not on the spin.

Figures 9 - 18:

The values of the $G_2(t)$ term as function of time for different values of spin, η , $\delta\omega$ and resolution time τ . Note that Fig. 9 is the $G_4(t)$ curve for spin 2. For all curves the first case is represented by the solid curve, the second by the dashed and the third by the dash dot line.

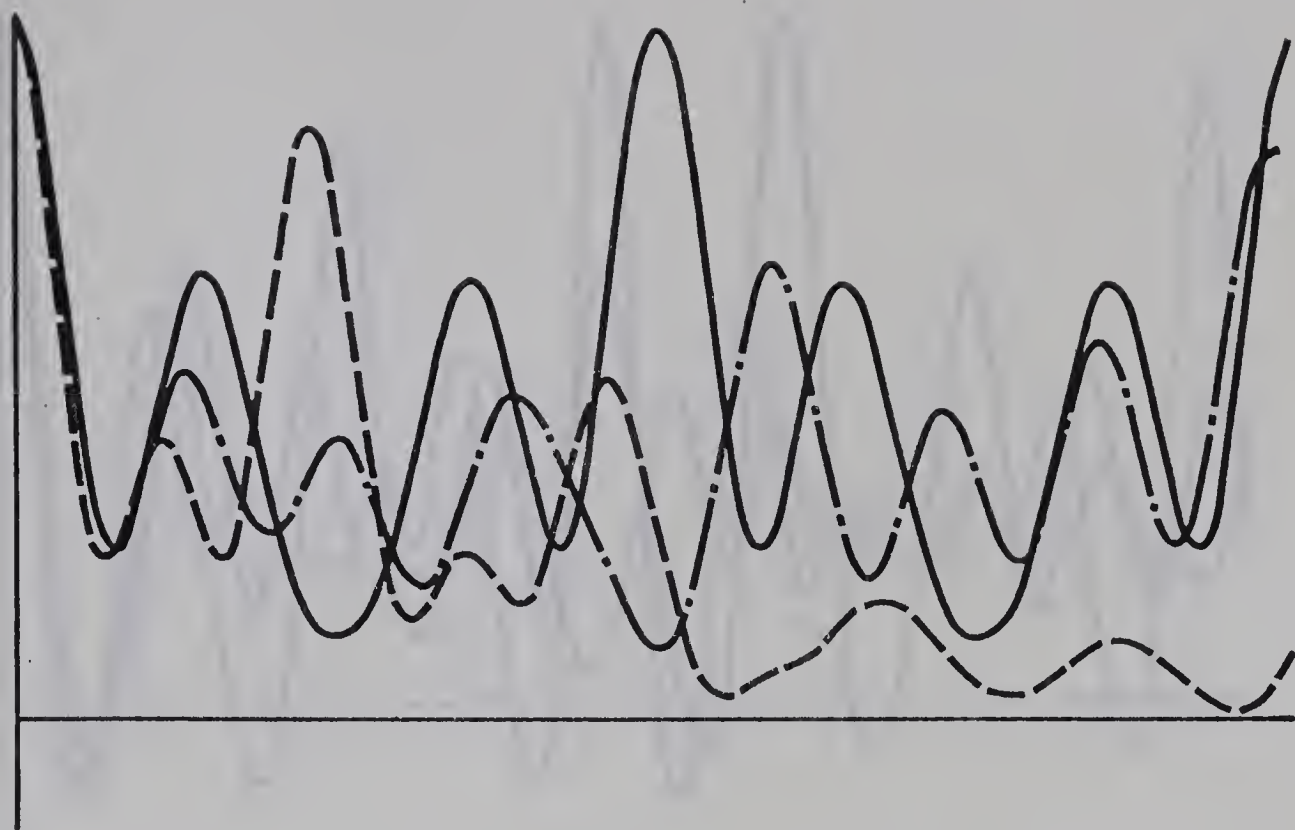


Fig 9: Spin = 2 $\eta = 0.0, 0.5, 1.0$ $\delta\omega = 0.0$ $\tau = 0.0$ The $G_4(t)$ term

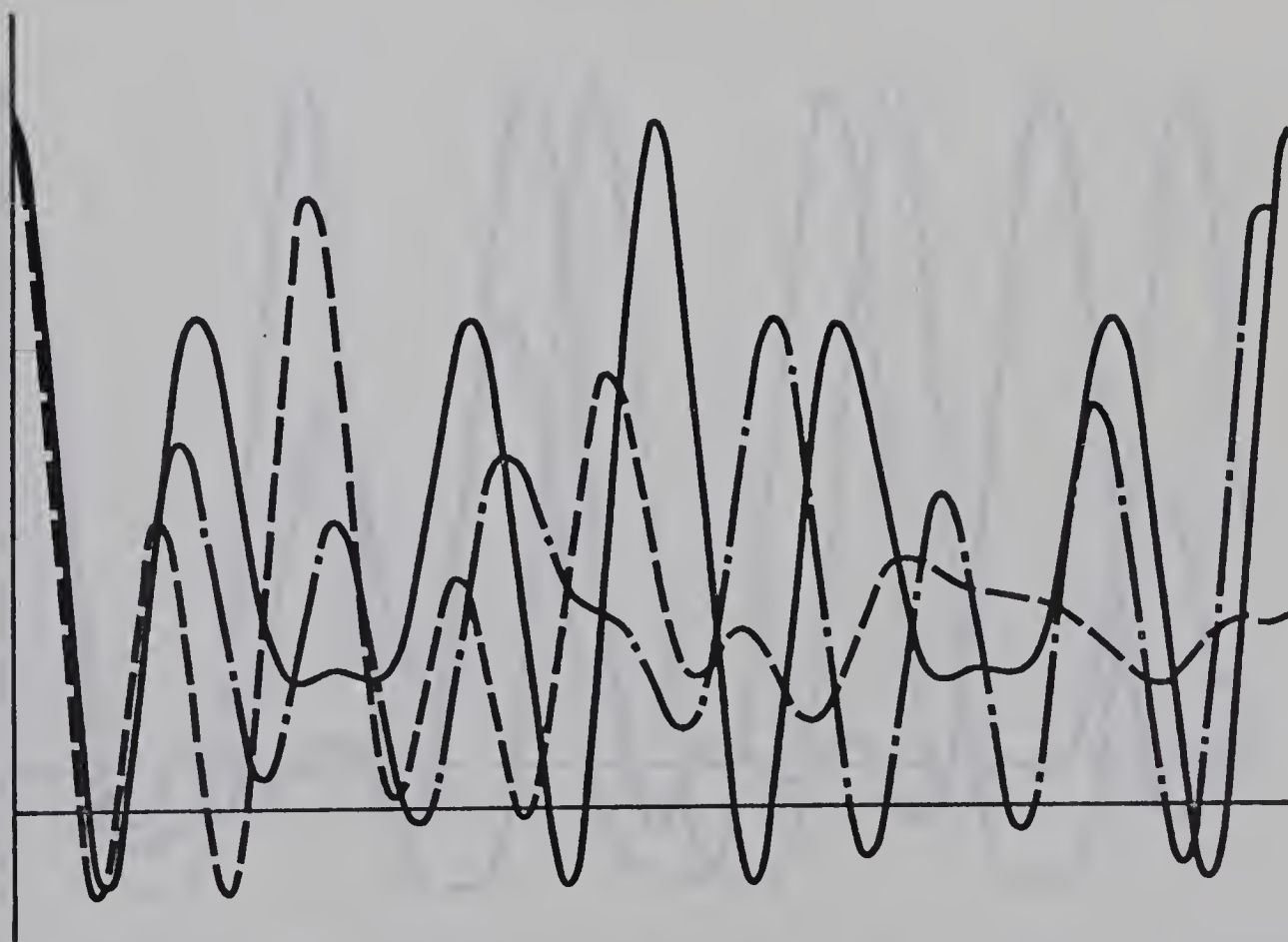


Fig 10: Spin 2 $\eta = 0.0, 0.5, 1.0$ $\delta\omega = 0.0$ $\tau = 0.0$ The $G_2(t)$ term

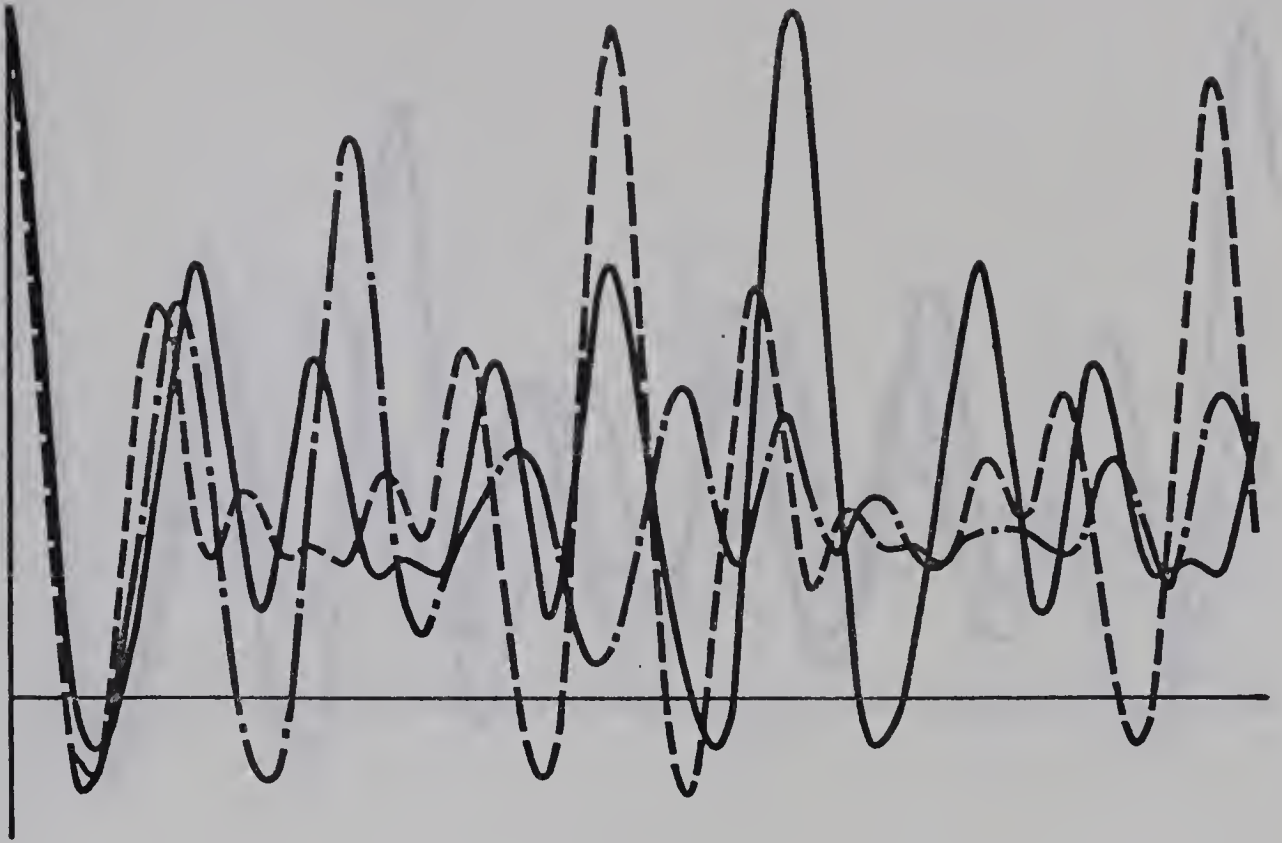


Fig. 11: Spin = 3 $\eta = 0.0, 0.5, 1.0$ $\delta\omega = 0.0$ $\tau = 0.0$

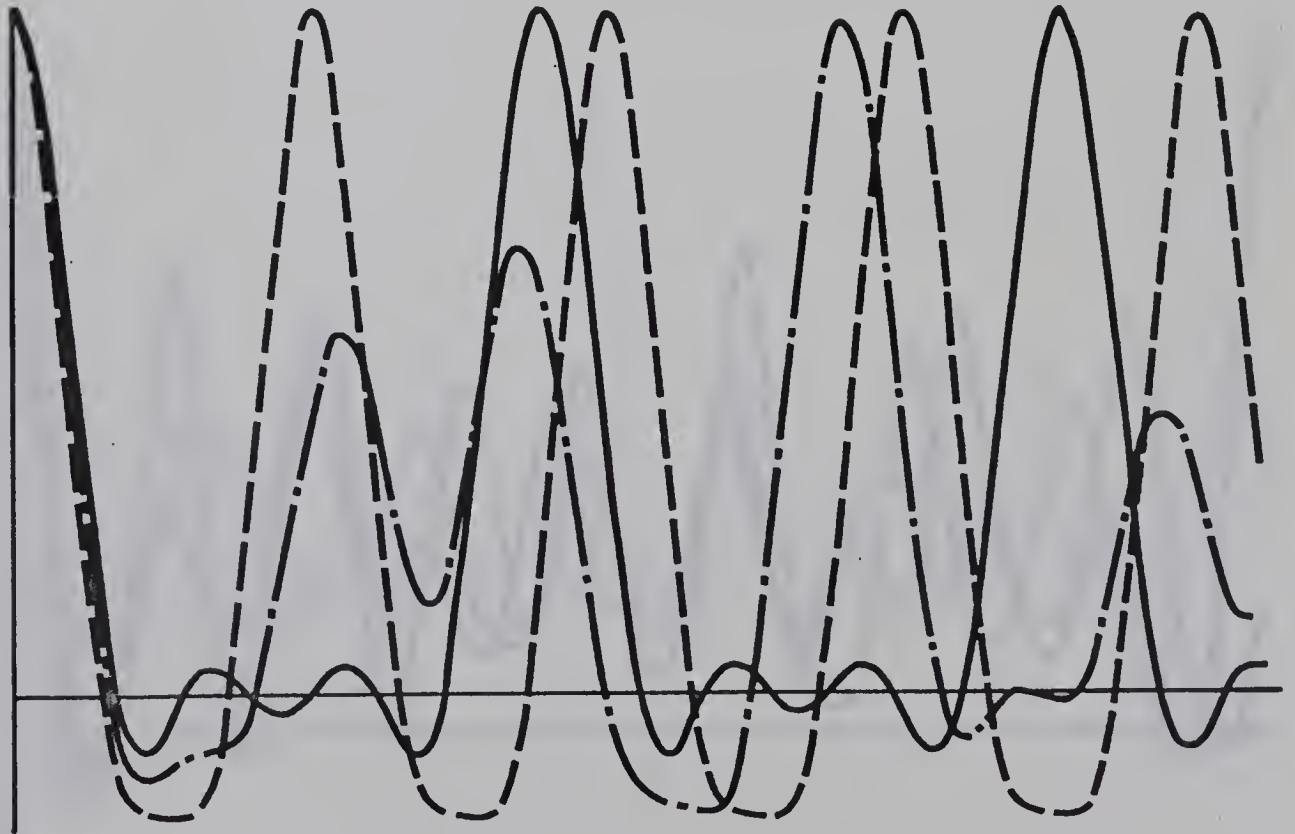


Fig. 12: Spin = 5/2 $\eta = 0.0, 0.5, 1.0$ $\delta\omega = 0.0$ $\tau = 0.0$

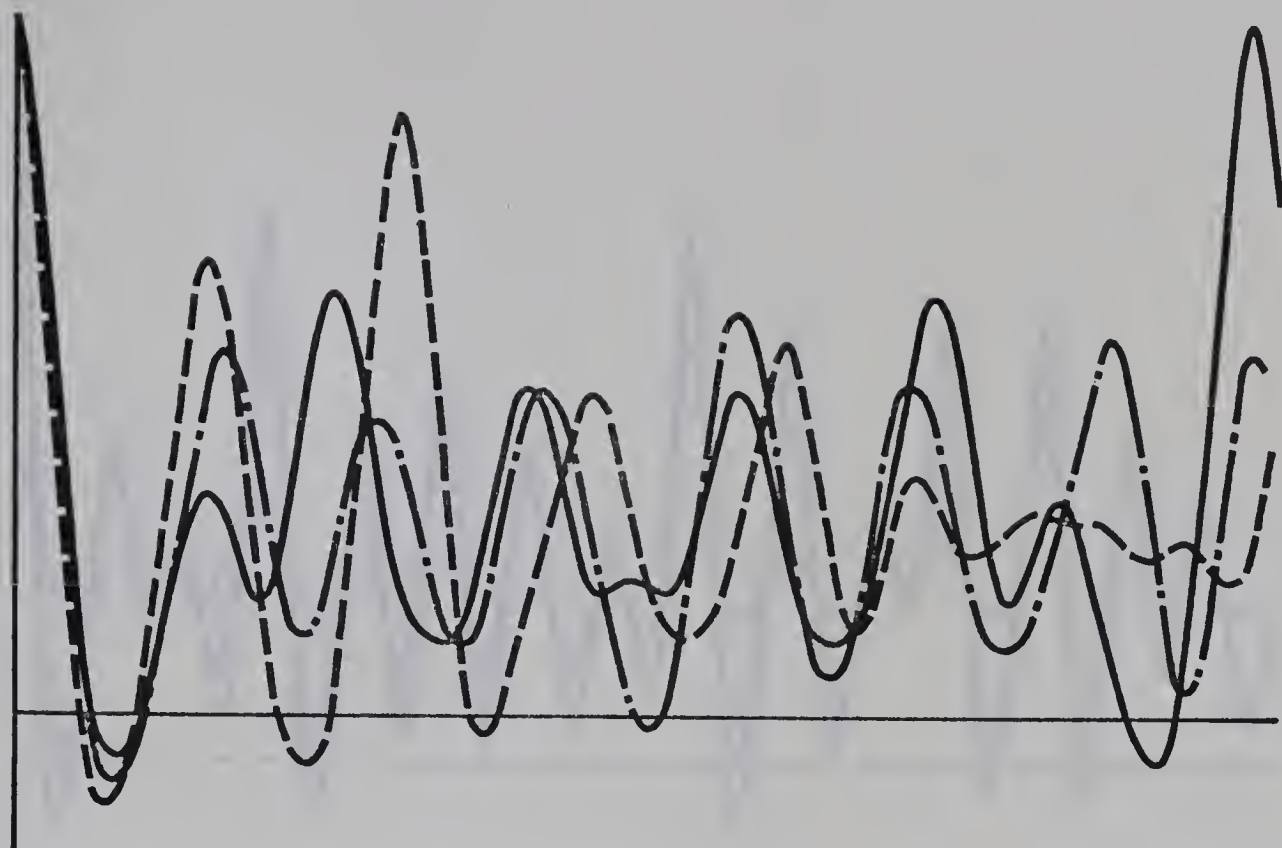


Fig 13: Spin = 4 $\eta = 0.0, 0.5, 1.0$ $\delta\omega = 0.0$ $\tau = 0.0$

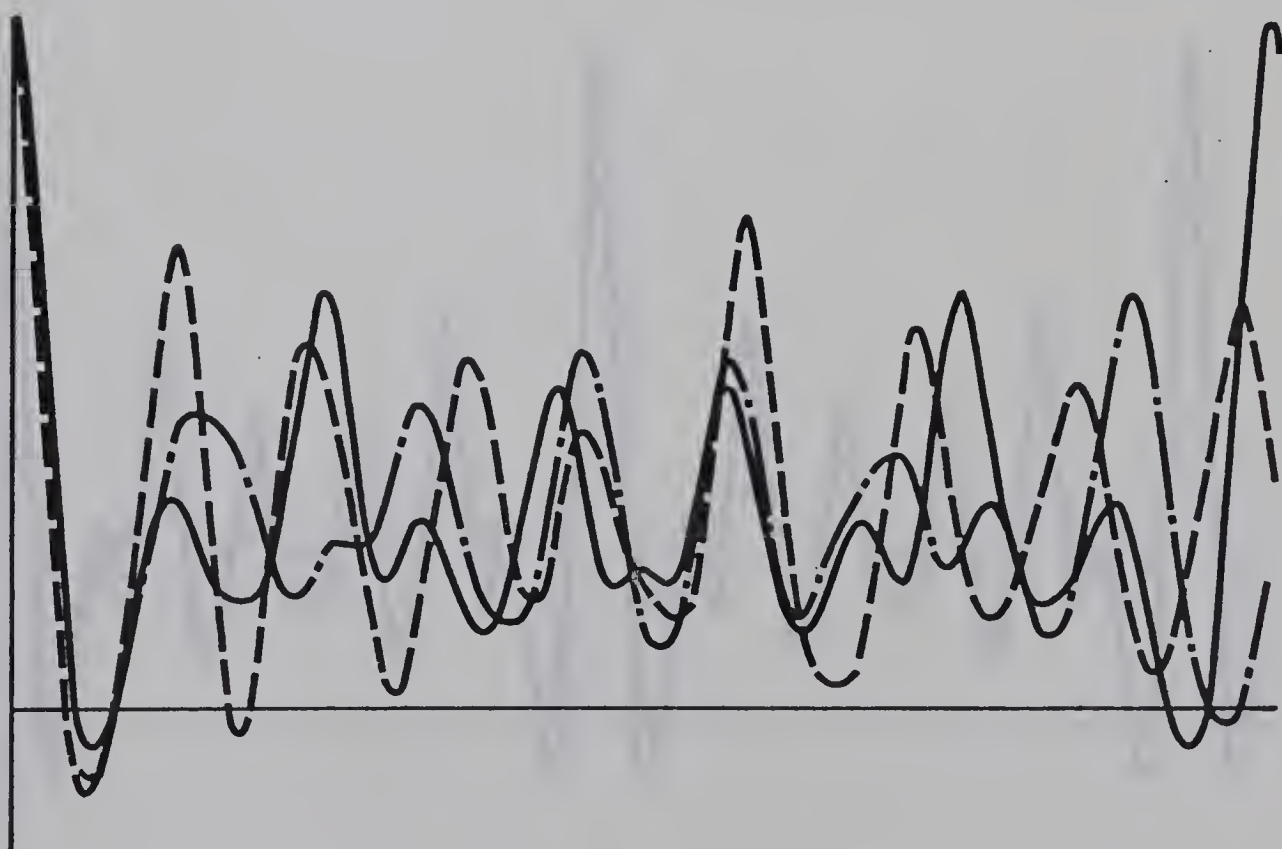


Fig 14: Spin = 5 $\eta = 0.0, 0.5, 1.0$ $\delta\omega = 0.0$ $\tau = 0.0$

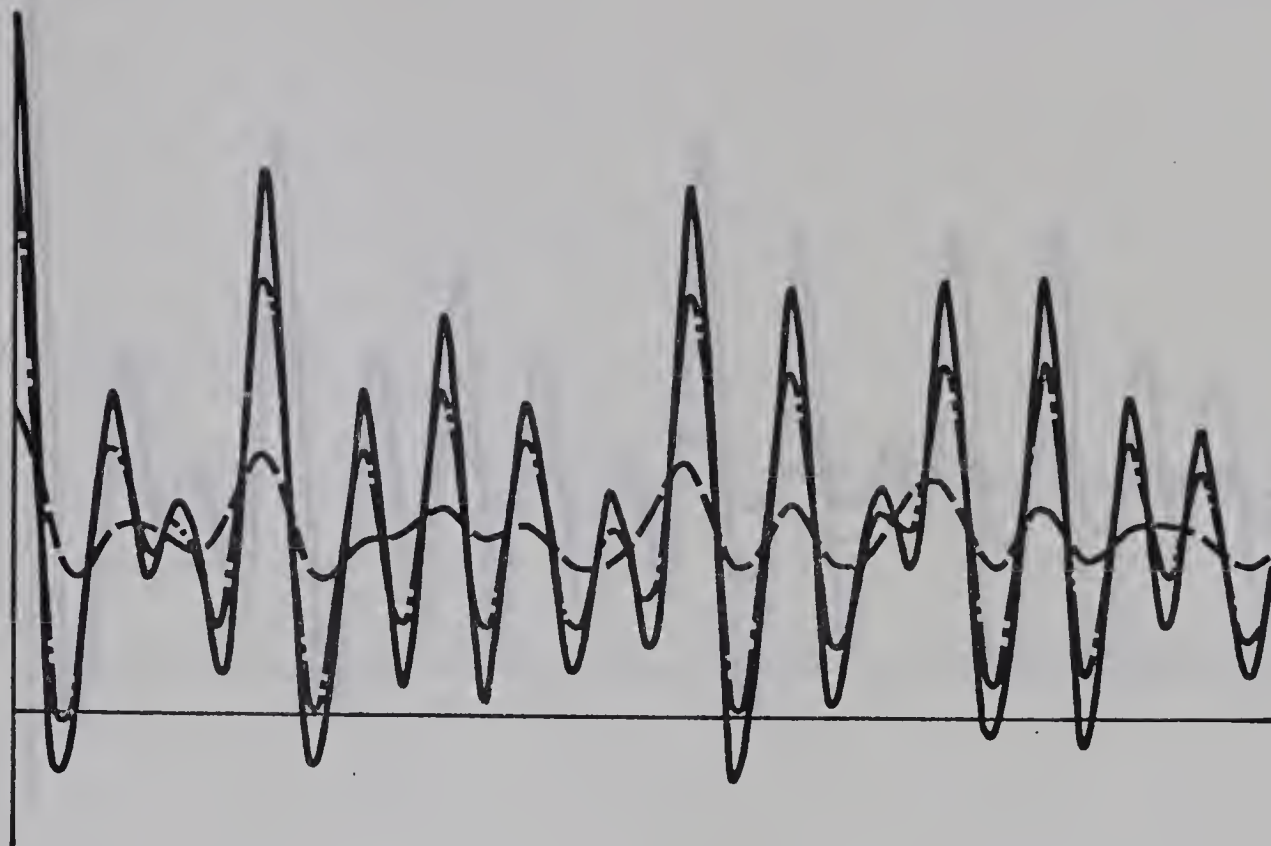


Fig 15: Spin = 4 $\eta = 0.4$ $\delta\omega = 0.0$ $\tau = 0.0, 1.0, 2.5$
Channels for $\omega = 5$ rad/ch.

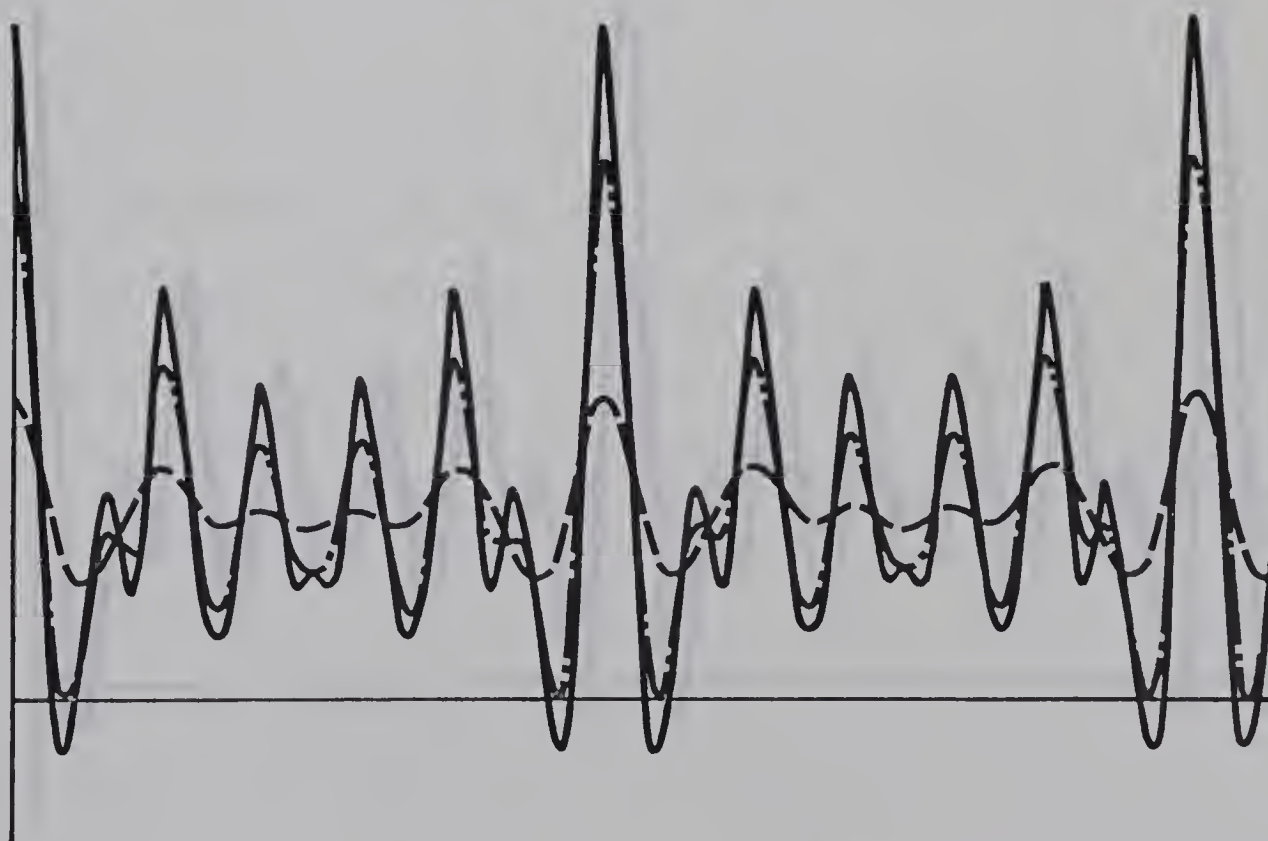


Fig 16: Spin = 4 $\eta = 0.0$ $\delta\omega = 0.0$ $\tau = 0.0, 1.0, 2.5$
Channels for $\omega = 5$ rad/ch.

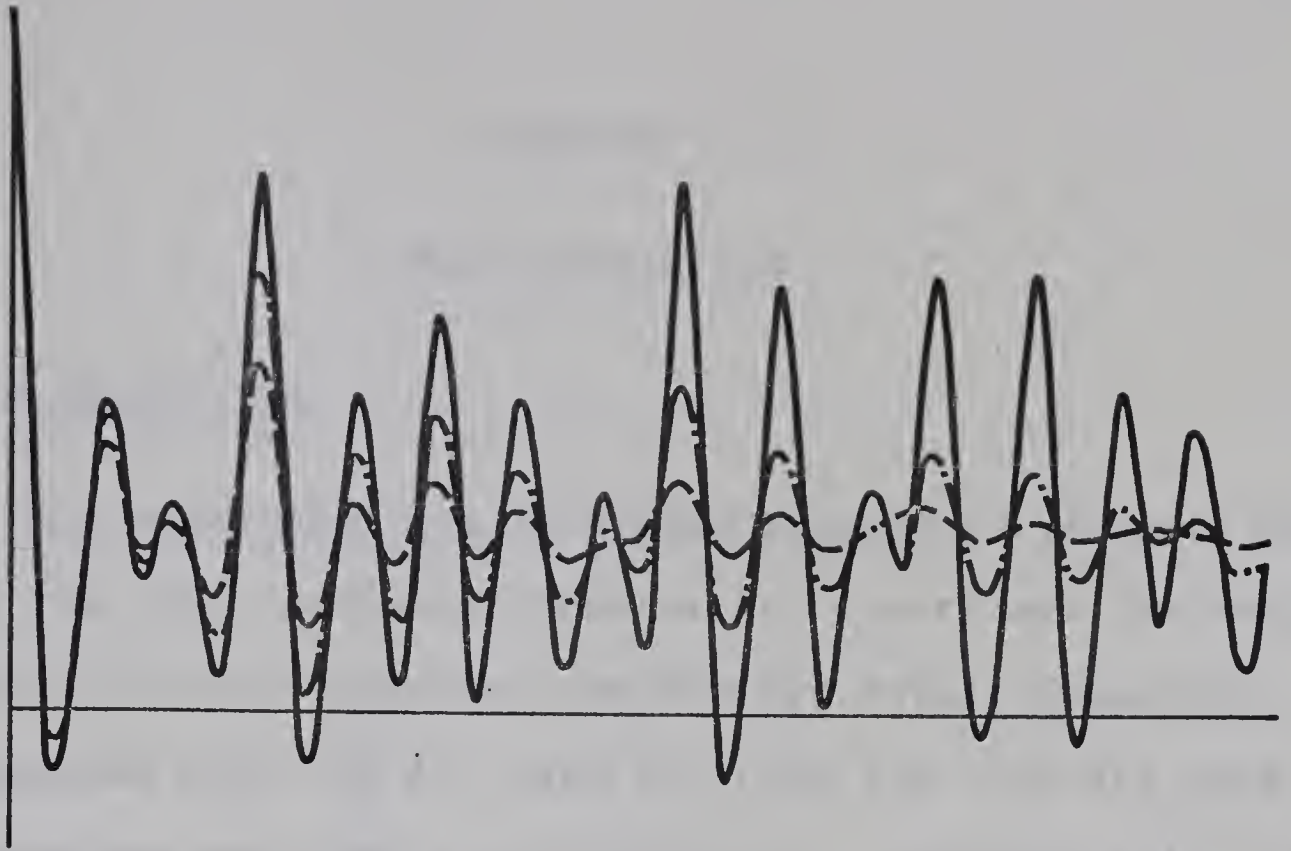


Fig 17: Spin = 4 $\eta = 0.4$ $\delta\omega = 0,2,5\%$ $\tau = 0.0$

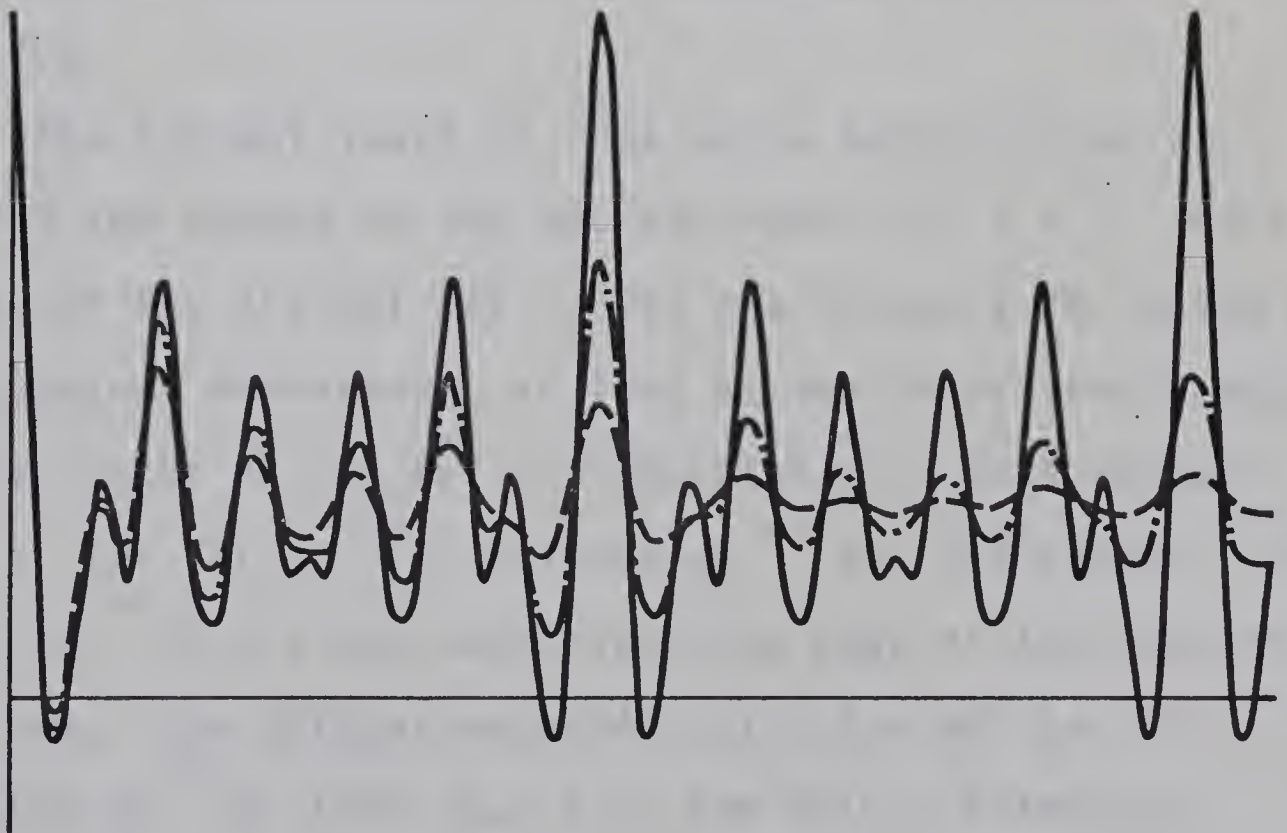
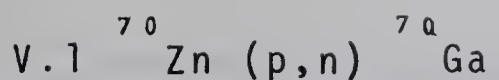


Fig 18: Spin = 4 $\eta = 0.0$ $\delta\omega = 0,2,5\%$ $\tau = 0.0$

CHAPTER V

THE EXPERIMENTS



The experiment was initiated because a discrepancy existed between the spin assignment from particle work and the measured anisotropy in the γ decay of the 879 keV level, especially when compared with the 411 keV γ ray from the 1102 keV level, which also was assigned a spin 4 (Do72). Together with the life time and the possibility of an Electric Field Gradient, we extracted the unperturbed value of the anisotropy, to see if this is in agreement with the prediction.

The 879 keV level of $\text{}^{70}\text{Ga}$ has a half-life of 22.7 ns (Hu75) and decays to the 691 keV level ($I^\pi = 2^-$). Both the 188 keV and the 691 keV γ rays are suitable for doing a time-dependent measurement as long as one takes into account that the region of 188 keV is populated with much abundant γ 's, i.e. 197 keV of $\text{}^{19}\text{F}$, 191 keV of $\text{}^{197}\text{Au}$, 185 keV of $\text{}^{64}\text{Cu}$, 175 keV of $\text{}^{71}\text{Ge}$ and the backscattering edge of the Comptons of 511 keV. The 691 keV coincides with the 692 keV E0 transition in $\text{}^{72}\text{Ge}$ from (n,n') in the Ge(Li) detectors. Another drawback is the relatively short lifetime of the decay.

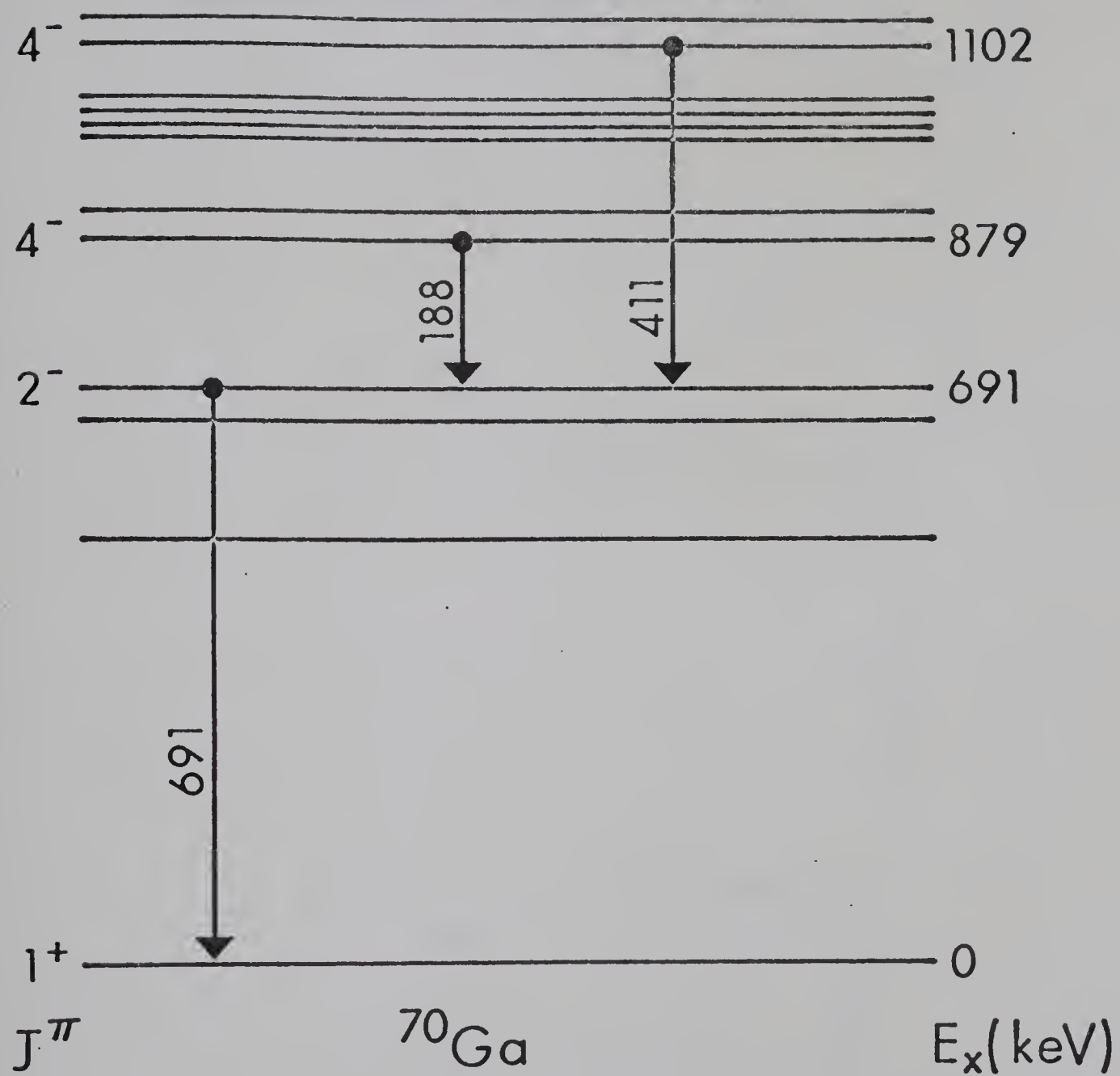
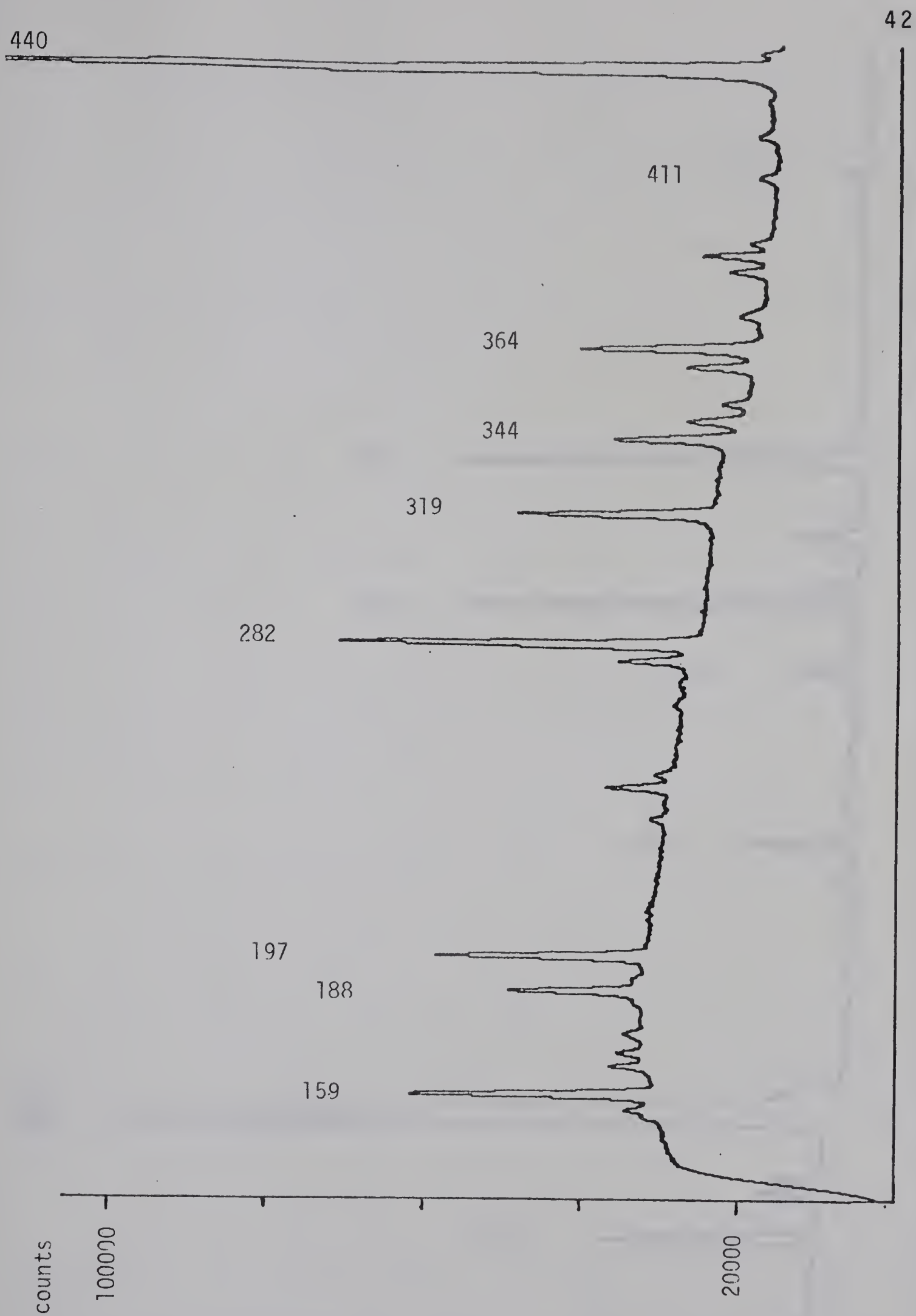
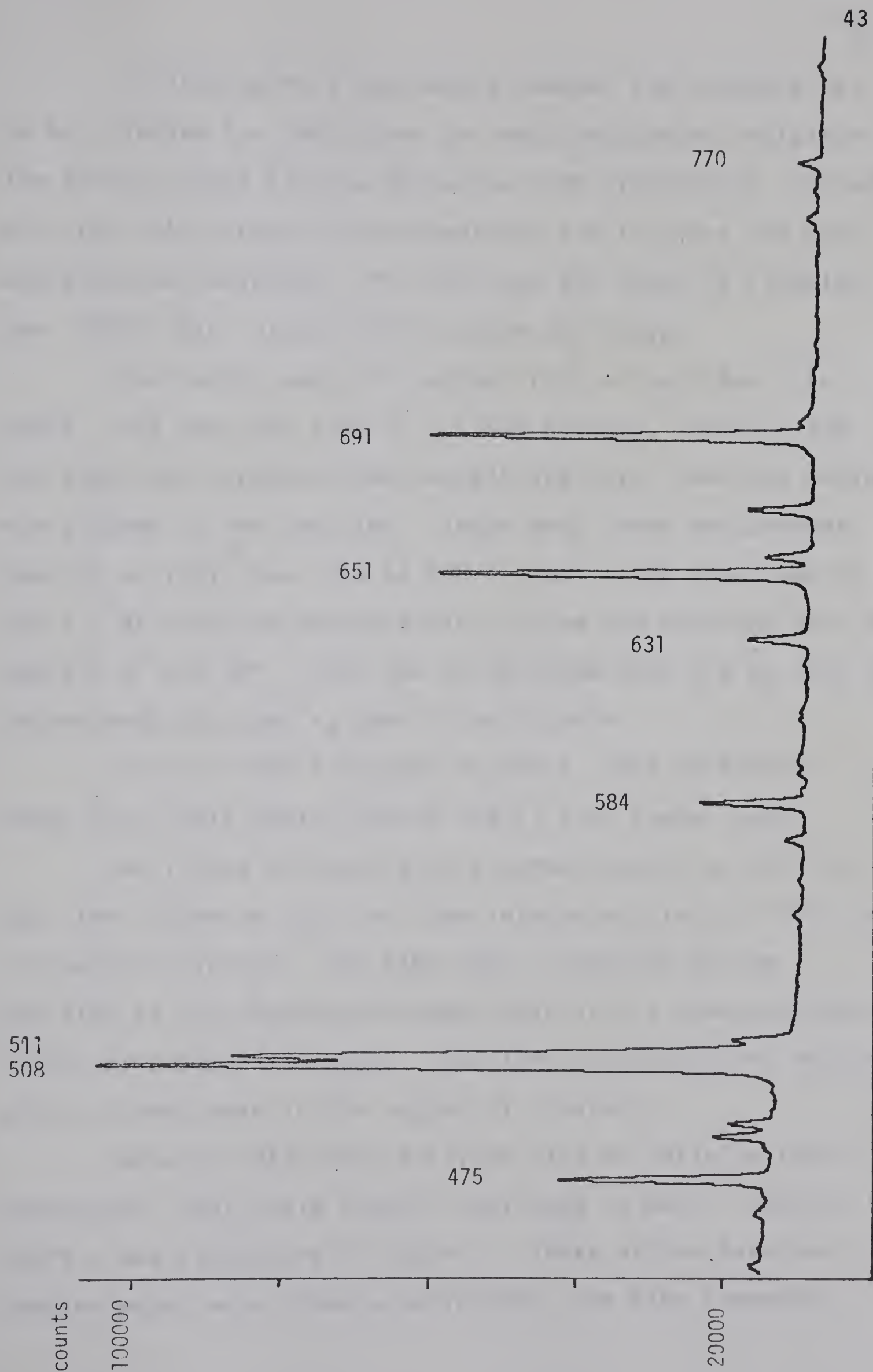


Fig. 19: The level scheme of ^{70}Ga with the transitions of interest.

Figure 20:

A typical γ - spectrum from ^{70}Zn (p,n) ^{70}Ga . The labels are the energies in keV.





In developing a hot-target chamber the aluminum has to be shielded for this gives too much background radiation. The target should also be prevented from evaporating. The use of mica for this purpose is unacceptable for it gives too much annihilation radiation. The solution was found in clamping two .0003" thick nickel foils around the target.

The target was a 1.9 mg/cm^2 foil of enriched ^{70}Zn (68%). The beam was 2.85 or 2.9 MeV protons, which is 300 keV above the threshold for the 879 keV level, and the nuclei are aligned by the reaction. There were three measurements done in a single run, one at 410 K, one at 420 K and one at 510 K. We used the double-timing system and measured only two angles, 0° and 90° . This has the problem that the a_2 term is determined only when a_4 term is negligible.

A run at 560 K and one at 340 K, were performed using the single timing set-up and at five angles each.

We fitted the data with a normalization to the 651 keV line, assuming that the time-integrated yield of this decay is isotropic (Do72). The time zero is defined by the position of the background prompt peak in the time-spectrum, fitted with peakfit program. The time resolution was measured with a prompt peak in the region of interest.

When the data were analyzed with an infinite time-resolution, they yield results published in Nucl. Physics (Hu75), and reproduced in Table 1. These values have one feature which makes them unbelievable, the high frequency

Table 1

UNPERTURBED VALUES OF LEGENDRE POLYNOMIAL COEFFICIENTS
(THE FIT IS DONE WITHOUT TIME RESOLUTION)

Target Temperature	E_p (MeV)	Transition				ω_q (MHz)	$\frac{\delta \omega}{\omega_q}$ (%)	χ^2/n
		$879 \rightarrow 691$		$691 \rightarrow 0$				
		a_2	a_4	a_2	a_4			
300 K	2.85	0.51 ± 0.03	-0.35 ± 0.04	-0.30 ± 0.02	0.05 ± 0.05			
	3.40	0.31 ± 0.02	-0.10 ± 0.03	-0.22 ± 0.01	0.05 ± 0.03	340	24	0.99
	2.85	0.43 ± 0.01	-0.26 ± 0.02	-0.33 ± 0.02	0.03 ± 0.03	298	40	1.47

spread. When we introduce the finite time resolution and the asymmetric field gradient, it turns out that the time resolution pushes the frequency spread down to zero.

Out of the analysis it followed that one cannot distinguish clearly between the various spins. Neither spin 3 nor spin 5 can be excluded for the 879 keV level with these experiments. This is caused by the short life time compared to the full period of the time-dependence. Only the first recovery of the anisotropy is seen and this is not sufficient to determine the spin. Only spin 3, 4, 5 were considered for the others are excluded on the basis of spin assignments from particle reactions. All the values calculated below are for spin 4. If spin 3 or 5 is chosen for the level, one must scale these values. When the recovery is set at a fixed time, ω_0 will be different for the three cases. Then $\omega_0 = 3\omega_q/(4I(2I-1))$, so ω_q is certainly different for the three cases.

TABLE 2

SCALING FACTORS FOR ω FOR DIFFERENT SPINS

Spin	ω_0	ω_q
3	1.520	0.814
4	1.000	1.000
5	0.847	1.361

($\eta = 0$, values normalized to spin 4)

This is confirmed with the analysis of the data with the three different spin values.

Neither is the value of η determined. For spin 4 the value of η is restricted to $0.0 \leq \eta \leq 0.6$. This large range is also due to the small part of the full cycle which is visible.

All values of a_2 and a_4 can be affected by a misalignment of the set-up up to 0.05. This error is not quoted in the table, but is common to the 188 and the 691, and will appear in the constant term c , which is a time-independent constant added to $a_k G_k(t)$ to get " $a'_k(t)$ ". This constant term absorbs also the normalization errors.

All data or typical samples of it are shown in the table and figures. The a_4 of the 691 γ ray is consistent with 0.00 and not quoted in the table.

V.2 The ^{18}F Trial

We tried to measure the quadrupole moment of the 1121 keV level of ^{18}F , which decays with a 184 keV γ ray to the 937 keV level, which subsequently decays to the ground state. The 1121 keV level has a spin 5^- and a half-life of 145 ns.

Since fluorine doesn't have a simple non-cubic crystal in any of its compounds, we wanted to compare ^{18}F with the 197 keV level in ^{19}F , which has a known Quadrupole moment. Radiation damage, which is dependent on the beam intensity and energy, can change the effective E.F.G.. So we wanted to

Table 3

THE DATA FROM THE VARIOUS RUNS FOR ^{70}Ga

188 keV ray						
T(K)	ω_q (MHz)	χ^2	Nf	C	$a_2(0)$	$a_2'(0)$
560	330	63.7	34	0.04	0.278 ± 0.008	0.32 ± 0.01
510	316	41.5	25	0.13	0.255 ± 0.026	0.38 ± 0.03
420	315	28.2	25	0.17	0.264 ± 0.021	0.43 ± 0.02
410	316	28.7	25	0.17	0.209 ± 0.020	0.38 ± 0.02
340	319	19.5	24	0.08	0.341 ± 0.022	0.42 ± 0.02
691 KeV ray						
560	330	25.6	23	-0.13	-0.156 ± 0.017	-0.29 ± 0.02
510	316	37.4	26	-0.06	-0.169 ± 0.020	-0.23 ± 0.02
420	315	32.9	26	-0.05	-0.170 ± 0.018	-0.22 ± 0.02
410	316	17.6	26	-0.03	-0.186 ± 0.020	-0.22 ± 0.02
340	319	14.7	22	-0.025	-0.257 ± 0.022	-0.29 ± 0.02
188 KeV ray						
					$a_4(0)$	$a_4'(0)$
560	330	41.2	34	-0.04	-0.051 ± 0.014	-0.09 ± 0.02
340	319	12.1	24	0.00	-0.144 ± 0.050	-0.14 ± 0.05

Nf is the number of degrees of freedom in fitting $a(t)$ to the theory

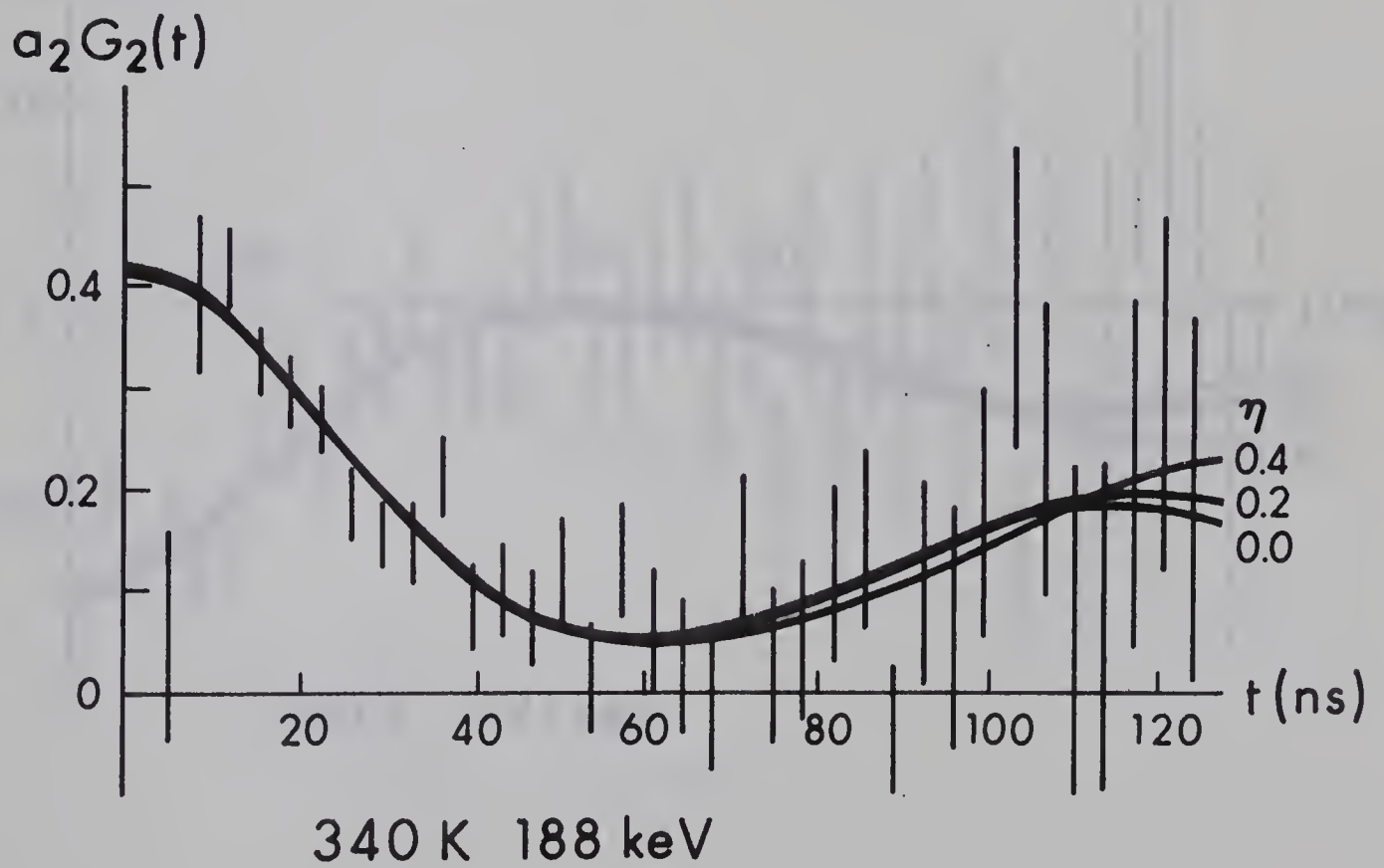
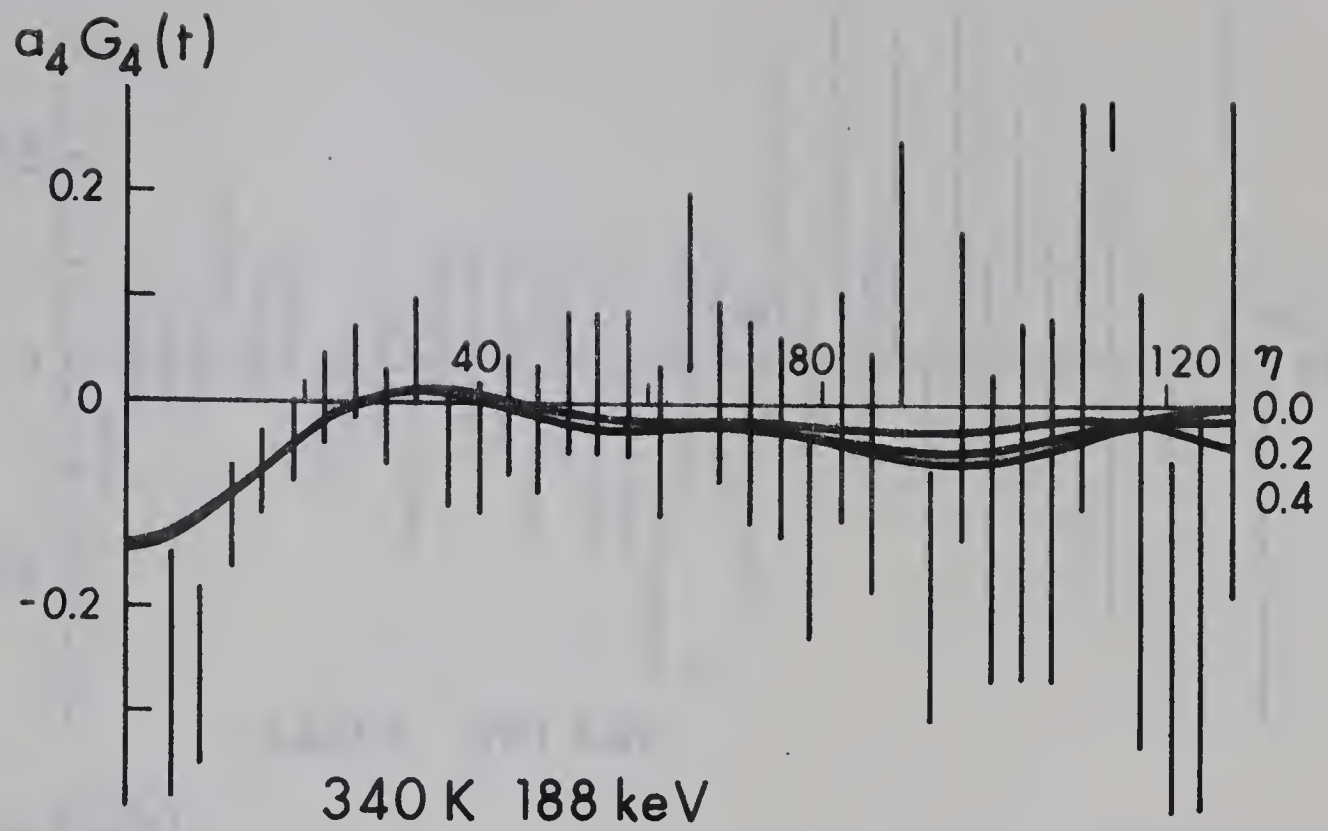
$$a'(0) = a(0) + C$$

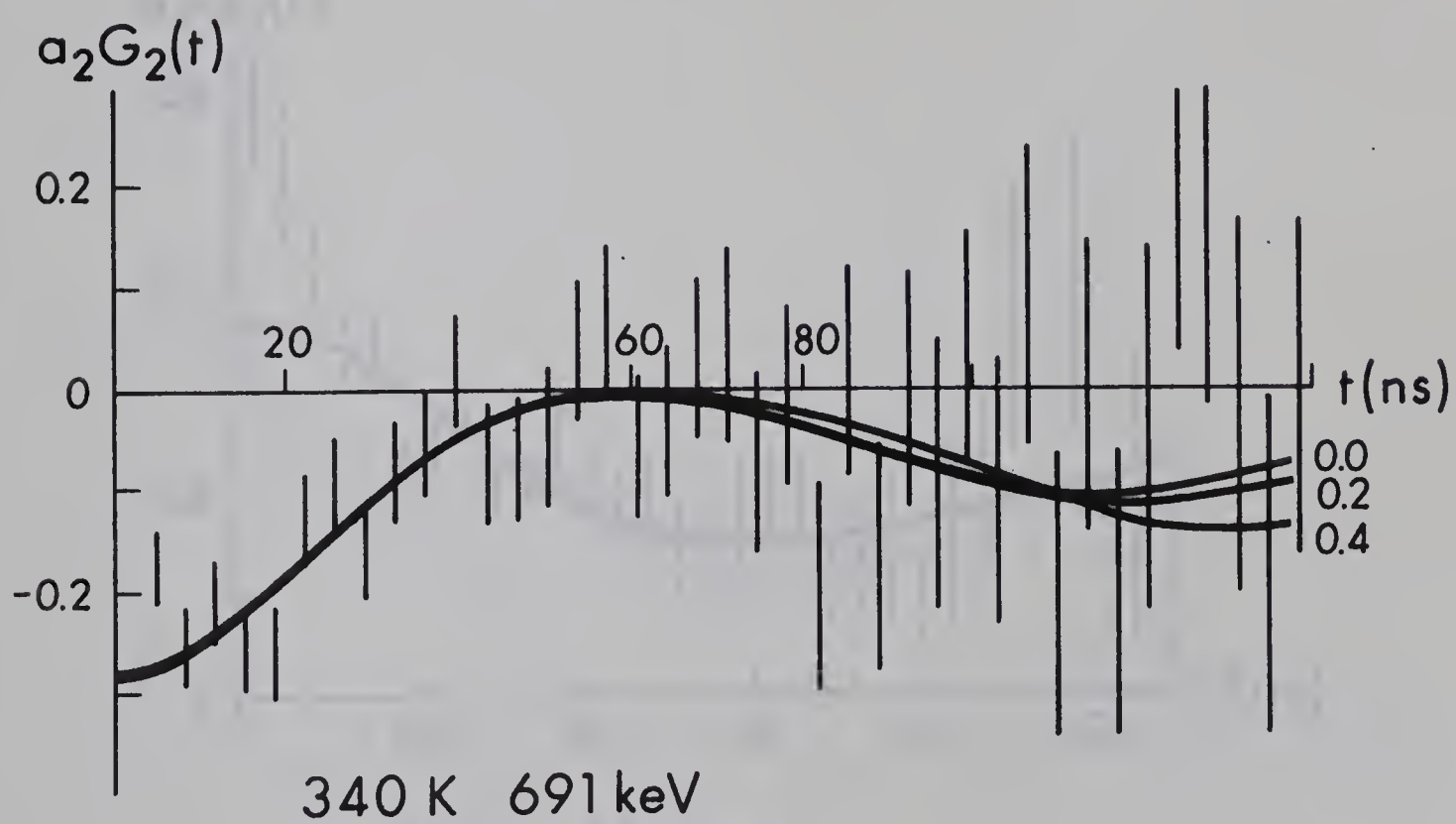
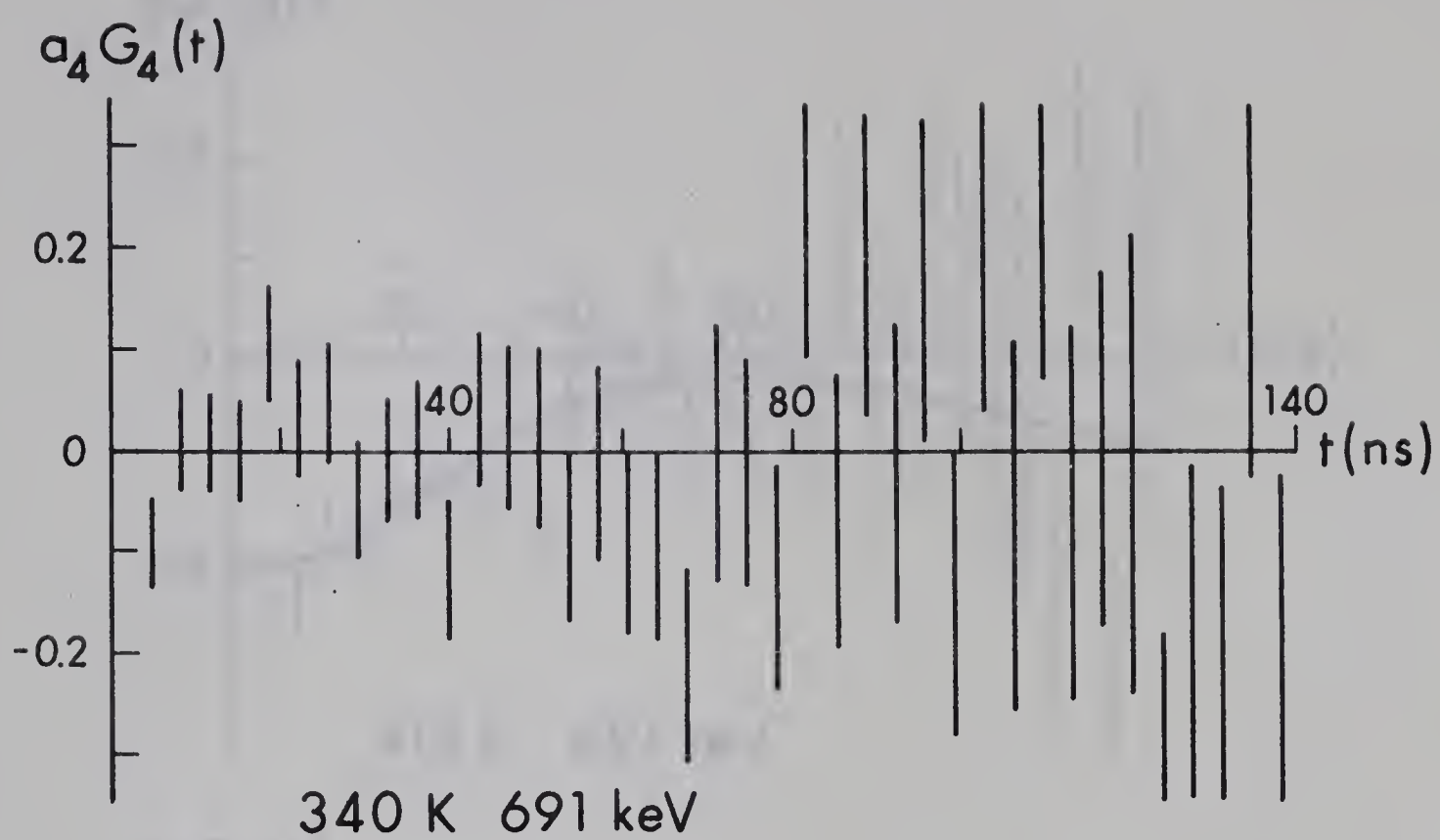
Time-integrated values for the 188 keV transition.

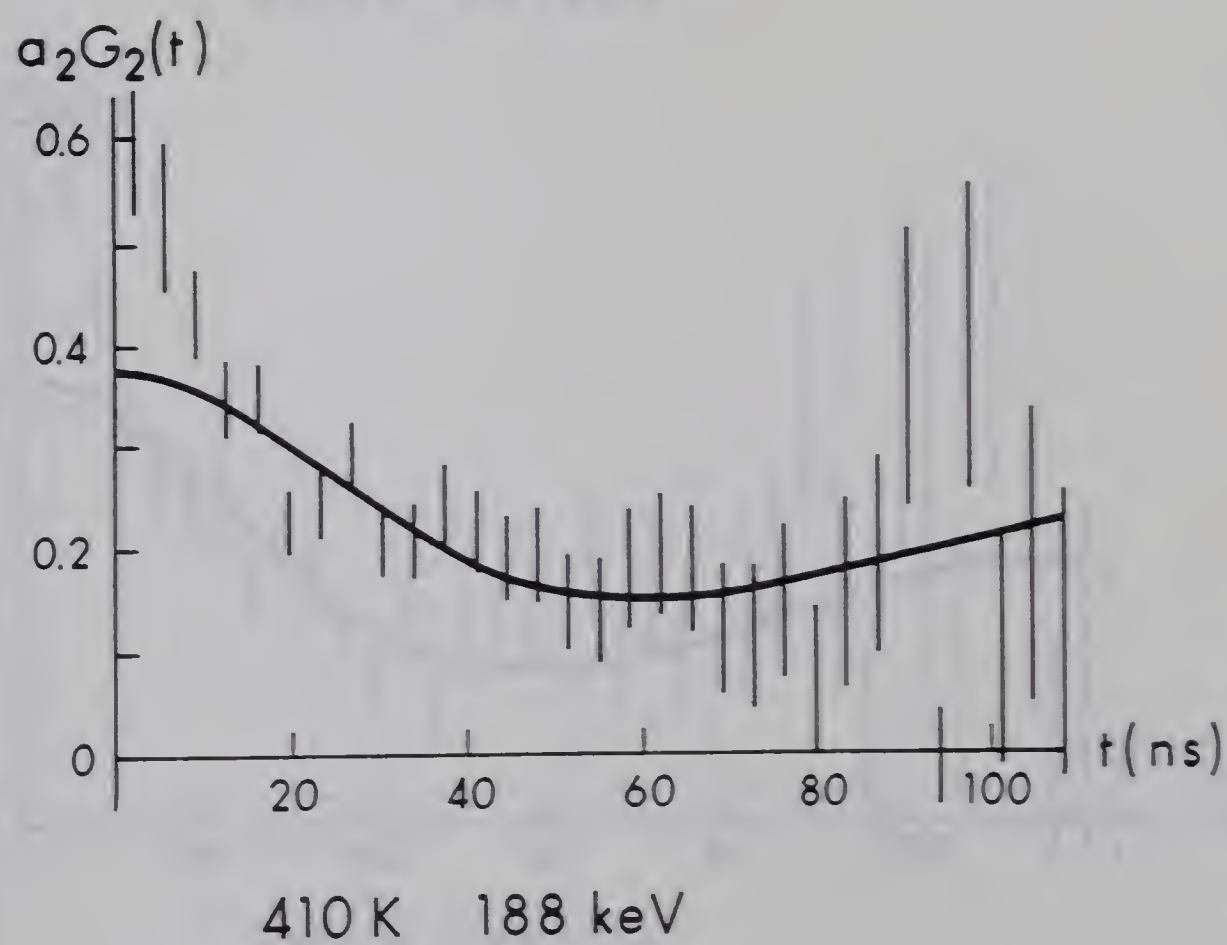
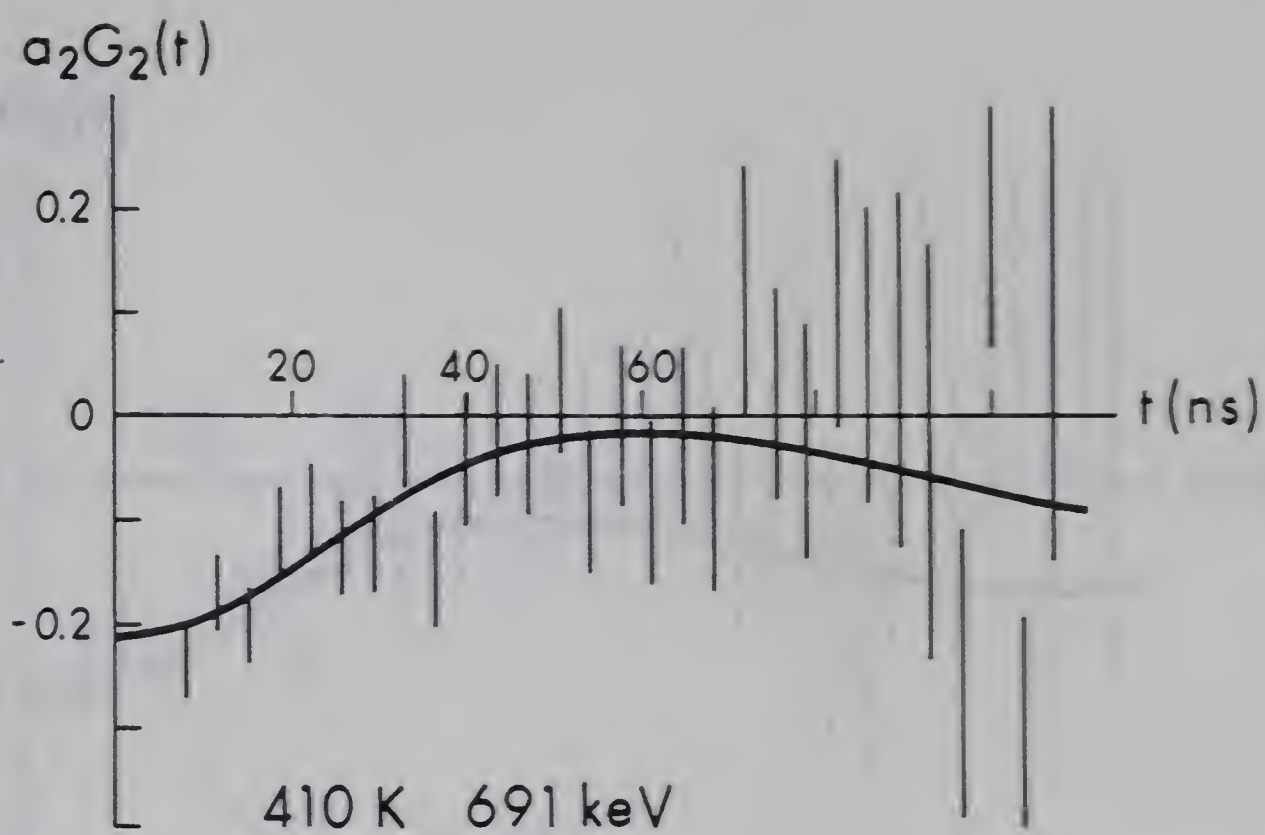
Temperature	a_2	a_4
340 K	0.20 ± 0.01	-0.11 ± 0.02
560 K	0.21 ± 0.01	-0.06 ± 0.02

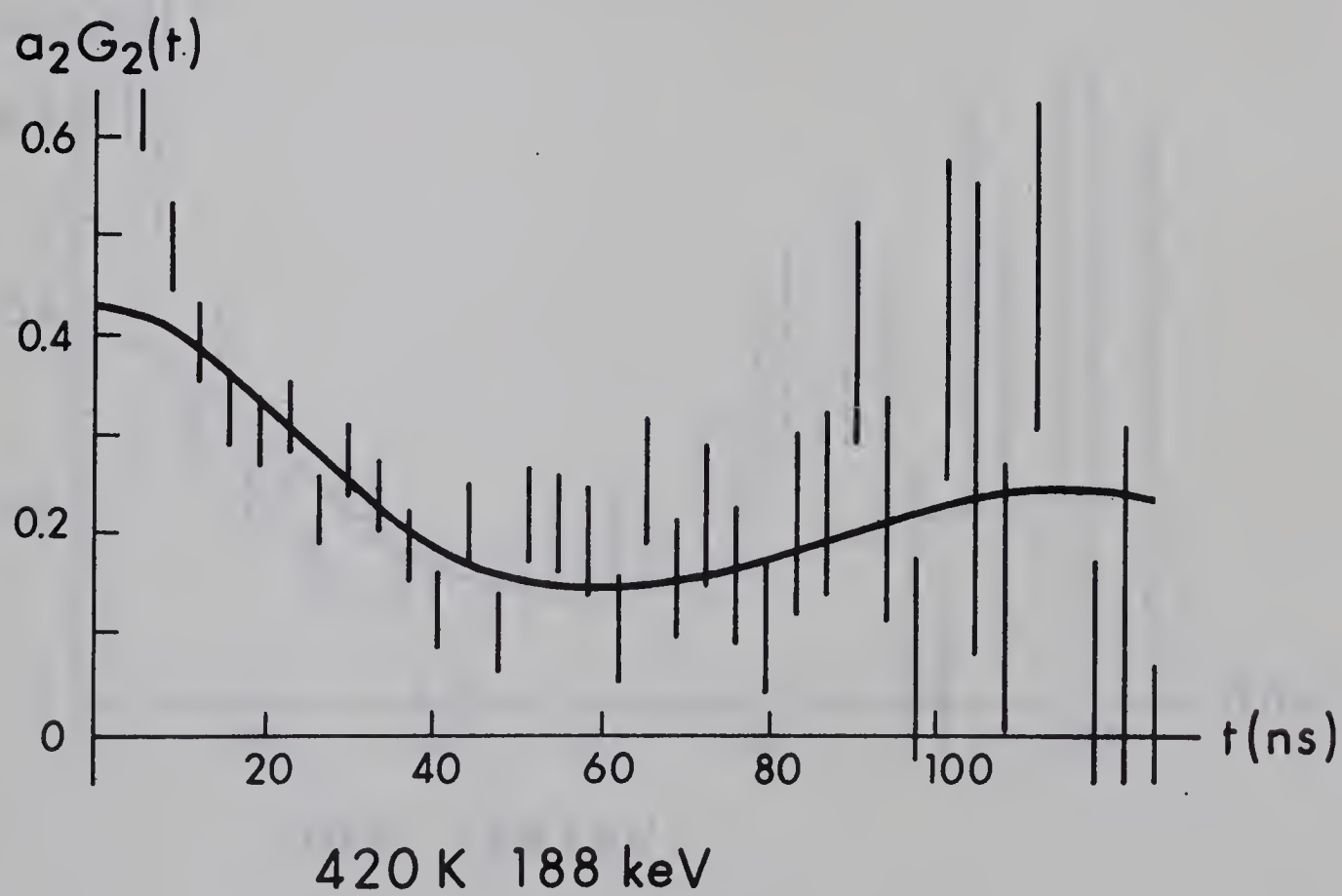
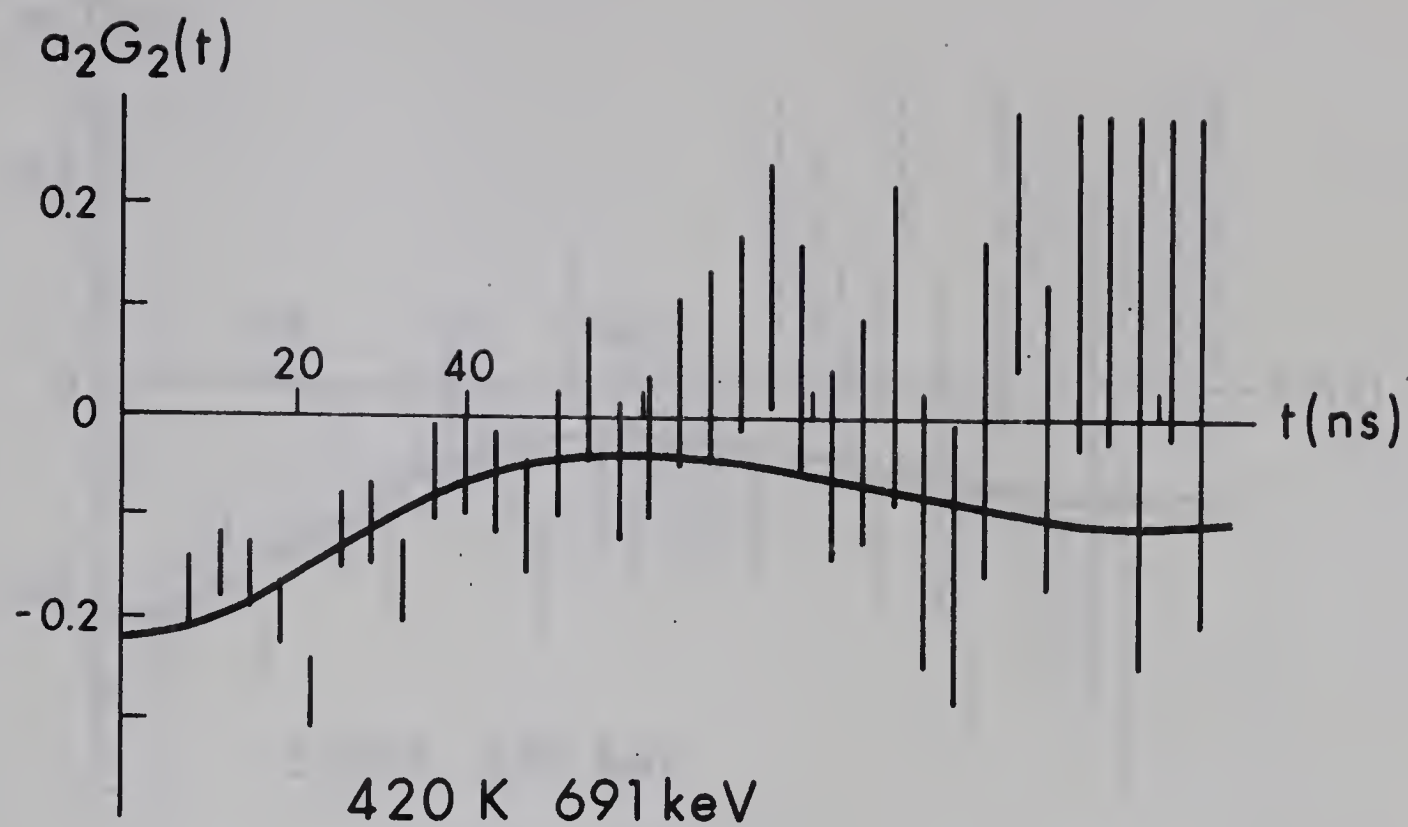
Fig. 21-34: The experimental results of ^{70}Ga in Zinc at various temperatures.

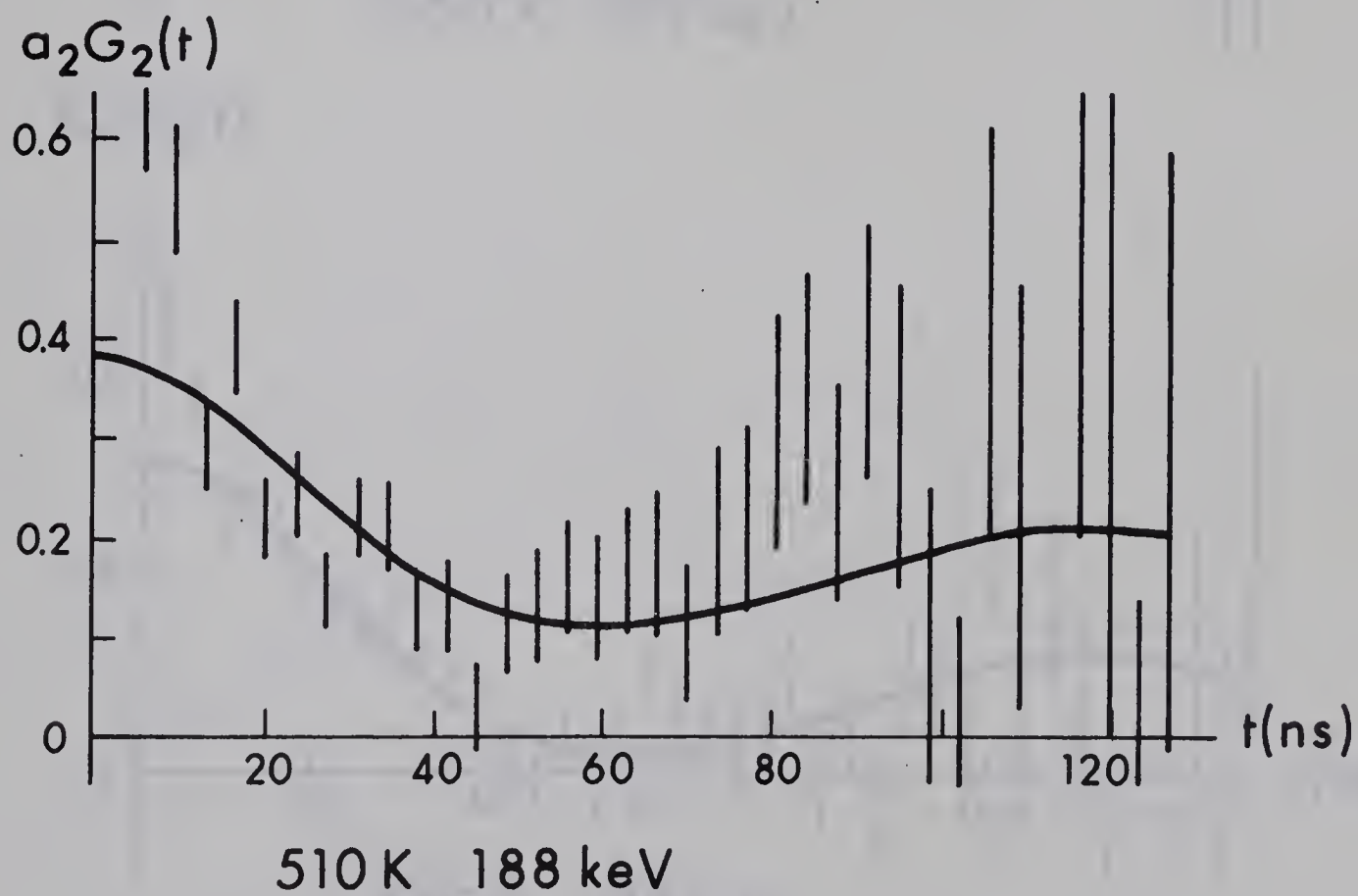
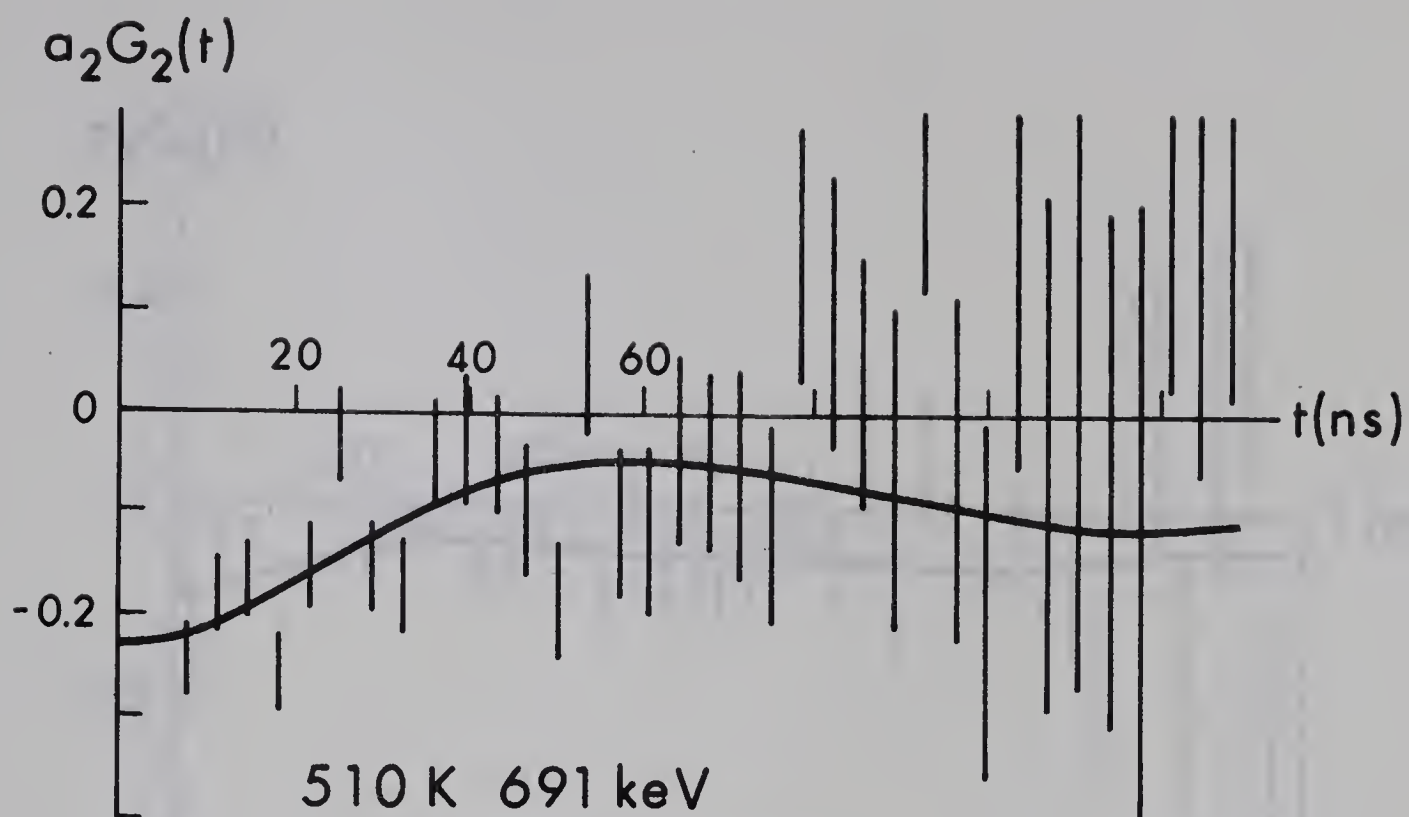


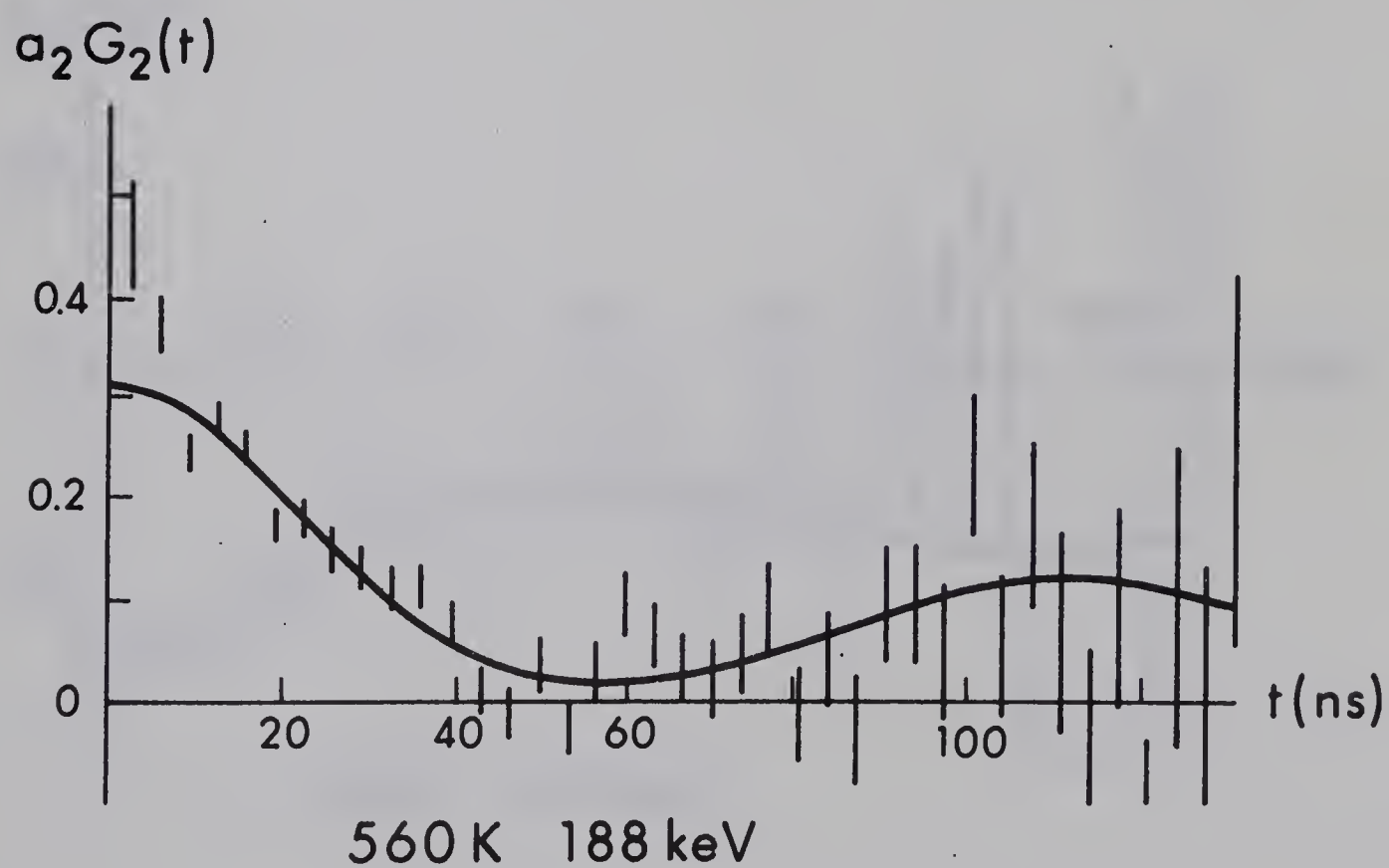
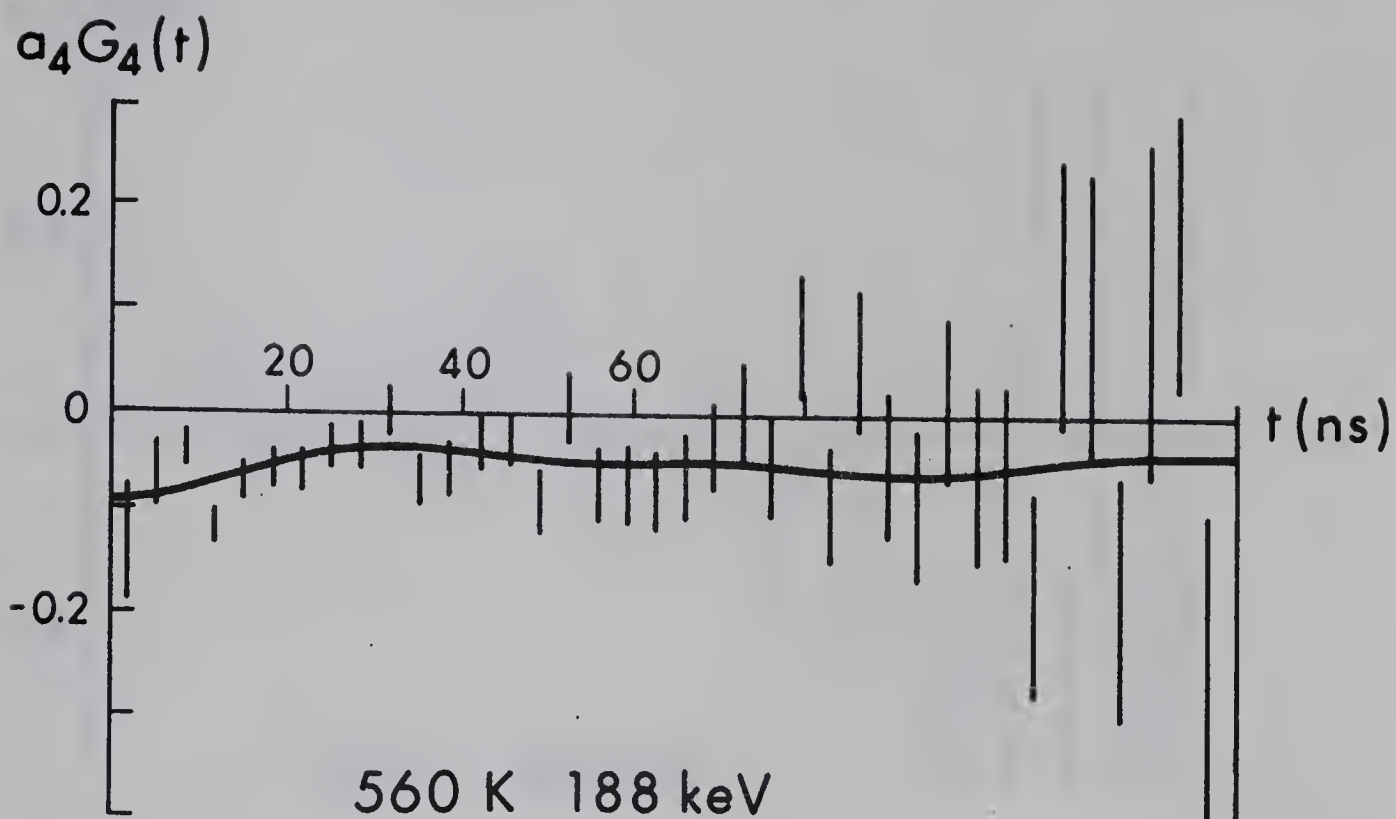


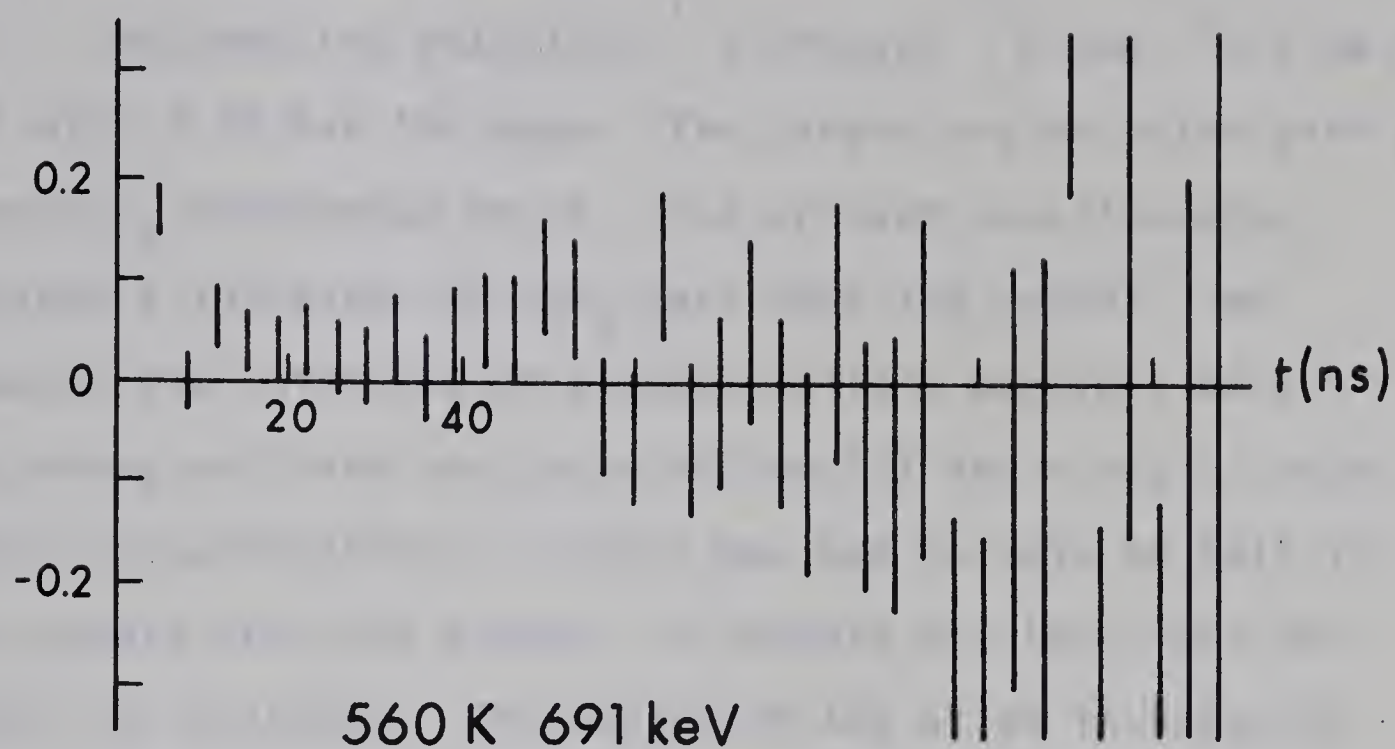
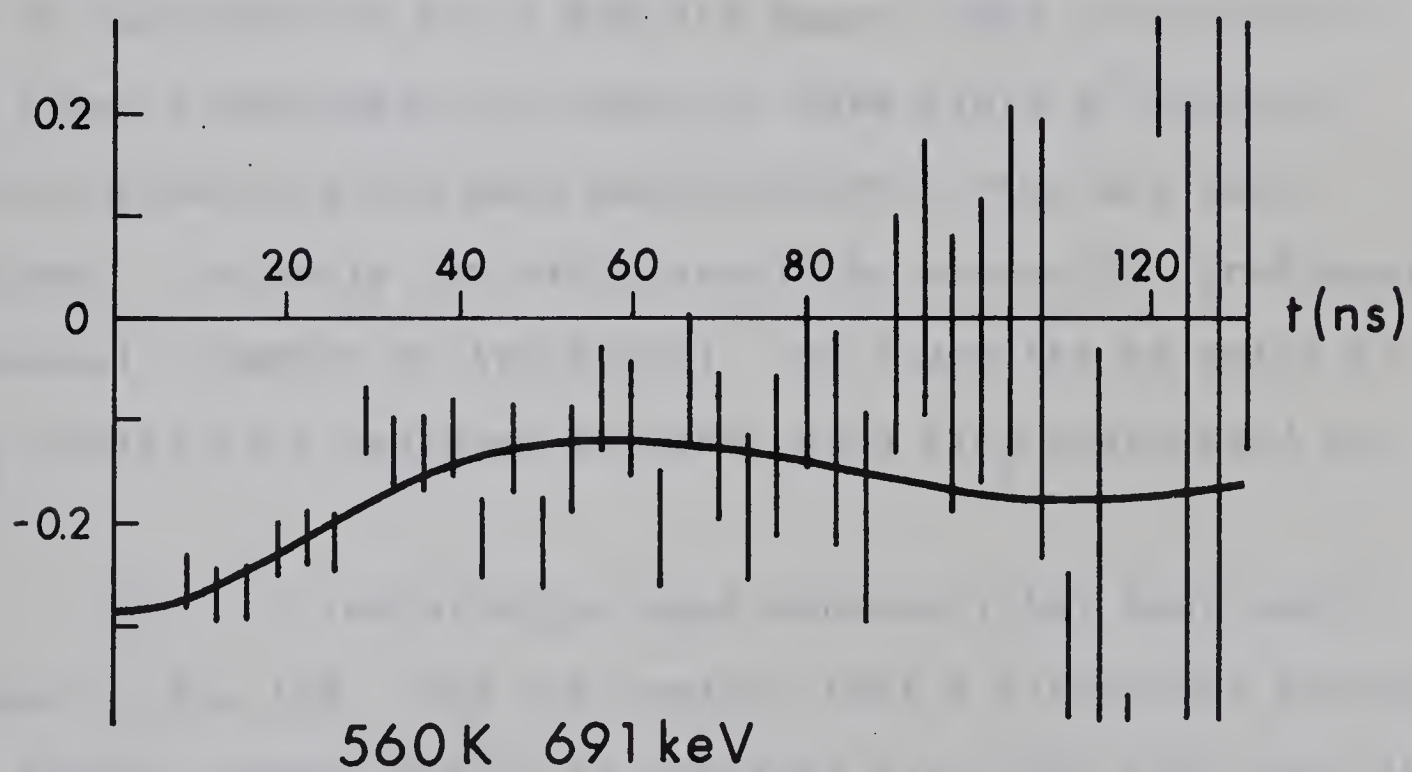










$a_4 G_4(t)$  $a_2 G_2(t)$ 

measure both frequencies in the same run, to ensure that both E.F.G. are the same.

We used the reactions $^{16}\text{O} (^3\text{He}, p) ^{18}\text{F}$ and $^{19}\text{F} (^3\text{He}, ^3\text{He}) ^{19}\text{F}^*$ with 2.95 MeV ^3He beam. The target was an oxide with a layer CaF_2 evaporated on it. The present recoil energy required a thickness of CaF_2 less than $100 \mu\text{g}/\text{cm}^2$. We measured the thickness of a sample with α particle back-scattering and used the yield of the 197 keV γ ray of this sample as calibration. In this way one is able to tell if the targets are thin enough. 5 targets are less than $100 \mu\text{g}/\text{cm}^2$ in thickness. The choice of the oxide is bound by some conditions. The anion in the oxide should not give a lot of radiation in the 3 MeV ^3He beam. This excludes Si and lower Z materials, for most of them yield β^+ -unstable nuclei, producing too many annihilation γ rays and their comptons. Secondly the oxide should be non-cubic, preferably hexagonal, rhombic or tetragonal. We found the solution in V_2O_5 molten on a tantalum backing, with CaF_2 evaporated on top.

The ^{18}F annihilation peak produced that much background in the 180 - 200 keV region, that a background suppressing target chamber had to be designed using the fact that the half-life of ^{18}F is 110 min. One target was used for 30 min. then shielded for the detectors while measuring on the other targets. This way one is able to reduce the background at 184 keV by a factor 3 to 4.

V.3 $^{69}\text{Ga} (d,p) ^{70}\text{Ga}$

With this experiment we start to get some comparison between gallium ions in Zn and Ga metallic surroundings. This already has been done with Ge as probe (Ha73a). We used natural Ga and excited the 879 keV level with 5.5 MeV deuterons. The only experimental difficulty was the low melting point of gallium metal which is only 29.8 °C. The target was cooled by using the background suppressing target chamber and immersing the rod of the target ladder into ice water. Probably due to poor thermal contact between the target and the ladder we didn't succeed in maintaining our target solid, and measured so the time differential pattern of ^{70}Ga in liquid Gallium. The results show the feasibility of studying the quadrupole interaction of ^{70}Ga with the (d,p) reaction. The unperturbed value of a_2 is approximately 0.1.

CHAPTER VI

DISCUSSION OF THE RESULTS

VI.1 The Frequencies

The frequencies quoted in Table 3 have an uncertainty of 3%, in which region the χ^2 changes by only up to 3% of the quoted minimal value. A change in the frequency will slightly affect the unperturbed a_k values.

The values with their uncertainties are plotted in Fig. 35 as function of the temperature. From this graph follows the value of ω_q at 300 K of (315 ± 10) MHz. The change in frequency from 300 K to 600 K is $(+3 \pm 6)\%$.

A definite calculation of the E.F.G. has not yet been performed. According to the current theory

$$eq = (1 - \gamma_\infty)eq_{lat} + (1 - R)eq_{loc} \quad (VI.1)$$

where q_{loc} is due to the electrons in a shell around the nucleus not containing other ions,

q_{lat} is due to the other ions in the lattice and the electrons outside the shell.

γ_∞ represents the effect of the displacement of the core electrons in the lattice electric field. It is called the Sternheimer anti-shielding factor.

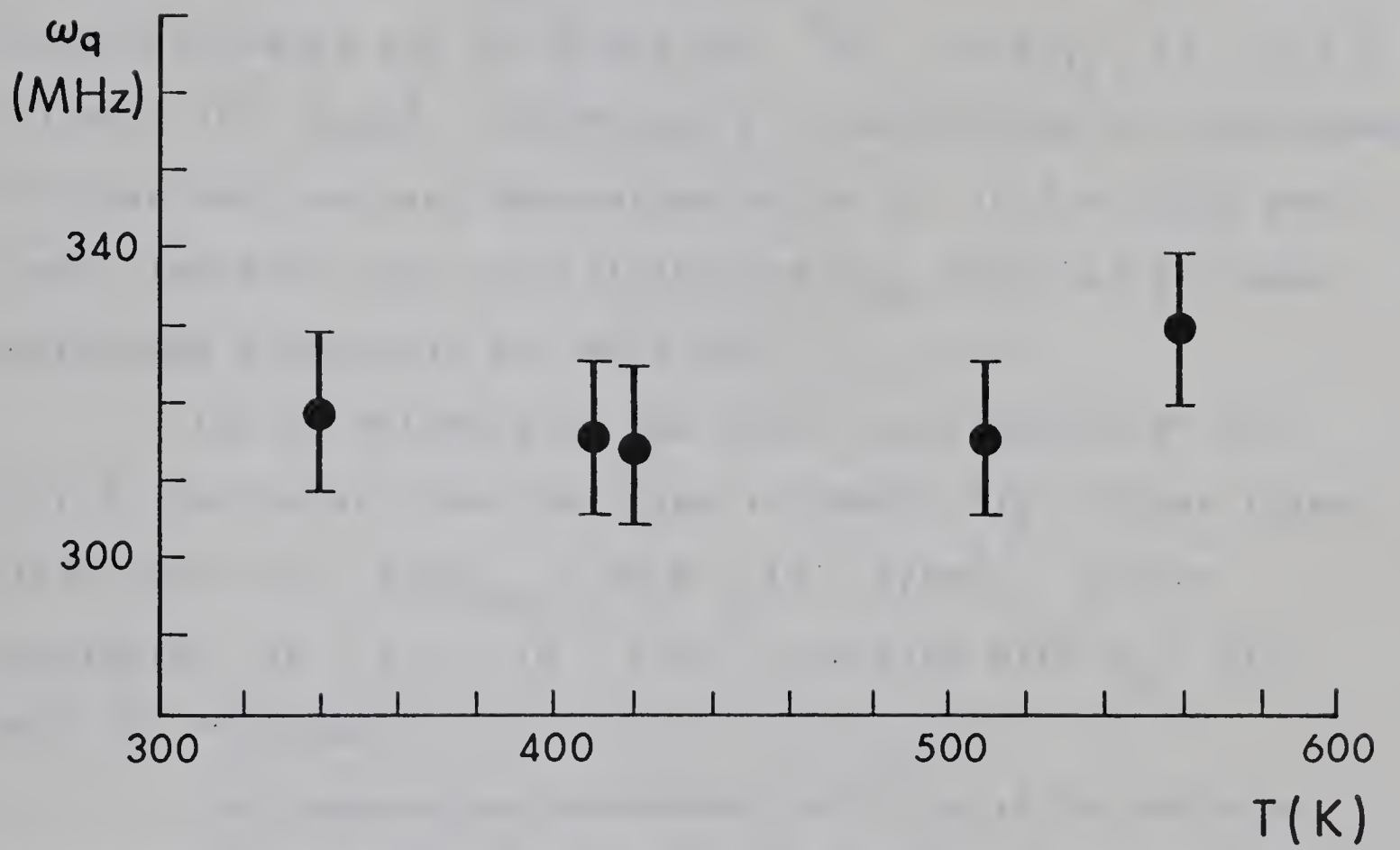


Fig 35: The dependence of ω_q on the temperature of ^{70}Ga in Zn

R is the shielding factor, which expresses the change in the E.F.G. of the electrons at the nuclear site due to the interaction of the nuclear quadrupole moment on the core electrons. (Wa65 and refs. therein).

q_{lat} can be calculated for various lattices (We61 and Da61), yielding for our hexagonal Zn lattice $eq_{lat} = -1.5 \times 10^{16} \text{ V/cm}^2$. γ_{∞} , the anti-shielding factor has been also calculated and is -9.905 for ^{70}Ga . So $eq_{lat} (1 - \gamma_{\infty}) = -1.63 \times 10^{17} \text{ V/cm}^2$. The factor R is calculated by Sternheimer for various ions and determined to be 0.1 to 0.4 (St63 and refs. therein), but calculations of q_{loc} have not yet been performed adequately for most ions.

For an estimate of the local contribution of the E.F.G. the value from the graph in (Ra75) Fig. 36 was taken. This gives $(1 - R)eq_{loc} = +5.8 \times 10^{17} \text{ V/cm}^2$. So one estimates $eq = 4.1 \times 10^{17} \text{ V/cm}^2$, yielding with $\omega_q = 315 \text{ MHz}$ $|Q| = 0.5 \text{ barn}$.

The temperature dependence of ^{70}Ga in Zn deviates certainly less from the temperature dependence of q_{lat} than the various other ions in Zn (Fig. 37); this might indicate that the lattice contribution is in comparison larger than in the other cases. This would increase the magnitude of the quadrupole moment.

The other part, the calculated value of Q is not established. In appendix II the results are quoted for the

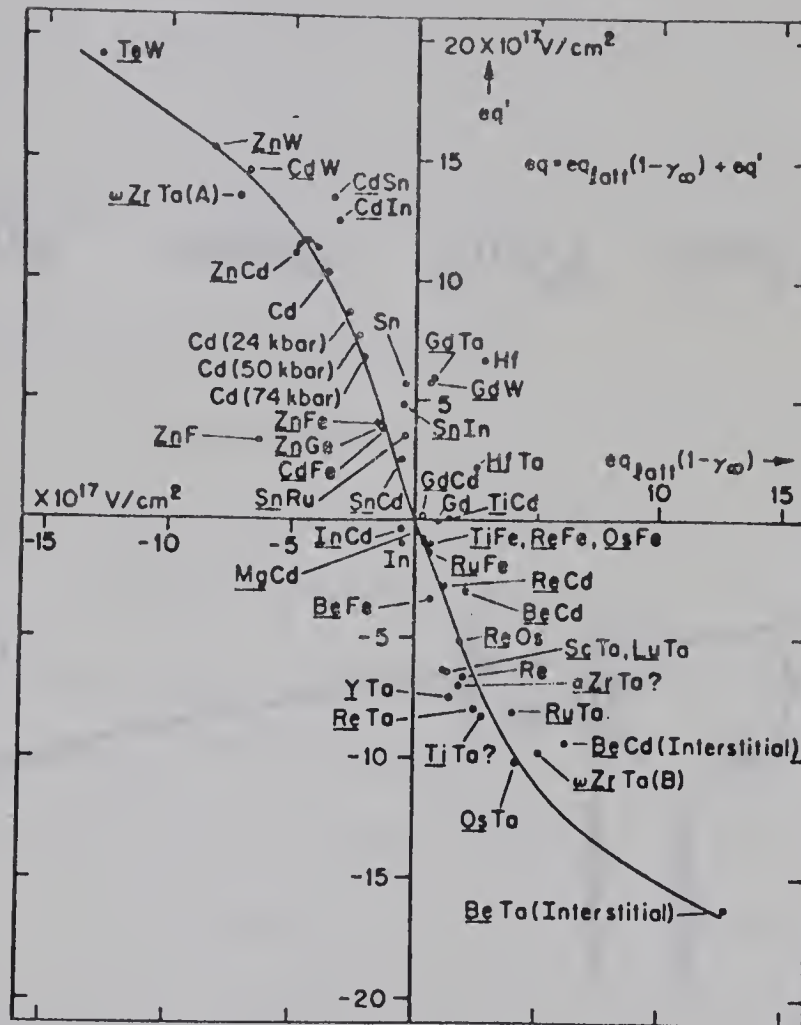


Fig. 36: Correlation of ionic and extraionic field-gradients in metals. Most values refer to room temperature. A typical temperature dependence is shown in the case of ZnCd by an arc of data points. Underlined symbols refer to the host metal. A and B refer to two inequivalent substitutional sites in ω -Zr. Filled circles indicate data from e^2qQ values of known signs. For open circles, e^2qQ signs are unknown. Locations of these points are predicted. (Ra75)

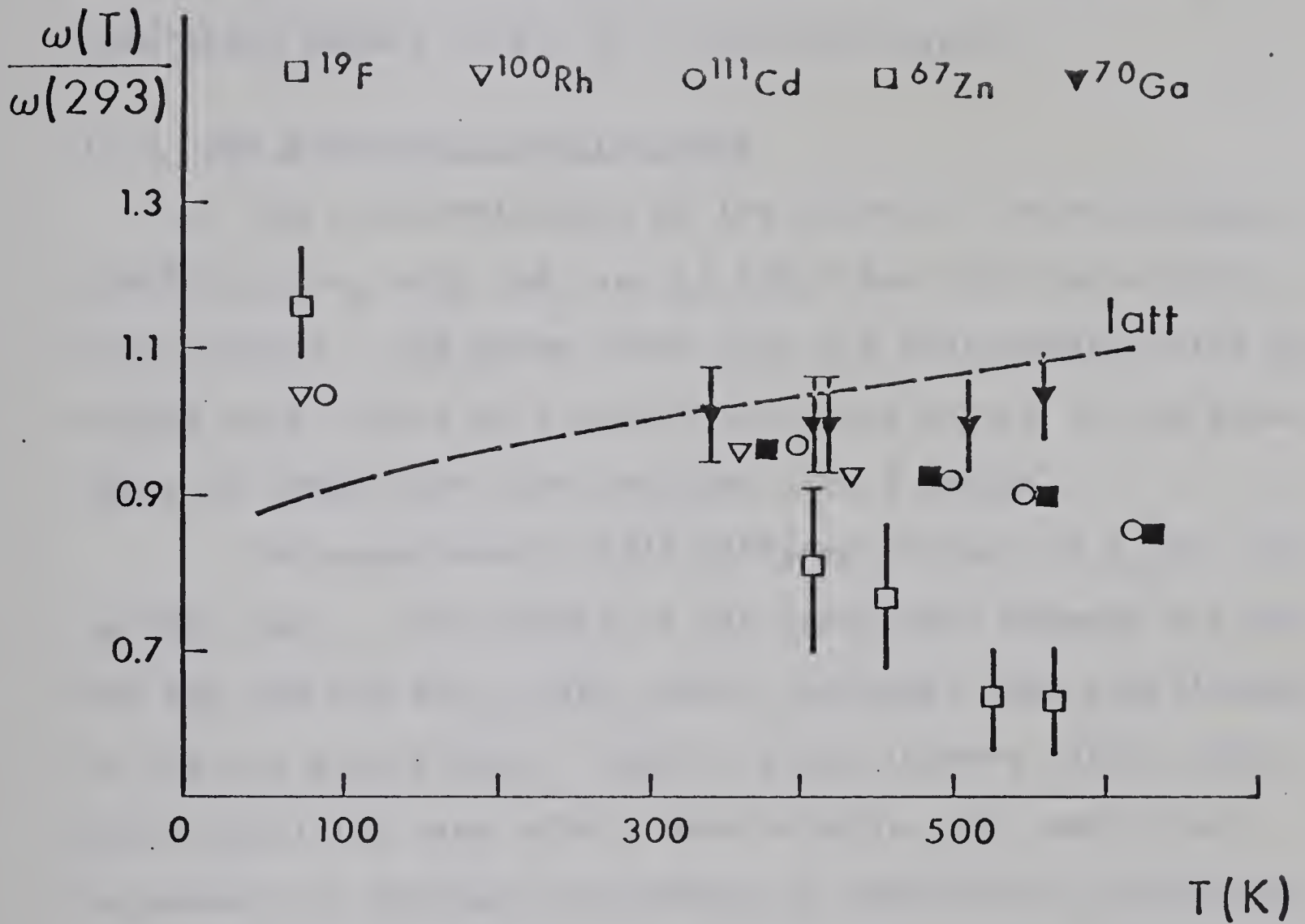


Fig. 37: The variation of the quadrupole frequencies of different ions in Zn with the temperature and the variation of the lattice part of the field gradient with the temperature.

calculation of the energy-levels in the Intermediate Coupling Model for ^{70}Ga . The results indicate that the results can be described with some admixing of phonon states. With the known quadrupole moment of the vibrational 2^+ state in ^{70}Ga of 0.38 b (Ch72) and the two particles outside the core, a quadrupole moment of 0.5 b is not unbelievable.

VI.2 The Anisotropy Coefficients

For a determination of the value of the anisotropy coefficient a_2 only the runs at 560 K and 340 K were taken into account. The three other runs are measurements with two angles only, which will easily introduce errors in the values large in comparison with the runs with 6 angles.

The experiments yield different values of a_2 for the various runs. This effect is not consistent between the 188 keV and the 691 keV γ rays, which indicates that misalignment is not the only effect. Various other authors (Be75, Va73, Bu74, Ha73) the same effect when studying the temperature dependence or pressure dependence of quadrupole interactions with the TDPAC technique. Two groups (Be74 and Ha73) report a reduction of the a_2 coefficient by a factor of two and more. All others show differences up to 25%.

Other γ rays of ^{70}Ga showed agreement between the two runs, and with the anisotropy coefficients as published by (Do72) and (Na73).

The theoretical expression for the time integrated attenuation coefficient is (Fr65)

$$\overline{G_k(\infty)} = \sum_N s_{kN} \frac{1}{1 + (N\omega_q\tau)^2} \quad (\text{VI.2})$$

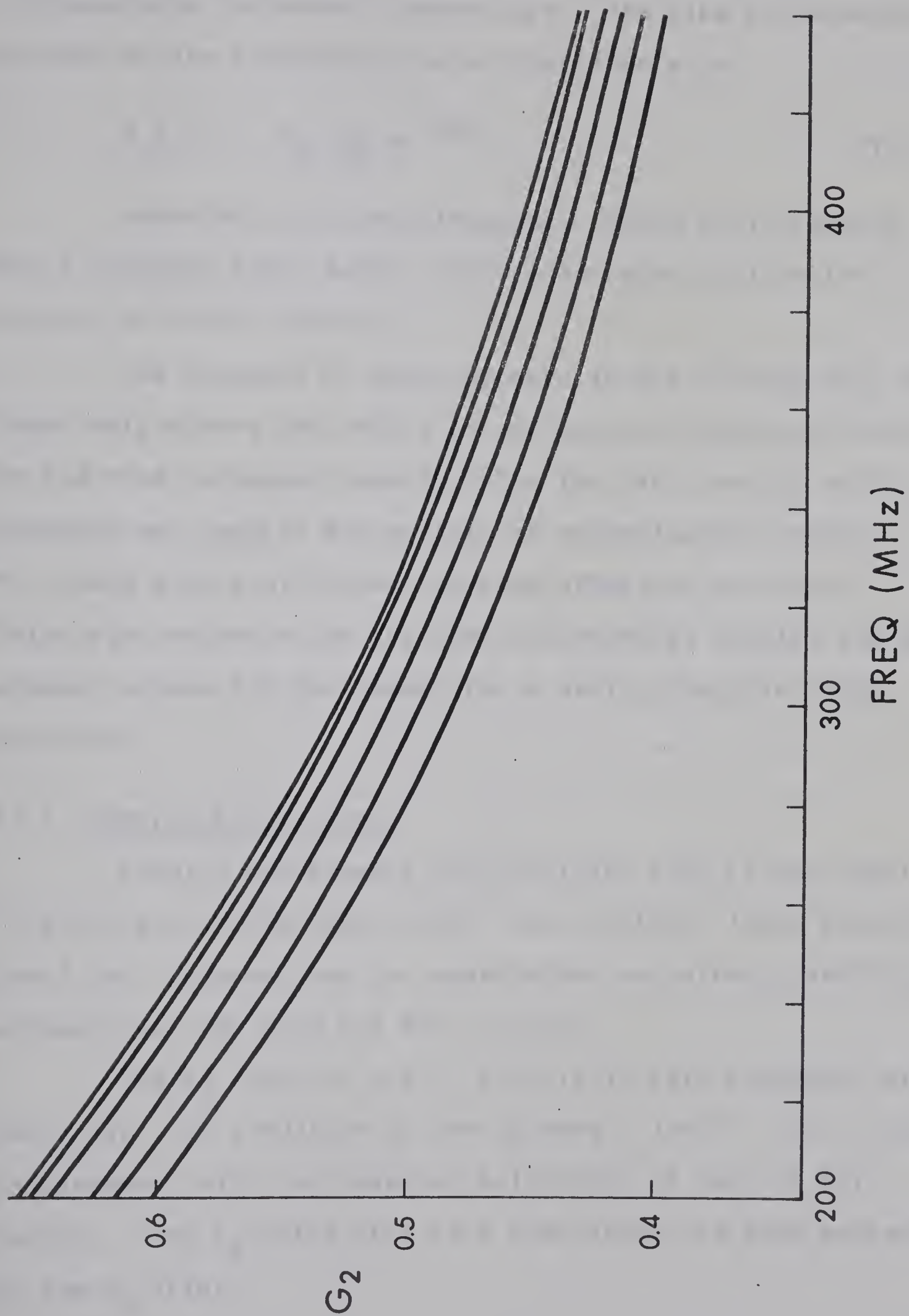
where τ is the lifetime.

The values for this expression for halflife of 23 ns and spin 4 are plotted in Fig. 38., as a function of ω_q . For the 560 K run the value of the time integrated attenuation coefficient is 0.66 and the value of ω_q is 330 MHz. For the 340 K run we have $\overline{G_2(\infty)} = 0.48$ with $\omega_q = 319$ MHz. If one compares these values with the curve it can be concluded that the 560 K run does not fit the theory of a static electric field gradient. The 340 K run does agree with the theory and it can be concluded that the $a_2(0)$ value is 0.42 ± 0.02 and $a_4(0) = 0.14 \pm 0.05$. For the 691 keV γ ray there is no possibility for such a check for the peak is obscured by the 692 KeV peak of ^{72}Ge .

The three other runs, which yield a mixture of a_2 and a_4 , have consistent values for the coefficients of both transitions, but a temperature dependence is not excluded with the present error bars.

If a temperature dependence is present the results might be explained with the occurrence of a fraction, that does not take substitutional lattice sites, but experiences a time-dependent quadrupole interaction. This fraction will

Fig. 38: The time integrated attenuation coefficient as function of ω_q for a level with spin 4 and $t_{1/2} = 23$ ns, for various values of η (0.0, 0.2, 0.4, 0.6, 0.8, 1.0, with 0.0 the highest values of $\overline{G_2(t)}$).



increase with increasing temperature. The time differential pattern of the anisotropy can be described with

$$G_2(t) = \sum_N s_{kN} e^{-N\delta\omega t} \quad (\text{VI.3})$$

where $\delta\omega$ is a large frequency spread as in formula (IV.2) (Be74a, Bo72, Va73). This might also explain the results of other results.

The constant c , which appears in the fitting will in these data absorb the effect of the non-substitutional fraction on the time dependent results. For the 340 K run it will probably not contain any effects of normalization errors, for these errors will have the same effect on the time integrated values as on the time differential results and the present values fit the theory for a static electric field gradient.

VI.3 General Conclusions

Despite experimental difficulties such as the short lifetime and a relatively small cross-section, these experiments yield the frequency and the unperturbed anisotropy coefficients, although not the spin and the η values.

The a_2 value of 0.42 ± 0.02 is in fair agreement with the value 0.38 predicted by the CN-model, (Hu75). It is also in agreement with the measured anisotropy of the 411 keV (Na73). The a_4 value of 0.14 ± 0.05 shows the same agreement as the a_2 value.

The ω_q value of 315 MHz is discussed in section VI.1 and indicate a quadrupole moment of 0.5 b, when it is assumed that the universal correlation of the components of the field gradient as suggested in Ra75 is true.

The TDPAD technique has the capability of measuring the quadrupole interaction, but has the drawback that it can only be performed with a pulsed beam. This gives us no possibility to place the nucleus in a particular place of a lattice TDPAC, which hasn't this drawback, has the disadvantage that the level of interest has to be fed by a long-lived parent ($t_{1/2} > 1$ day). If these techniques are performed in combination with Mossbauer and NQR experiments, both of which have their own drawbacks, one is able to measure field gradients and quadrupole moments of most nuclei in various surroundings. But the difficulties in the measurements are clearly indicated by the fact, that the theory was well developed in 1962, and only in recent years have the experimental results been available in reasonable number.

REFERENCES

- Be74 H. Bertschat, E. Recknagel, B. Spellmeyer. Phys. Rev. Lett. 32 (1974) 18.
- Be74a H. Bertschat, H. Haas, F. Pleiter, E. Recknagel, E. Schlodder, B. Spellmeyer.
Int. Conf. on Hyperfine Interactions studied in Nuclear Reactions and Decay. Conf. Uppsala 1974, p. 40.
- Be75 H. C. Binski, J. Berthier, G. Teisseron, S. Choulet. Phys. Lett. 51A (1975), 467.
- B172 J. Bleck, R. Butt, H. Haas, W. Ribbe, W. Zeitz, Phys. Rev. Lett. 29 (1972), 1371.
- Bo72 E. Bodenstedt, U. Ortabasi, W. H. Ellis, Phys. Rev. B6 (1972), 2909.
- Br62 D.M. Brink, G. R. Satchler, Angular Momentum (Oxford University Press 1962).
- Br74 R. Brenn, G. Yue, G. D. Sprouse, O. Klepper, Int. Conf. on Hyperfine Interactions studied in Nuclear Reactions and Decay. Conf. Uppsala 1974, p. 206.
- Bu74 T. Butz, G. Wortmann, G. M. Kalvius, W. B. Holsapfel, Phys. Lett. 50A (1974), 127.
- Ch67 D. C. Choudhury, T. F. O'Dwyer, Nucl. Phys. A93 (1967) 300.
- Ch72 A. Christy, O. Häusser, Nucl. Data Tables 11 (1972) 281.
- Da61 T. P. Das, M. Pomerantz, Phys. Rev. 123 (1961) 2070.
- De53 H. G. Dehmelt, Am. J. Phys. 22 (1953) 110.
- Do72 D. A. Dohan, Thesis McMaster University (unpublished) 1972.
- Fe69 F. D. Feiock, W. R. Johnson, Phys. Rev. 187 (1969) 39.
- Fr65 H. Frauenfelder and R. M. Steffen in α , β and γ ray spectroscopy Vol. II ed. K. Siegbahn (North Holland Publishing Comp. 1965).

- Ha72 Handbook of Chemistry and Physics (Chemical Rubber edition 1972).
- Ha73 H. Haas, D. A. Shirley, J. Chem. Phys. 58 (1973) 3339.
- Ha73a H. Haas, W. Leitz, H. E. Mahnke, W. Semmler, R. Sielemann, Th. Wichert, Phys. Rev. Lett. 30 (1973) 656.
- Ha74 L. Hasselgren, F. Falk, B. S. Ghuman, C. Fahlander, J. E. Thun, Int. Conf. on Hyperfine Interactions studied in Nuclear Reactions and Decay, Uppsala 1974, p. 136.
- Hu75 D. A. Hutcheon, D. M. Sheppard, P. Kitching, J. M. Davidson, C. W. Luursema, L. E. Carlson, Nucl. Phys. A245 (1975) 306.
- Lu75 C. W. Luursema, D. A. Hutcheon, Internal Report Nucl. Research Centre U. of A. added as appendix III.
- Ma62 E. Matthias, W. Schneider, R. Steffen, Phys. Rev. 125 (1962) 261.
- Ma63 E. Matthias, W. Schneider, R. Steffen, Arkiv för Physik 24 (1963) 97.
- Ma71 E. Matthias, B. Olsen, D. A. Shirley, J. E. Templeton, R. M. Steffen, Phys. Rev. A4 (1971) 1626.
- Mc72 J. M. McDonald, P. M. S. Lesser, D. B. Fossan, Phys. Rev. Lett. 28 (1972) 1057.
- Na73 M. R. Najam, L. E. Carlson, W. F. Davidson, W. M. Zuk Nucl. Phys. A211 (1973) 77.
- Ra75 R. S. Raghavan, E. N. Kaufmann, P. Raghavan. Phys. Rev. Lett. 34 (1975) 1280.
- Re74 R. C. Reno, R. L. Raseria, G. Schmidt. Phys. Lett. 50A (1974) 243.
- Ro67 H. J. Rose, D. M. Brink, Rev. Mod. Phys. 39 (1967) 306.
- St63 R. M. Sternheimer. Phys. Rev. 130 (1963) 1423.
- Va73 A. Vasquez, J. D. Rogers, A. Maciel. Phys. Lett. 45A (1973) 253.
- Wa65 R. E. Watson, A. C. Gossard, Y. Yafet. Phys. Rev. 140 (1965) A375.
- We61 F. W. de Wette. Phys. Rev. 123 (1961) 103.

APPENDIX I

TARGET HEATING

When a beam deposit its energy Q on the target, radius b and thickness d , in a circle with radius a ($a < b$) in the centre, the centre will have a higher temperature than the edge. The edge is assumed to absorb the heat without a temperature rise. The temperature as function of the radius is:

$$T(0) - T(r) = \frac{Q}{4\pi dK} \left\{ \frac{r}{a} \right\}^2 \quad r \leq a$$

$$T(r) - T(a) = \frac{Q}{2\pi dK} \ln \frac{r}{a} \quad a \leq r \leq b$$

where K is the constant of thermal conductivity.

Define $P = Q/d$, the energy loss of the beam per cm material.

In this way

$$T(b) - T(0) = \frac{P}{4\pi K} \left\{ 1 + 2 \ln \frac{b}{a} \right\}.$$

Substitute the appropriate values for 3 MeV protons on a zinc target.

$$P = 70 \frac{\text{keV}}{\text{mg/cm}^2} \times 7200 \text{ mg/cm}^2 = 504 \text{ W cm}^{-1} \mu\text{A}^{-1}$$

$$K = 1.2 \text{ W / (cm K)}$$

for	b/a	=	3.0	ΔT	=	106.9	K/ μA
		=	2.7			99.8	
		=	2.5			94.7	
		=	2.0			79.7	
		=	1.8			72.7	

The sublimation rate of zinc, which was used as a check on the approximate temperature can easily be calculated. Every material has a vapor pressure, which will be pumped away in the high vacuum beam line. This pressure is given by

$$p_0 = \frac{1}{3} \rho \overline{v^2}$$

where ρ is the density of the gas and v the velocity of the gas molecules. Per unit time the average distance travelled by the molecules is v_{av} . The mass escaping per unit time and per unit area is

$$\Delta m = 3 p_0 v_{av} / \overline{v^2}$$

$$= p_0 \sqrt{\frac{8m}{\pi kT}}$$

(For the formulae for v_{av} and $\overline{v^2}$ see ref. 1).

With the vapor pressure quoted in ref. 2 the sublimation rate of ^{70}Zn can be calculated and the values are tabulated in Table 4.

TABLE 4
 SUBLIMATION RATE OF ZINC AS FUNCTION
 OF THE TEMPERATURE

T (K)	p_0 (mm Hg)	Δm ($\mu\text{g}/\text{cm}^2\text{s}$)
421	10^{-10}	9.7×10^{-5}
449	10^{-9}	9.4×10^{-4}
481	10^{-8}	9.1×10^{-3}
517	10^{-7}	8.8×10^{-2}
559	10^{-6}	8.4×10^{-1}
611	10^{-5}	8.1×10^0

ref. 1 D. Halliday, R. Resnik, Physics (J. Wiley and Sons, N.Y., 1966)

ref. 2 American Institute of Physics Handbook, ed. D. E. Gray, 1972, p. 4 - 300.

APPENDIX II

THE LEVEL SCHEME OF ^{70}Ga IN THE INTERMEDIATE COUPLING MODEL

The Intermediate Coupling Model couples one or two particles in shell model states outside an even-even core to the vibrations of the core. The coupling is characterized by the energy of the phonons, the number of phonons and the coupling constant ξ (Ch67).

For ^{70}Ga the even-even core is ^{68}Zn . An estimate of the phonon energy of this nucleus is 1 MeV. The particle levels can be taken as the single-particle levels of ^{57}Ni and yield for the energies

$$E(|2p\ 3/2\rangle) = 0.0\ \text{MeV}$$

$$E(|1f\ 5/2\rangle) = 0.78\ \text{MeV}$$

$$E(|2p\ 1/2\rangle) = 1.08\ \text{MeV}$$

$$E(|1g\ 9/2\rangle) = 2.00\ \text{MeV}$$

except for the g 9/2 state, which is not observed in ^{57}Ni . The quoted value is the estimate of Dohan (Do72).

When the calculations are done with one phonon and 3 orbitals available for the proton and 2 orbitals for the neutron, the results predict a reasonable part of the observed level scheme. The other levels might have an admixture of two-phonon states.

The 4^- state at the calculated energy of 795 keV above the lowest state is built up as:

$$\begin{aligned}
 |4^- \rangle = & 0.977 |0; p_{3/2} g_{9/2}; 4\rangle + 0.017 |0; f_{5/2} g_{9/2}; 4\rangle + \\
 & -0.030 |0; p_{1/2} g_{9/2}; 4\rangle - 0.140 |1; p_{3/2} g_{9/2}; 3\rangle + \\
 & -0.084 |1; p_{3/2} g_{9/2}; 4\rangle + 0.062 |1; p_{3/2} g_{9/2}; 5\rangle + \\
 & -0.079 |1; p_{3/2} g_{9/2}; 6\rangle - 0.028 |1; f_{5/2} g_{9/2}; 2\rangle + \\
 & +0.024 |1; f_{5/2} g_{9/2}; 3\rangle - 0.004 |1; f_{5/2} g_{9/2}; 4\rangle + \\
 & -0.020 |1; f_{5/2} g_{9/2}; 5\rangle + 0.034 |1; f_{5/2} g_{9/2}; 6\rangle + \\
 & +0.042 |1; p_{1/2} g_{9/2}; 4\rangle - 0.058 |1; p_{1/2} g_{9/2}; 5\rangle
 \end{aligned}$$

where $|1; f_{5/2} g_{9/2}; 4\rangle$ means a state with 1 phonon, the proton in the $f_{5/2}$ orbit, the neutron in the $g_{9/2}$ orbit and both particles coupled to spin 5.

Exp.		Calc.	
$E(\text{keV})$	J^π	$E(\text{keV})$	J^π
		1110	3^-
		1094	1^+
996	2^+	998	0^+
901	4^+	925	4^+
879	4^-	912	2^+
691	2^-		
651	1^+		
508	2^+	475	2^+
		130	1^+
0	1^+		

Fig. 39: Comparison between the experimental and calculated level scheme for ^{70}Ga . The calculation is done with one phonon in the Intermediate Coupling Model.

APPENDIX III

INTERNAL REPORT #77

PROGRAM TDPAD

PROGRAM TDPAD

*Nuclear Research Centre
University of Alberta
Edmonton, Alberta*

INTERNAL REPORT #77

C.W. Luursema, and D.A. Hutcheon

Introduction

This program is meant for the analysis of a time dependent γ ray angular distribution due to static electric Quadrupole Interaction in randomly oriented microcrystals with the plane of detection containing the beam. It starts with time-delay spectra of the transition of interest and of background data for two or more angles and gives the least χ^2 fit parameters to the theoretical formula.

It is developed for the SDS, 940 for the Nuclear Research Centre, makes use of all 32K core and works only with Rad Monarch system.

TDPAD is a Fortran Linking program consisting out of three links. The three links 'Data', fitting the raw data to the anisotropy coefficients at various delay times, 'Display', fitting the coefficients to the theoretical expression and central processor and 'Sun' calculating the S_{kN} coefficients, are reasonably independent so the program doesn't switch very often during running.

It is assumed that the raw data, i.e. the yield as function of delay, are stored in maximal 1024 channels with the time running backwards, i.e. increasing channel number corresponds to decreasing delay.

Time dependent Perturbed Angular Distribution is given by (all refs.)

$$W(\theta) = \sum_k (a_k G_k(t) + c) P_k(\cos\theta)$$

where c is a time independent constant.

$$G_k(t) = \sum_{qmm''} \frac{1}{2k+1} (I -m I m' | k q) \times \\ \sum_{nn'} (I -m'' I m'' | k q) e^{-i(E_n - E_{n'})t/\hbar} \times$$

$$U_{mn} U_{m''n}^* U_{m''n'} U_{m'n'}^*$$

where U is the transformation matrix which diagonalizes the Hamiltonian ($UHU^{-1} = E$).

Since $(E_n - E_{n'}) = -(E_{n'} - E_n)$ we end up with only cosine terms

$$G_k(t) = \sum_N s_{kN} \cos N\omega t$$

where $\omega = e^2 q Q / \hbar$ and $N = \frac{(E_n - E_{n'})}{e^2 q Q}$

The Hamiltonian is given by the elements

$$H_{m,m} = \frac{eQ}{4I(2I-1)} (3m^2 - I(I+1)) V_{zz}$$

$$H_{m,m\pm 2} = \eta \frac{eQ}{4I(2I-1)} \times \\ \{(I \mp m-1)(I \mp m)(I \pm m+1)(I \pm m+2)\}$$

with $V_{zz} = \frac{\partial^2}{\partial z^2} V$, evaluated at the nuclear site

and $\eta = \frac{V_{yy} - V_{xx}}{V_{zz}}$ and $0 \leq \eta \leq 1$

By taking into account a spread of frequencies around the central one and a finite resolution time of the detecting system, the formula is:

$$G_k(t) = \sum_N S_{kN} \cos N \omega t e^{-\delta \omega N t} e^{-1/2(\omega N \tau)^2}$$

$\delta \omega$ = absolute frequency spread

τ = resolution time of system

The fitting is done to

$$a_k(t) = G_k(t) a_k(0) + c,$$

where c is a time-independent constant.

Procedure

The program is split up in three parts

- (a) 'Data'. This part reads in the data from magnetic tape unit number 1 and calculates the a_k coefficients as a function of time. The input data consist of the time spectrum for the region of interest and the appropriate background spectrum, both should be in the same run on the tape. It is possible that there are two angles in one run. After reading in data for a least two angles, it orders the data into groups (maximum of 512) and fits each group to

$$W(\theta) = \sum_k a_k P_k(\cos \theta) \text{ for } k=0,2,4.$$

If desired a list of calculated values and their errors is printed out (time runs backwards on this list).

The search for next runs is according to run number, i.e. a higher run number causes a search forward of the tape and a lower search backwards. By reading in a faked high or low run number with a blank card behind it, it is possible to direct the search freely without changing the data.

- (b) 'Display' The central processing and fitting unit. This part asks for the other information necessary for fitting to the formula.
- (1) The out put from 'Data', i.e. $a_k(0)$ and the error in $a_k(0)$. After calculation of $a_k(0)$ and χ^2 it can be directed to all parts of the program (see listing in Table I). The program types after each step the number of channels used for the fit, the $a_k(0)$ value, its the error in $a_k(0)$ and the χ^2 .
- (c) 'Sun' This part calculates the S_{kN} coefficients and the values of N for formula (1) as function of spin, η and k. It calculates the matrix and diagonalizes it with the method of Jacobi then it calculates S_{kN} for each N, making use of the fact that for each n only half of the magnetic substates contribute.

Table I List of options in 'Display' on question '0'

0. Types out all possibilities.
1. Goes to 'Data' and read in new set of data.
2. Goes to 'Sun' and asks for new values of k, spin and η and recalculates S_{kN} and N.
3. Print out all relevant parameters, e.g. S_{kN} coefficients, N-values, $a_k(0)$, error in $a_k(0)$, χ^2 , spin, η , k first and last channel of the region of fitting, time-zero, frequency, spread in frequency and fudge.
4. Asks for new value of time-zero.
5. Asks for new region of fitting.
6. Asks for a new frequency, constant term and relative spread.
7. Goes to show-routine, which shows experimental data with upper and lower limit of the error bar, the calculated curve and the zero line

if the upper and lower limits (amax and amin) contain zero. To leave this routine set breakpoint 4.

8. Goes to the plotting routine, if and only if the program has displayed the data after the last calculation, otherwise it does the same as 7.
9. Goes to the plotting routine, taking old values for the plotting parameters except for YOFF, unless they are zero, in which case it goes to 7.

Input for Data

Card I: NGRP, NCPG, NLEG, IDIR, TITLE (FORMAT 414, 10A4).

NGRP number of groups less than 513.

NCPG number of channels per group $\text{NGRP} * \text{NCPG} \leq 1024$.

NLEG number of Legendre polynomials (maximum 3).

IDIR direction first search (0 forward, 1 backward).

Title (less than 40 characters).

Card II: Date, Month, Year Run, Angle

Format 413, F6.0.

Year = 0 calculations follows.

Card III: IBASE, ZNORM

FORMAT 15, F7.3

IBASE: First Channel of spectrum to be read.

ZNORM: Normalization constant with which the data are multiplied before processing. $\text{ZNORM} < 0$ Background

$\text{ZNORM} > 0$ Real data

$\text{ZNORM} = 0$ go to next angle.

So proper order is:

I, II, III (background), III(real data), III(blank), II, III(background),
III(real data), III(blank), II(blank)

Teletype input

PRINT YES(1) OR NO (0) (11)

1: PRINTS out ALL a_k for each group normalized to $a_0=1$ and not normalized with group number, error in a_k and χ^2 of fit for each group.

0: Suppresses this output, and this information is lost, except for the nomalized values, which are used by 'DISPLAY' and may be plotted.

ENTER 1 TO RESTART, 0 TO EXIT (11)

1: Begins again at the beginning of the program (reread all data)

0: Stops

Resolution Time (FWHM)

Floating point input of the resolution time of the electronics and detector expressed in number of groups.

FREQ IN RAD/GR, C, REL SPREAD

Format 3F10.0

Asks for the essential parameters in the formulae, the frequency being ω_q and relative spread being $\frac{\delta\omega}{\omega_q}$

TZ(F 10.0)

Input of time zero, as group number according to the output listing of 'Data'.

AMIN, AMAX

The lower and upper limit of the values for the show-routine and for the plot routine. Values outside this region are set to the upper or lower limit.

GROUPS/INCH, YSC, YOFF (Floating point)

GROUPS/INCH X-scale

YSC, number of inches over which the y-scale extends.

YOFF, vertical offset of AMIN in inches, zero being point of pen location.

EXP(1) CAL(2), AXIS(3), SLEW(4), DONE(5)

Format I1

1. Plots experimental error bars.
2. Plots the current theoretical curve.
3. Plots the x-and y-axis, from time-zero to the last channel to plot and the y-axis from amin to amax, and x-axis at $a_k=0$ and the y-axis on time =0.
4. Slews the paper up till the second integer inch after the plot and cannot be returned.
5. Returns to the rest of the program.

Plot same as above

Other questions are self-explanatory.

All input parameters are floating point unless otherwise indicated.

References

1. C.W. Luursema, Thesis University of Alberta (October 1975).
2. H. Frauenfelder and R. Steffen, In α , β and γ ray Spectroscopy.
Ed. K. Siegbahn, North-holland Publishing Co. A'dam ('65).
3. H. Haas and D.A. Shirley, Journal of Chemical Physics 58, 3339 ('73).
4. E. Matthias, W. Schneider and R.M. Steffen,
Physics Letters 4, 41 ('63).
5. E. Bodenstedt, In 'Angular Correlations in Nuclear Disintegration'.
Rotterdam University Press, Groningen, Nederland, Ed. H. van Krugten
and B. van Nooyen ('71).

LISTING OF THE PROGRAM


```

1 LINK 1
2 DATA
3
4 FITTING DATA TO ANGULAR DISTRIBUTIONS
5 FIRST OF THREE PROGRAMS TO HANDLE DATA
6 OF PERTURBED ANGULAR DISTRIBUTION DUE TO EFG
7
8 DIMENSION TITLE(10),WMAT(3,3,171),DVEC(4,512),KS(1024)
9 DIMENSION INFO(26),X(3),WINV(3,3),A(3),ERR(3)
10 DIMENSION SUMSQ( 512)
11 DIMENSION DUM(1691),DST0(4,171)
12 COMMON DUM,CRAP,AKP,NI,IT,TZ,SIP,ICL,ICU,W,FUD,SPR,NGRP,ETA
13 EQUIVALENCE (DUM(1),WMAT(1),DST0(1))
14 EQUIVALENCE (VAR,TEMP)
15
16 CONTINUE
17 1000
18 5001
19 TYPE 6001
20
21 OUTPUT LIST
22
23 FORMAT ($PRINT N0(0),YES(1)$)
24 ACCEPT 6002,IK
25 FORMAT (I1)
26
27 READ MAIN PARAMETERS
28
29 READ 200,NGRP,NCPG,NLEG,IDIR,(TITLE(I),I=1,10)
30 FORMAT(4I4,10A4)
31 PRINT 220,NGRP,NCPG,NLEG,IDIR
32 FORMAT(1H1,I3,$ GROUPS $,I3,$ CH/GRP $,I1,$ POLYS $,I1,$ F/R$)
33 IF(NGRP)1,1,2002
34 STOP
35
36 CHECK SIZES OF THINGS

```


37	2002	KSSIZE=NGRP*NCPG
38		IF(NGRP-512)2003,2003,180
39	2003	IF(KSSIZE-1024)2004,2004,181
40	2004	IF(NLEG-3)2005,2005,182
41	2005	IF(IDIR-1)2006,2006,183
42	2006	IF (IDIR) 6010,6010,6011
43	6010	IRUN=0
44		GETB 6012
45	6011	IRUN=1000.
46	6012	CENTINUE
47	C	
48	C	INITIALIZE MATRICES
49	C	
50		DB 61 J=1,512
51		DVEC(4,J)=0.
52	61	SUMSQ(J)=0.
53		ZHOLD=0.
54		DB 9 L=0,2
55		CALL MEMSWT(L+5)
56		DB 9 I=1,171
57		IP=I+L*171
58		DB 8 J=1,3
59		DB 7 K=1,3
60	7	WMAT(K,J,I)=0.
61	8	DVEC(J,IP)=0.
62	9	CENTINUE
63	C	
64		CALL INITKS(1,KS,KSSIZE)
65	C	
66	C	READ CARD FOR MIDDLE LOOP
67	C	
68	10	READ 201,(INF0(J),J=3,6),THETA
69		PRINT 221,(INF0(J),J=3,6),THETA
70	201	FORMAT(4I3,F6.1)
71	221	FORMAT(5X,\$D,M,Y,RUN,ANGLE \$,3I3,15,2X,F6.1)
72		IF(INF0(5)-1)30,30,2011


```

73 2011 THETA=3.1416*THETA/180.
74 YX=COS(THETA)
75 YX=YX*YX
76 X(1)=1.
77 X(2)=1.5*YX*0.5
78 X(3)=0.125*(35.*YX*YX - 30.*YX + 3.0)
79 IS=1
80 IF (INF0(6)-IRUN)6004,6004,6005
81 IS=3
82 IRUN=INF0(6)
83
84 READ CARD FOR INNER LOOP
85
86 READ 202,IBASE,ZN0RM
87 FORMAT(15,F7.3)
88 PRINT 222,IBASE,ZN0RM
89 FORMAT(10X,I5,2X,F7.3)
90 IF(ZN0RM-0.)219,21,22
91 GO TO 10
92 ZH0LD=ZN0RM
93 CALL READKS(IS,IBASE,INF0,IERR)
94 IF(IERR-2)23,184,184
95 IS=3
96
97 DATA READ IS OK, NOW PROCESS IT
98
99 DO 29 L=0,2
100 CALL MEMSWT(L+5)
101 DO 29 IP=1,171
102 I=IP+L*171
103 IF (NGRP-I)20,2023,2023
104 IBEG=(I-1)*NCPG+1
105 IEND=IBEG+NCPG-1
106 SUM=0.
107 DO 2024 J=IBEG,IEND
108 SUM=SUM+FL0AT(KS(J))

```


109		IF(ZN0RM)241,21,249				
110	241	DVEC(4,I)=SUM				
111		GO TO 29				
112	249	VAR=ZN0RM*ZN0RM*SUM+ZH0LD*ZH0LD*DVEC(4,I)				
113		SUM=SUM*ZN0RM+DVEC(4,I)*ZH0LD				
114		IF(VAR-10.)25,26,26				
115	25	VAR=10.				
116	26	DO 28 J=1,NLEG				
117		DVEC(J,I)=DVEC(J,I)+SUM*X(J)/VAR				
118		DO 2027 K=1,NLEG				
119	2027	WMAT(K,J,IP)=WMAT(K,J,IP)+X(J)*X(K)/VAR				
120	28	CONTINUE				
121		SUMSQ(I)=SUMSQ(I)+SUM*SUM/VAR				
122		DVEC(4,I)=0.				
123	29	CONTINUE				
124		GO TO 20				
125	C					
126	C					
127	C	INVERT MATRIX, CALC. COEFFS AND ERRORS				
128	C					
129	30	IF (IK) 4004,4004,4003				
130	4003	PRINT 203,(TITLE(I),I=1,10)				
131	203	FORMAT(10A4,/,,\$ GR0UP A0	ERR	A2		
132	4004	TYPE 4008,(TITLE(I),I=1,10)				
133	4008	FORMAT(10A4)				
134		DO 50 L=0,2				
135		CALL MEMSWT(L+5)				
136		DO 50 K=1,171				
137		KA=K+L*171				
138		IF (NGRP-KA) 51,4002,4002				
139	4002	GO TO (2031, 32,33),NLEG				
140	2031	DET=WMAT(1,1,K)				
141		IF(DET)311,485,311				
142	485	PRINT 207,KA				
143	207	FORMAT(1X,I3,\$ MATRIX SINGULAR\$)				
144		GO TO 50				


```

145 311 WINV(1,1)=1./DET
146 GO TO 34
147 32 DET=WMAT(1,1,K)*WMAT(2,2,K)-WMAT(1,2,K)*WMAT(2,1,K)
148 IF(DET) 321,485,321
149 321 WINV(1,1)=WMAT(2,2,K)/DET
150 WINV(2,1)=-WMAT(1,2,K)/DET
151 WINV(1,2)=WINV(2,1)
152 WINV(2,2)=WMAT(1,1,K)/DET
153 GO TO 34
154 33 C0F11=WMAT(2,2,K)*WMAT(3,3,K)-WMAT(2,3,K)*WMAT(3,2,K)
155 C0F12=WMAT(2,3,K)*WMAT(3,1,K)-WMAT(2,1,K)*WMAT(3,3,K)
156 C0F13=WMAT(2,1,K)*WMAT(3,2,K)-WMAT(2,2,K)*WMAT(3,1,K)
157 C0F22=WMAT(1,1,K)*WMAT(3,3,K)-WMAT(1,3,K)*WMAT(3,1,K)
158 C0F23=WMAT(1,2,K)*WMAT(3,1,K)-WMAT(1,1,K)*WMAT(3,2,K)
159 C0F33=WMAT(1,1,K)*WMAT(2,2,K)-WMAT(1,2,K)*WMAT(2,1,K)
160 DET=WMAT(1,1,K)*C0F11 + WMAT(1,2,K)*C0F12 + WMAT(1,3,K)*C0F13
161 IF(DET)331,485,331
162 331 WINV(1,1)=C0F11/DET
163 WINV(1,2)=C0F12/DET
164 WINV(2,1)=WINV(1,2)
165 WINV(1,3)=C0F13/DET
166 WINV(3,1)=WINV(1,3)
167 WINV(2,2)=C0F22/DET
168 WINV(2,3)=C0F23/DET
169 WINV(3,2)=WINV(2,3)
170 WINV(3,3)=C0F33/DET
171 C
172 34 DO 36 I=1,NLEG
173 A(I)=0.
174 DO 35 J=1,NLEG
175 A(I)=A(I)+WINV(I,J)*DVEC(J,KA)
176 36 ERR(I)=SQRT(WINV(I,I))
177 C
178 C CALCULATE CHI**2
179 CHISQ=0.
180 DO 362 I=1,NLEG

```



```

181 SUM=0.
182 DO 361 J=1,NLEG
183 SUM=SUM+WMAT(I,J,K)*A(J)
184 CHISQ=CHISQ+SUM*A(I) - 2.*A(I)*DVEC(I,KA)
185 CHISQ=CHISQ+SUMSQ(KA)
186
187 PRINT RESULTS
188
189 IF (IK) 4006,4006,4005
190 PRINT 204,KA,(A(I),ERR(I),I=1,NLEG),CHISQ
191 FORMAT(1X,I3,2X,4(F8.1,1X,F5.1,1X))
192 IF(A(1)=0.)50,50,37
193 IF(NLEG=1)50,50,38
194 DO 41 J=2,NLEG
195 TEMP=A(J)*A(J)*WINV(1,1)/A(1)**4 -2.0*A(J)*WINV(1,J)/A(1)**3
196 1 +WINV(J,J)/A(1)**2
197 IF(TEMP)39,39,40
198 TEMP=9801.
199 ERR(J)=SQRT(TEMP)
200 A(J)=A(J)/A(1)
201 DVEC(3,KA)=A(3)
202 DVEC(1,KA)=A(2)
203 DVEC(2,KA)=ERR(2)
204 DVEC(4,KA)=ERR(3)
205 IF (IK) 50,50,4007
206 PRINT 205,(A(J),ERR(J),J=2,NLEG)
207 FORMAT( 9X,$1.0$,8X,2(F8.3,1X,F5.3,1X))
208 CONTINUE
209
210 STORE RESULTS FOR NEXT PARTS
211
212 CALL MEMSWT(4)
213 DO 400 K=1,NGRP
214 DO 401 I=1,4
215 DST0(I,K)=DVEC(I,K)
216 CONTINUE

```



```

217 CALL MEMSWT(3)
218 IF (IT)500,500,501
219 CALL LINK(2)
220 CALL LINK(3)
221 C
222 C
223 C
224 TYPE 230
225 TYPE 231
226 ACCEPT 6002,IN
227 IF(IN-1) 1,1000,1
228 FORMAT($ ENTER 1 TO RESTART, 0 TO EXIT (I1)$)
229 FORMAT($ 512 GROUPS MAX $)
230 C
231 TYPE 232
232 FORMAT($ 1024 MAX TOTAL CHANNELS$)
233 GO TO 1801
234 TYPE 233
235 FORMAT($ 3 LEGENDRE POLYS. MAX $)
236 GO TO 1801
237 TYPE 234
238 FORMAT($ DIRECTION CONTROL MUST BE 0 OR 1 $)
239 GO TO 1801
240 TYPE 235, IERR
241 FORMAT($ TAPE READ ERROR $,I2)
242 GO TO 1801
243 END

```



```

1 LINK 2
2 DISPLAY
3
4 FIT TO FORMULA FOR QUADRUPOLE INTERACTION PERTURBATION
5 AND OUTPUT ROUTINES
6
7 DIMENSION KC(512), IR(6), KSADR(4), LIST(5), IREP(4), IORG(4), IFR0(4)
8 DIMENSION IBAC(4)
9   DIMENSION DVEC(4,171), SKN(106), XN(106)
10  DIMENSION KB(512), KL(512), KU(512)
11  DIMENSION SUN(106), XUN(106)
12  DIMENSION DUM(1691)
13  COMMON DUM, CRAP, AK, NN, IT, TZ, SI, ICL, ICU, W, FUD, SPR, NGRP, ET
14  EQUIVALENCE(DUM(1), DVEC(1), SUN(1))
15  EQUIVALENCE(DUM(107), XUN(1))
16  EQUIVALENCE(DUM(358), TR)
17
18 2ND OF 3 PROGRAMS TO HANDLE DATA OF TDPAD
19
20 TYPE 108
21 FORMAT ($RESOLUTION TIME (FWHM)$)
22 ACCEPT 102, TR
23 TR=TR/2.3548
24 IF (IT) 5006, 5006, 4999
25
26 TYPE 103
27 CALL MEMSWT(3)
28 ACCEPT 102, W, FUD, SPR
29 FORMAT($FREQ IN RAD/GROUP, CONST, .REL SPREAD $)
30
31 DO1 I=1, NN
32 SKN(I)=SUN(I)*EXP(-.5*(W*XUN(I)*TR)**2)
33 XN(I)=XUN(I)
34 CALL MEMSWT(4)
35 IF (IT) 5004, 5004, 5000
36

```



```

37 C      GOTO PRGR 1 DATA INPUT AND A2/A4 CALCULATION
38 C
39 5001 CALL MEMSWT(3)
40 CALL LINK(1)
41 C
42 C      GOTO PRGR 3 CALCULATION OF SKN COEFF.
43 C
44 5002 CALL MEMSWT(3)
45 CALL LINK(3)
46 FORMAT(10F10.5)
47 FORMAT( I3,F10.0)
48 C
49 C      PRINT OUT RELEVANT PARAMETERS
50 C
51 5003 PRINT 155,SI,ET,AK
52 155  FORMAT(/,6H SPIN= , F4.1,6H ETA= ,F6.3,6H K=,I1)
53
54 151  FORMAT($ NUM FREQ=$ ,I3)
55 PRINT 201
56 201  FORMAT(/,$XN(I)$)
57 PRINT 102,(XN(I),I=1,NN)
58 PRINT 202
59 202  FORMAT(/,$SKN(I)$)
60 PRINT 102,(SKN(L),L=1,NN)
61 PRINT 156,TZ,ICL,ICU,W,SPR,FUD
62 156  FORMAT(5H TZ=,F5.1,6H ICL=,I3,6H ICU=,I3,4H W=,F7.3,6H SPR=,
63 1 F4.3,6H FUD=,F4.3)
64 PRINT 104,AZ,DAZ,CHI
65 GOTO 5013
66 C
67 C      INPUT TIMEZERO, ACCORDING TO OUTPUT LIST OF A2/A4
68 C
69 5004 TYPE 5100
70 5100 FORMAT ($TZ (F10.0)$)
71 ACCEPT 5110,TZ
72 5110 FORMAT (F10.0)

```



```

73 TZ =NGRP-TZ
74 IF (IT) 5005,5005,5000
75
76 TYPE 4001
77 FORMAT($ LOWER, UPPER GROUP FOR FITTING$)
78 ACCEPT 4002, ICL,ICU
79 FORMAT(2F5.0)
80
81 C
82 FITTING CALCULATION
83 SQ=0.
84 AB=0.
85 DVEB=0.
86 P=FIX(AK+.1)
87 WMAB=0.
88 NF=ICU-ICL+1
89 DO 4 J=NGRP-ICU+1,NGRP-ICL+1
90 WT=(FLOAT(J-1)-TZ)*W
91 CAL=0.
92 I=NGRP-J+1
93
94 C
95 CAST OUT ZERO ERRORS
96
97 IF (DVEC(P,I))2,6,2
98 DO 3 N=1,NN
99 CAL=CAL+SKN(N)*COS(XN(N)*WT)*EXP(-XN(N)*SPR*WT)
100 SQ=SQ+((DVEC(P-1,I)-FUD)/DVEC(P,I))**2
101 DVEB=DVEB+(DVEC(P-1,I)-FUD)*CAL/DVEC(P,I)**2
102 WMAB=WMAB+(CAL/DVEC(P,I))**2
103 GOT0 4
104 NF=NF-1
105 CONTINUE
106 AZ=DVEB/WMAB
107 DAZ=SQRT(1./WMAB)
108 CHI=SQ+AZ*AZ*WMAB-2.*DVEB*AZ
109 TYPE 107,NF
110 FORMAT(6H NF=,I3)

```



```

TYPE 104,AZ,DAZ,CHI
FORMAT($ T=O C$EFF,ERROR $,2F7.3,$ CHI**2=$,F7.1)
WHAT TO DO NEXT
IT=1
TYPE 105
FORMAT ($0$)
ACCEPT 106,IJ
FORMAT(I1)
IJ=IJ+1
GOTO(5010,5001,5002,5003,5004,5005,5006,5007,5008,5009),IJ
TYPE 5011
FORMAT($DATA(1),S(K,N) (2),PRINT (3),TZ (4),FIT REGION (5),FREQ.
1 (6),SHOW (7),PLOT (8),PLOT (9),(I1)$)
GOTO 5012
DISPLAY DATA AND FITTED VALUES
TYPE 110
FORMAT($ AMIN,AMAX $)
ACCEPT 102, AMIN,AMAX
IF(AMIN*AMAX)12,12,14
DO 13 J=1,NGRP
KB(J)=FIX(-1000.*AMIN/(AMAX-AMIN))
D02023J=1,NGRP
I=NGRP-J+1
XX=DVEC(P-1,I)+DVEC(P,I)
IF (XX-AMIN) 6015,6016,6016
XX=AMIN
IF (AMAX-XX) 15,16,16
XX=AMAX
KU(J)=FIX(1000.*(XX-AMIN)/(AMAX-AMIN))
XX=DVEC(P-1,I)-DVEC(P,I)
IF (AMAX-XX) 6017,6018,6018
XX=AMAX

```



```

145 6018 IF (XX=AMIN) 17,18,18
146 17 XX=AMIN
147 18 KL(J)=FIX(1000.*(XX=AMIN)/(AMAX=AMIN))
148 18 WT=(FL0AT(J-1)-TZ)*W
149 18 XX=0.
150 19 D0 19 N=1,NN
151 19 XX=XX+AZ*SKN(N) *COS(XN(N)*WT)*EXP(-XN(N)*SPR*WT)
152 19 XX=XX+FUD
153 200 IF (XX=AMIN)200,201,2021
154 200 XX=AMIN
155 201 IF (AMAX=XX)202,203,2023
156 202 XX=AMAX
157 203 KC(J)=FIX(1000.*(XX=AMIN)/(AMAX=AMIN))
158 158 KSADR(1)=L0CF(KC(1))
159 159 KSADR(2)=L0CF(KU(1))
160 160 KSADR(3)=L0CF(KL(1))
161 161 KSADR(4)=L0CF(KB(1))
162 162 D0 24 J=1,4
163 163 IREP(J)=1
164 164 I0RG(J)=0
165 165 IFR0(J)=0
166 166 IBAC(J)=NGRP
167 24 LIST(J)=J
168 24 LIST(5)=0
169 2025 IF (AMIN*AMAX)2026,2026,2025
170 2025 LIST(4)=0
171 2026 IREP(1)=2
172 172 CALL SH0SET(IREP,I0RG,KSADR,IFR0,IBAC)
173 27 CALL SH0W(0,LIST,IR)
174 174 IF (IR(2))5,2028,2028
175 2028 LIST(4)=0
176 176 IF (IR(1))2029,2029,2026
177 2029 LIST(4)=4
178 178 G0 T0 27
179 5 IT=2
180 180 G0T0 5013

```



```

181 C
182 C
183 C
184 5008
185 129
186 131
187
188
189 4101
190
191 4102
192 5700
193 130
194
195 31
196 5710
197 5720
198
199 2032
200 C
201 C
202 C
203 2033
204
205
206
207
208
209
210
211 2331
212
213
214
215
216

```

```

      PLOT ROUTINE
      IF (IT-1) 5000,5007,129
      TYPE 131
      FORMAT($ GROUPS/INCH, YSC,YOFF $)
      ACCEPT 102,GPI,YSC,YOFF
      TYPE 4101
      FORMAT($FIRST AND LAST GROUP TO PLOT$)
      ACCEPT 4102, ICK,ICV
      FORMAT (2F5.0)
      TYPE 130
      FORMAT($ EXPT(1) OR CAL(2), AXIS(3), SLEW (4), DONE(5)$)
      GOT0 5720
      TYPE 5710
      FORMAT ($PLOT$)
      ACCEPT 106,IJ
      IF(IJ*(6-IJ))5700,5700,2032
      GOT0 (2033,2050,5500,5600,5013),IJ
      PLOT EXPERIMENTAL VALUES
      D0 2034 J=NGRP-ICV+1,NGRP-ICK+1
      XX=(-TZ+FL0AT(J-1))/GPI
      IX=FIX(200.*XX)
      XX=Y0FF+(FL0AT(KL(J))/1000.)*YSC
      IY=FIX(200.*XX)
      IFC=0
      CALL DRAW(IFC,IX,IY,M)
      IF (M*(3-M)) 2331,2331,65
      IFC=1
      XX=Y0FF+(FL0AT(KU(J))/1000.)*YSC
      IY=FIX(200.*XX)
      CALL DRAW(IFC,IX,IY,M)
      IF(M*(3-M))2034,2034,65
      CONTINUE

```



```

217 GO TO 65
218
219 C
220 C
221 C
222 C
223 C
224 C
225 C
226 C
227 C
228 C
229 C
230 C
231 C
232 C
233 C
234 C
235 C
236 C
237 C
238 C
239 C
240 C
241 C
242 C
243 C
244 C
245 C
246 C
247 C
248 C
249 C
250 C
251 C
252 C

PL0T CALCULATED VALUES

TYPE 150
FORMAT($ P0INTS/GR0UP $)
ACCEPT 102,PPG
WTP=W/PPG
NT0T=IFIX((FL0AT(NGRP-ICK)-TZ)*PPG)
IFC=0
D0 56 J=1,NT0T
XT=FL0AT(J-1)*WTP
XX=0.
D0 51 N=1,NN
XX=XX+AZ*SKN(N) *COS(XN(N)*XT)*EXP(-XN(N)*SPR*XT)
XX=XX+FUD
IF(XX-AMIN)52,52,53
XX=AMIN
IF(AMAX-XX)54,55,55
XX=AMAX
XX=Y0FF+(XX-AMIN)*YSC/(AMAX-AMIN)
IY=IFIX(200.*XX)
IX=IFIX(200.*FL0AT(J-1)/(PPG*GPI))
CALL DRAW(IFC,IX,IY,M)
IFC=1
IF(M*(3-M))56,56,65
CONTINUE
G0T0 65

PL0T AXIS

XX=Y0FF
IY=IFIX(200.*XX)
IX=0
IFC=0
CALL DRAW(IFC,IX,IY,M)

```



```

253 IF (M*(3-M)) 5510,5510,65
254 XX=Y0FF+YSC
255 IY=IFIX(200.*XX)
256 IFC=1
257 CALL DRAW(IFC,IX,IY,M)
258 IF (M*(3-M)) 5520,5520,65
259 XX=Y0FF-AMIN*YSC/(AMAX-AMIN)
260 IY=IFIX(200.*XX)
261 IFC=0
262 CALL DRAW(IFC,IX,IY,M)
263 IF (M*(3-M)) 5530,5530,65
264 XX=(NGRP-TZ-ICK)/GPI
265 IX=IFIX(200.*XX)
266 IFC=1
267 CALL DRAW(IFC,IX,IY,M)
268 C
269 C
270 65
271 IFC=0
272 IX=0
273 IY=0
274 CALL DRAW(IFC,IX,IY,M)
275 GOT0 31
276 C
277 SLEW PAPER
278 C
279 XX=(NGRP-TZ-ICK)/GPI
280 IX=IFIX(XX+3)
281 IX=200*IX
282 IY=0
283 IFC=2
284 CALL DRAW(IFC,IX,IY,M)
285 IF (M*(3-M)) 31,31,65
286 C
287 PLOT WITHOUT CHANGING GPI,YSC AND CHANNELS
288 C
5009 IF (GPI) 5007,5008,5900

```



```
289 TYPE 5901
290 F0RMAT($Y0FF$)
291 ACCEPT 102,Y0FF
292 G0T0 31
293 END
```



```

1  C      LINK 3
2  C      SUN
3  C
4  C      CALCULATION OF SKN COEFFICIENTS AS FUNCTION OF SPIN AND ETA
5  C      FOR NON-AXIAL SYMMETRIC EFG
6  C      THIRD PROGRAM OF THREE TO HANDLE DATA
7  C
8  C      DIMENSION CL(15,9)
9  C      DIMENSION H(15,15),U(15,15),VALU(15)
10 C      DIMENSION XV(106),SKN(106)
11 C      DIMENSION DUM(1691)
12 C      COMMON DUM,CRAP,AKP,NI,IT,TZ,SIP,ICL,ICU,W,FUD,SPR,NGRP,ET
13 C      EQUIVALENCE (DUM(1),SKN(1))
14 C      EQUIVALENCE(DUM(107),XV(1))
15 C      EQUIVALENCE(DUM(215),CL(1))
16 C
17 C      PARAMETERS MATCHED WITH OTHER PARTS
18 C
19 C      TYPE 3003
20 C      FORMAT($A2 (2) OR A4 (4) (I1)$)
21 C      ACCEPT 3001,(AK)
22 C      FORMAT (I1)
23 C
24 C      TYPE 101
25 C      FORMAT($SPIN,ETA$)
26 C      ACCEPT 102,SI,ET
27 C      FORMAT(2F10.0)
28 C      N=2*SI+1.1
29 C
30 C      CALCULATE HAMILTONIAN
31 C
32 C      DO 1600 I=1,15
33 C      DO 1600 J=1,15
34 C      H(I,J)=0
35 C      DO 1650 I=1,(2*SI+1)
36 C      H(I,I)=3*(I-SI-1)**2.-SI*(SI+1)

```



```

37      DO 1680 I=1,(2*SI-1)
38      H(I,I+2)=.5*SQRT((I+1)*(I)*(2*SI-I+1)*(2*SI-I)) *ET
39      H(I+2,I)=H(I,I+2)
40      C
41      C  DIAGONALIZATION OF HAMILTONIAN
42      C  GIVES EIGENVALUES AS R0WA
43      C
44      DO 20 I=1,N
45      DO 20 J=1,N
46      U(I,J)=0
47      DO 30 I=1,N
48      U(I,I)=1.
49      ITALY=0
50      NMIN1=N-1
51      DO 220 L=1,NMIN1
52      LPLUS1=L+1
53      DO 220 M=LPLUS1,N
54      0FF=H(L,M)
55      SPLIT=H(L,L)-H(M,M)
56      Q=ABS(0FF)
57      R=ABS(SPLIT)
58      IF(10**6*Q-R-1.0E-24) 220,110,110
59      IF (SPLIT) 112,111,112
60      S=SIGN(0.5,0FF)
61      GOT0 130
62      IF (2.*Q-R) 116,113,113
63      S=SIGN(0.5,0FF*SPLIT)
64      GOT0 130
65      S=0FF/SPLIT
66      C=SQRT(1.0-S*S)
67      C
68      C  LEFT MATRIX MULTIPLICATION
69      C
70      DO 173 J=1,N
71      X=C*H(L,J)+S*H(M,J)
72      H(M,J)=C*H(M,J)-S*H(L,J)

```



```

73 173 H(L,J)=X
74 C
75 C RIGHT MATRIX MULTIPLICATION
76 C
77 DO 210 I=1,N
78 X=C*H(I,L)+S*H(I,M)
79 H(I,M)=C*H(I,M)-S*H(I,L)
80 H(I,L)=X
81 X=C*U(I,L)+S*U(I,M)
82 U(I,M)=C*U(I,M)-S*U(I,L)
83 U(I,L)=X
84 ITALY=ITALY+1
85 CONTINUE
86 IF (ITALY) 250,250,89
87 DO 260 I=1,N
88 VALU(I)=H(I,I)
89 C
90 C
91 C
92 C
93 GLEBSCH-GORDON CALCULATION(SI M1,SI M2/K M3)
94
95 SKN(1)=0.
96 XV(1)=0.
97 NI=1
98 IF(AK-2.*SI-0.1)300,1400,1400
99 CONTINUE
100 SAME K AND SPIN DEN,T CALCULATE CLEBSCH-GORDON'S
101 IF (ABS(AK-AKP)+ABS(SI-SIP)) 450,550,450
102 AKP=AK
103 SIP=SI
104 DO 500 AM1=-SI,SI
105 DO 500 AM3=-AK,AK
106 CL(IFIX(SI+AM1+1.1),IFIX(AK+AM3+1.1))=
107 1 CG(SI,AM1,SI,AM3-AM1,AK,AM3)
108 C

```


109	C		
110	C		
111	550	I=1	
112		D8 800 NN=1,N	
113		D8 780 NP=1,NN	
114		I=I+1	
115		XV(I)=ABS(VALU(NN)-VALU(NP))	
116		P=0.	
117		D8 730 AM3=-AK,AK	
118		JKM3=FIX(AK+AM3+1.1)	
119		D8 710 AM1=-SI,SI	
120		JIM1=FIX(SI+AM1+1.1)	
121		IF(M8D(JIM1+NP,2))710,670,710	
122	670	JIM2=FIX(SI+AM1-AM3+1.1)	
123		IF(M8D(JIM2+NN,2))710,675,710	
124	675	T1=CL(JIM1,JKM3)*(-1.)*FIX(SI+AM3-AM1+0.1)	
125		T5=U(JIM2,NN)	
126		T3=U(JIM1,NP)	
127		D8 690 AM4=-SI,SI	
128		JIM4=FIX(SI+AM4+1.1)	
129		IF(M8D(JIM4+NP,2))690,680,690	
130	680	JIM5=FIX(SI+AM4-AM3+1.1)	
131		IF(M8D(JIM5+NN,2))690,685,690	
132	685	T2=CL(JIM4,JKM3)*(-1.)*FIX(SI+AM3-AM4+0.1)	
133		T4=U(JIM4,NP)	
134		T6=U(JIM5,NN)	
135		P=P+T1*T2*T3*T4*T5*T6	
136	690	CONTINUE	
137	710	CONTINUE	
138	730	CONTINUE	
139	C		
140	C	PUT THEM ON THE RIGHT SPOT	
141	C		
142		IF(NP-NN)732,735,732	
143	732	P=2.*P	
144	735	IF(XV(I))760,740,760	


```

145 SKN(1)=SKN(1)+P
146 I=I-1
147 GET9 780
148 SKN(I)=P
149 CONTINUE
150 CONTINUE
151 LIMIT=I
152 C
153 C
154 C
155 DO 1100 I=2,LIMIT-1
156 IF(XV(I)+5.)1100,1010,1010
157 DO 1050 J=I+1,LIMIT
158 IF (ABS(XV(I)-XV(J))-1.0E-4) 1020,1050,1050
159 SKN(I)=SKN(I)+SKN(J)
160 SKN(J)=0.
161 XV(J)=-10.
162 CONTINUE
163 CONTINUE
164 C
165 C
166 C
167 DO 1200 I=2,LIMIT
168 IF(ABS(SKN(I))-0.0001) 1200,1150,1150
169 NI=NI+1
170 SKN(NI)=SKN(I)
171 XV(NI)=XV(I)
172 CONTINUE
173 C
174 C
175 CC
176 CONTINUE
177 DO 1330 L=1,NI
178 XV(L)=XV(L)/(4.*SI*(2.*SI-1.))
179 SKN(L)=SKN(L)/(2.*AK+1.)
180 CONTINUE

```

TAKING SAME ENERGIEDIFF. TOGETHER

CAST OUT ZERO AMPLITUDES

MAKE THEM PROPRE

181 C
182 C
183 C

GOTO DISPLAY PART

RETURN
END

184
185


```

1 2 3 4 5 6 7 8 9 10 11 12 13 14 15 16 17 18 19 20 21 22 23 24 25 26 27 28 29 30 31 32 33 34 35 36
C C C 1 2 32 34 44 3 4 C 5 C
FUNCTION CG(A,C,B,D,E,F)
DIMENSION FACT(26)
COMPUTES CLEBSCH-GORDAN COEFFS (J',M',J'',M',M'/J,M)
DEFINITION IS THAT OF M.E.ROSE
IF(ABS(FACT(3)-0.693)-0.002) 2,1,1
CALL FACTOR(FACT)
CG=0.0
IF(B-ABS(D)+0.1)99,99,32
IF(A-ABS(C)+0.1)99,99,34
IF(E-ABS(F)+0.1)99,99,44
IF(ITRI(A,B,E))3,99,3
IF(ABS(C+D-F)-0.1)4,99,99
I1=A+C+0.1
I2=A-C+0.1
I3=B+D+0.1
I4=A+B-E+0.1
I5=B-E-C+0.1
I6=A+D-E+0.1
CALCULATE LIMITS OF THE SUM
ISTART=MAX(0,I5,I6)
IEND=MIN(I2,I3,I4)
IF(IEND-ISTART)99,5,5
I4=B-D+0.1
I5=E-F+0.1
I6=E+F+0.1
S=0.0
NOW DO THE SUM
DO 10 I=ISTART,IEND
RI=FLBAT(I)
J1=E+RI+C-B+0.1
J2=E+RI-A-D+0.1
J3=A+B-E-RI+0.1
J4=A-RI-C+0.1
J5=B+D-RI+0.1
T1=FACT(I+1)+FACT(J1+1)+FACT(J2+1)+FACT(J3+1)+FACT(J4+1)
T1=T1+FACT(J5+1)

```


37		RI=(-1)**I
38		S=S+RI*EXP(-T1)
39	10	CONTINUE
40		T1=FACT(I1+1)+FACT(I2+1)+FACT(I3+1)+FACT(I4+1)
41		T1=T1+FACT(I5+1)+FACT(I6+1)
42		CG=SQRT(DELTA(A,B,E,FACT)*EXP(T1))*SQRT(2.0*E+1.0)*S
43	99	RETURN
44		END


```
1  FUNCTION DELTA(A,B,C,FACT)
2  DIMENSION FACT(26)
3  I1=A+B-C+0.1
4  I2=B+C-A+0.1
5  I3=A+C-B+0.1
6  I4=A+C+B+1.1
7  DELTA=FACT(I1+1)+FACT(I2+1)+FACT(I3+1)-FACT(I4+1)
8  DELTA=EXP(DELTA)
9  RETURN
10 END
```



```

1      C
2      C
3      C
4      C
5      ITRI=0
6      IF(A+B+0.1-C) 99,2,2
7      IF(ABS(A-B)-0.1-C)3,99,99
8      S=A+B+C
9      S1=FLOAT(INT(S+0.1))
10     IF(S-S1-0.1) 4,4,99
11     ITRI=1
12     RETURN
13     END

```

FUNCTION ITRI(A,B,C)
 TESTS TRIANGLE INEQUALITY OF 3 ANGULAR MOMENTA
 ALSO REQUIRES INTEGER SUM TO GIVE VALID RETURN OF VALUE 1


```

1 2 3 4 5 6 7 8 9 10 11 12
C
C
C
SUBROUTINE FACTOR(FACT)
CALCULATE AND STORE FACTORIALS FOR C-G ROUTINES
ACTUALLY STORES LOG FACTORIALS
DIMENSION FACT(26)
FACT(1)=0.
FACT(2)=0.
DO 1 I=3,26
RI=FLOAT(I-1)
FACT(I)=FACT(I-1) + ALOG(RI)
CALL LINK(2)
END

```


B30127